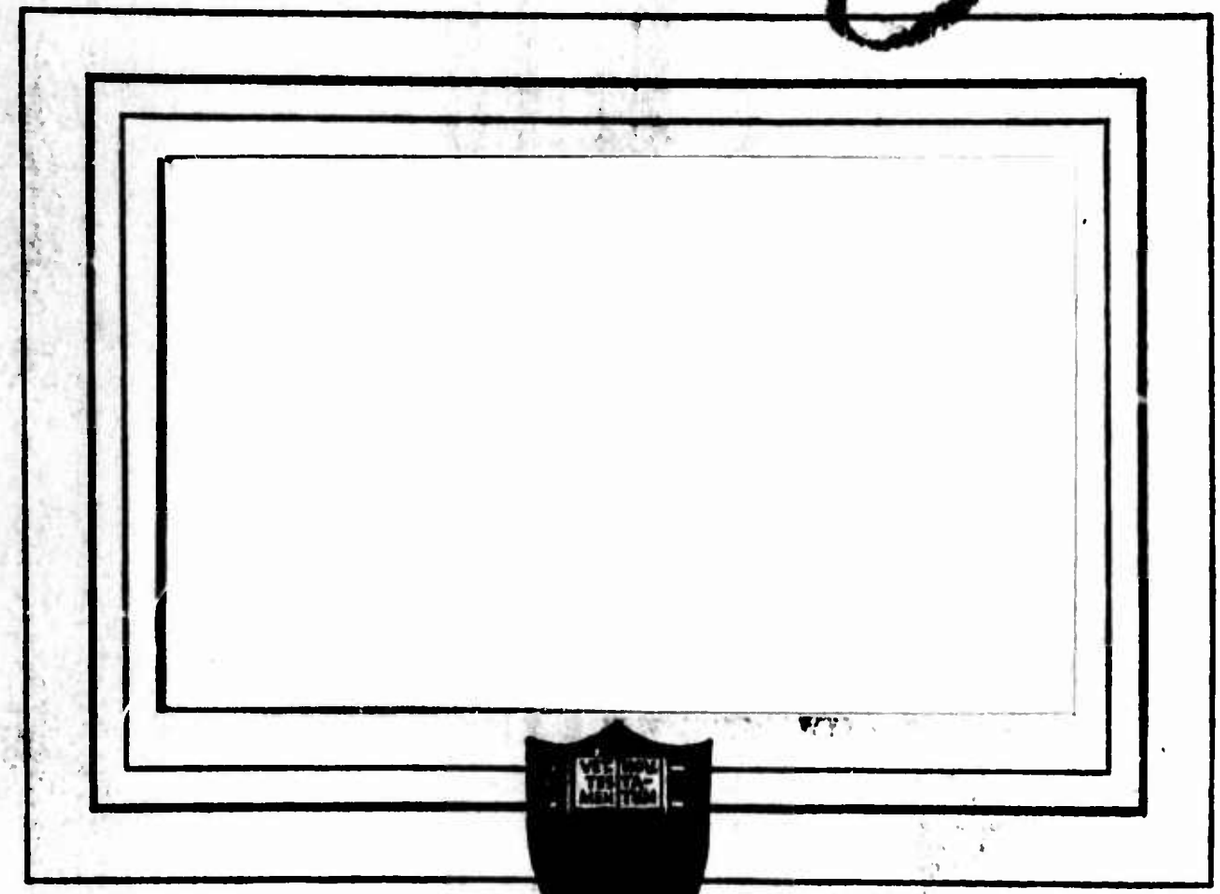

PRINCETON UNIVERSITY

DEPARTMENT OF AEROSPACE AND MECHANICAL SCIENCES

ELECTRICAL POWER SYSTEMS FOR THE MANNED ORBITING LABORATORY

by

Michael R. Anderberg

October 1965

Michael R. Anderberg

Supervised by: Morris Handelsman

Morris Handelsman, Visiting Senior Research Aerospace Scientist and Lecturer

Martin Summerfield

Martin Summerfield, Professor of Aerospace Engineering

Submitted in partial fulfillment of the requirements for the Degree of Master of Science in Engineering from Princeton University

ACKNOWLEDGEMENTS

The author wishes to thank Dr. Morris Handelsman for his advice, challenges, and encouragement during the preparation of this thesis. The spacecraft power group of RCA's Astro-Electronics Division, Hightstown, New Jersey, offered much useful advice and information. Thanks are also due to Mr. J. H. Rodgers of the Beech Aircraft Corporation for the analysis of cryogenic storage systems used in this study. Special thanks go to Mrs. Grace Arnesen who typed the final draft.

ABSTRACT

This paper is a detailed design study of possible electrical power systems for the Air Force's Manned Orbiting Laboratory. The mission requirements and details are reviewed to the extent that they are known in the open literature and a set of power requirements is derived. On the basis of reliability, availability, and weight considerations, only solar cells, fuel cells, secondary batteries and combinations thereof are selected for detailed analysis. For the 30 day mission it is concluded that if no experiments are required during the shadow portion of the orbit, the integrated battery/ solar cell system is superior by a large margin. If experiments are required in the shadow period, it is found that either the fuel cell system or the battery/ solar cell system may be optimum depending on the magnitude and type of power required. It is also found that for a 60 day mission only the battery/ solar cell system can be seriously considered. The analysis of the three power systems in support of the design study is developed step by step and may be used as a detailed guide for analyzing the characteristics of these systems for other missions.

TABLE OF CONTENTS

TABLE OF CONTENTS (Continued)

TABLE OF CONTENTS (Continued)

TABLE OF CONTENTS (Continued)

TABLE OF CONTENTS (Continued)

LIST OF TABLES

LIST OF TABLES (Continued)

LIST OF FIGURES

LIST OF FIGURES (Continued)

1. MISSION REQUIREMENTS

1.1 General Mission Description

Simultaneously with the cancellation of the X-20 (Dyna Soar) in December 1963 the Air Force was given responsibility for developing the Manned Orbiting Laboratory (MOL) to evaluate the military usefulness of man in space. After extensive study and many delays, the President announced in August 1965 that Douglas Aircraft Company would build the MOL spacecraft and that the General Electric Company will be responsible for experiments.

While many of the exact details of MOL are either classified or undecided, some general descriptive information has been made public. The orbital vehicle is to consist of a modified Gemini capsule mated to a cylinder 41 feet long and 10 feet in diameter.[52] During launch and re-entry phases of the mission, the crew of two will occupy the Gemini capsule. For the remainder of the flight, they will live and work in the cylinder which is to provide "a shirt sleeve environment."[89] The cylinder will be divided into three compartments: one will be a living area, the second a work area, and the third an unpressurized section for equipment and experiments. The latter compartment will be adjacent to the transstage and is to be about 20 feet long.[52] It is planned that the complete spacecraft will weigh about 25000 pounds including the 6000 pound modified Gemini capsule.[91]

The launch vehicle is to be the Titan IIIC. According to published data, this booster has a gross payload capacity of 28,500 pounds for a 100 nautical mile circular orbit or 25000 pounds for a 350 nautical mile orbit.[74, 83] The effects of atmospheric drag will limit the circular satellite to a minimum of 160 nautical miles while the radiation belts will limit the maximum altitude to about 350 nautical miles, the upper limit of booster capability.[50] Apparently, the Air Force is planning orbits near the upper end of this range as two used Gemini capsules have been procurred in order to test a thicker heat

shield for re-entry from high altitudes.[90] For the purposes of this study, the orbital altitude will be taken as 250 NM.

Initially the MOL program is to consist of five manned launches with 30 day durations, beginning in late 1968. The manned flights will originate from the Western Test Range using polar orbits. There will be unmanned launches of the two used Gemini capsules and a complete MOL spacecraft from the Eastern Test Range prior to any manned flights.[28,52,91] The program is considered to be open ended and after the first few flights the mission duration may be extended or there may be rendezvous attempts. As a result, this study will analyze power systems for both the 30 day mission and an extended 60 day mission.

To insure mission success, minimize cost, and reduce development time, Air Force spokesmen have emphasized that maximum use must be made of existing hardware and technology.[6] Only in the event of gross unsuitability or established improvements should any new development programs be initiated.[22] The MOL project will draw heavily on the experience of NASA in its manned spaceflight programs and it can be expected that much of the MOL equipment will be modified Gemini and Apollo hardware.

1.2 Power Requirements

The Air Force has released no information on the power requirements for MOL. However, from the published information summarized above, it is possible to delimit a range of power requirements by drawing on the results of published space station studies for NASA.

The fact that the crew consists of only two men will severely restrict the time available for activities other than routine duties. The astronauts will be awake together only eight out of twenty-four hours as only one man may sleep at a time. A typical day for one man might be broken up as in Table 1.1 below.

ACTIVITY	Total Hours	Hours when both are awake
Sleeping	8	0
Eating	1-3/4	3/4
Personal Hygiene	3/4	1/4
Physical Fitness	3-1/2	1/2
Relaxation and Recreation	1-1/2	1-1/2
Station Management	2-1/2	1/2
Maintenance and Housekeeping	2	3/4
Experiments	3-1/2	3-1/2
Unassigned (contingency)	1/2	1/4
Total	24	8

TABLE 1.1, CREW SCHEDULE

The division of time in the second column of Table 1.1 is based upon crew schedule studies for NASA's MORL.[7] Assuming that both men must be on duty during experiments, it is of interest to know whether 3-1/2 of the 8 hours when both are awake will actually be available for such activities. The figures in the third column are the author's own idea of how these eight hours will be allocated for one man. This schedule is based upon performance of as much of the routine duties as possible while the other man is asleep. For instance, during a 24 hour day, each man will eat three meals requiring one-half hour each and a quarter hour snack. It should be possible to eat two of the meals while the other man is asleep.

With a crew schedule of this type, electrical loads should occur as in Table 1.2 below which is derived in part from a study for NASA's MOSS.[33]

Type of load	Peak load	Average load	Average time used	Peak time used
Life support:				
Continuous	1-2.5 KW	1-2.5 KW	24 hrs/day	24 hrs/day
Periodic	200 W	100 W	10 min/day	20 min/day
Transient	600 W	500 W	45 sec/rev	10 sec/rev
Communications:				
Voice	20 W	20 W	20 min/rev	50 min/rev
Telemetry	20 W	20 W	2 hrs/day	4 hrs/day
Experiments:				
High load	1.5-4 KW	1-3 KW	90 min/day	45 min/rev 2 hrs/day
Medium and low load	0.75-2 KW	0.5-1.5 KW	60 min/day	45 min/rev 2 hrs/day
Biomedical monitors	25 W	25 W	24 hrs/day	24 hrs/day

TABLE 1.2, ELECTRICAL DEMANDS

Life support loads consist of air conditioning and purification systems, lights, stabilization and control, system performance monitors, etc. The continuous loads are constant power throughout the course of the mission. The magnitude of the continuous loads will depend upon the type and quantity of life support equipment. The periodic loads serve such functions as waste disposal, food heating, and water pumping. These functions may be performed whenever convenient. The transient loads are associated with motor starting, valve actuation, switching, and other functions which occur in conjunction with the periodic loads. Transient loads should never occur simultaneously. Emergency operations may be conducted at one-half the continuous life support power.

Communication loads are for transmission only. The receiver loads are considered to be negligible. Voice communication with ground stations must be continuously available. However, it is unlikely that the crew will be speaking more than half the time even during continuous communication; hence, a maximum of 50 minutes per orbit has been allotted. This is a very generous figure when one considers that the present network of ground receivers does not allow continuous voice communication. Telemetry is only for reporting of data from experiments. The data is stored in tape recorders and read out when the power

supply has excess capacity. The biomedical monitors report data in real time and power for telemetry is included in the power allotted for that function.

Experiments may be classified as biomedical, behavioral, scientific, and engineering. Each MOL vehicle will have a unique complement of experiments and so will impose unique demands on the electrical power system. Hence, a range of load conditions are given in Table 1.2. Only one experiment will be performed at a time. The maximum time allotted to power consuming experiments will be 45 minutes per orbit (3 hours per day) in order to not unduly prejudice the solar cell systems. It has been assumed that an average of one hour out of the 3-1/2 hours per day available for experiments is spent in activities which consume no power. Since experiments are non-coincident and the high load experiments determine the peak power requirement, the other experiments may be conveniently lumped together as they influence only the total energy consumed. The magnitude of the medium and low loads is assumed to be half that of the high loads.

Biomedical monitors report data on the astronauts themselves. The power level specified provides for continuous telemetry.

As a result of uncertainties in the power requirements for MOL and variation of requirements among the five flights, a range of demands has been specified for the life support and experimental loads. Small loads are taken as constant since their influence on total demand is very small.

Most space electrical equipment is well developed for 28 volt systems and there appears to be no good reason to deviate from this standard.[77] According to MIL-E-26144 the allowable voltage variation of a nominally 28 volt system is over the range of 25 to 29.5 volts.[8] The demands shown in Table 1.2 are based upon the minimum voltage of 25 volts. If the power source output is at a higher voltage, the power rating of the source must be correspondingly higher in order to deliver the required current, which is constant regardless of voltage.

Because the various power sources considered in this study have similar power conditioning requirements, the weight of regulators and inverters will vary by only a few pounds among power systems and so will not significantly affect the comparisons. Further, the division of power between AC and DC loads is unknown as is the quantity of very closely regulated power required for special uses. Thus, an analysis of power conditioning requirements could not be performed with any significant validity.

The power system should not require any maintenance during the course of the mission. On the other hand, the system should not be designed in such a manner as to hinder or preclude emergency repairs.

Since the Gemini capsule is the astronauts' only means of returning to earth, the MOL power system should be completely independent of that in the Gemini. A possible exception to this rule is a provision of a trickel charge for the capsule's primary batteries.

Should there be a failure in the primary electrical system, there must be an emergency battery capable of providing continuous life support loads for about two hours in order to give the crew time to don suits and enter the Gemini. Since all candidate primary power systems must have such a back-up system, the emergency battery will not be considered in detail here as it will not influence system comparisons.

1.3 Attitude Control

The experiments to be performed in the MOL missions are for the most part related to reconnaissance and probably have been the primary reason for the secrecy surrounding the program. For instance, two experiments have to do with assembling large optical devices and antennas in space while a third involves surveillance and cataloging of the world's ocean traffic.[86] Because of the nature of these experiments, the spacecraft will require very high pointing accuracies, probably about ± 0.001 radian.[51]

The orientation of the spacecraft will probably be earth-pointing as such an orientation is advantageous for both the reconnaissance sensors and communications antennas. Further, the gravitational potential acting on the spacecraft will exert a strong force tending to align the axis of least inertia (the longitudinal or yaw axis) with the local vertical. This orientation is also quite stable and so aids the attitude control system in overcoming the various disturbance torques.[88]

These pointing requirements are mentioned here because the power system interacts with the attitude control system. In the case of some devices,

weight can be traded for use of higher power levels so that an excess capacity in the power source can result in a weight saving in the attitude control system. Another possibility is that product water from a fuel cell could be used as a monopropellant in a gas jet attitude control system. An analysis of attitude control systems and requirements is presented in Appendix B.

1.4 Power System Reliability

Because space exploration is an expensive proposition, and more recently because human lives are involved, system reliability has become one of the most significant parameters in describing a piece of space hardware. Weight and volume comparisons among candidate systems for a given task are meaningless unless reliability is specified.

Reliability is defined as the probability that a given system will adequately perform a given task under certain conditions for a specified period of time. In the case of a power system, a failure is said to have occurred when the system can no longer provide the requisite power at the minimum voltage. Under this definition, the system might never fail catastrophically but just slowly decay until it is inadequate to the task. Further, failure has several levels. For instance complete mission success may require P watts, but only 0.5P watts may still allow many objectives to be fulfilled while possibly only 0.2 P watts are needed to comfortably sustain the crew.

This distinction brings us to the subject of mission success and crew safety reliabilities. For mission success, the power system must be able to satisfy the peak load resulting from the schedule of demands in Table 1.2. For crew safety, the power system only needs to provide half the continuous life support load. There is a world of difference between the two respective power levels and an even larger difference between the required reliability associated with each of them. For the Gemini spacecraft, the power system reliability is 0.995 for mission success and 0.9999 for crew safety.[47] The difference in probability of success between these two figures seems very small; but the probability of failure is 50 times greater for mission

success criteria than for crew safety criteria. These Gemini reliability figures will be used in this analysis for the full 30 and 60 day missions in designing a power system for the MOL.

A word about the quality of available reliability data is in order. In order to establish system reliability figures at the levels specified above, lengthy and costly test programs are needed. For instance, if 60 complete systems were tested under simulated mission conditions and none of the systems failed before the required mission duration was reached, it could be said to the 95% confidence level that the system reliability was at least 0.95.[25] Now, there has never been such a test on a space power system and there likely never will be because of the immense cost. Rather, reliability is estimated from component failure rates. The inherent system reliability is enhanced at every opportunity by making the design as simple as possible and employing redundant components whenever the need is indicated. Even so, power system designers shun being pinned down on the statistical confidence associated with their reported reliability figures. In this study, reliability figures necessarily are taken as given in the literature and used as though the same confidence level is implied among different systems.

Systems which are subject to sudden total failures are analyzed in this study on the basis of numerical reliability figures using a cumulative binomial probability distribution. Other systems which are not subject to failures of this type but slowly decay are analyzed on the basis of providing sufficient excess capacity at the beginning of the mission to allow for expected rates of deterioration. Batteries and fuel cells are examples of the former while solar cells and radioisotope thermoelectric generators are representative of the latter.

2. POSSIBLE POWER SYSTEMS

2.1 The Spectrum of Choice

A few years ago, preliminary selection of possible power systems for space use was relatively simple as the alternatives were few. This fact is evident when one considers that the only power systems that have been operationally flown are primary batteries, solar cells combined with secondary batteries, fuel cells, and small radioisotope thermoelectric generators (RTG's). However, the spectrum of choice is broadening and will continue to do so. It is reasonable to expect that by 1968 several systems now in development will have flown with a few of these actually in operational use and not merely a part of the experimental payload.

However, having passed orbital tests or even being qualified as an operational off the shelf piece of equipment does not mean that a system is man rated. In some cases, man rating can be a tremendous hurdle requiring possibly years of further development and very sizable levels of funding. For instance, an otherwise attractive system may involve noise or vibration levels that interfere with crew performance. Or the system might present a radiation or toxicity hazard to the crew and so require additional weight for protective devices. Or, finally and most important, the probability that the system will be able to provide sufficient power for mission success and crew safety may be far from the mission requirements.

The only system designed from the outset to be man-rated has been the fuel cell. Experience with batteries and solar cells has been so extensive and successful that there cannot be any question about them being adequate for manned missions. But new power system concepts which are in the hardware stage now, or will be in a few years, have not been initially designed for the stringent requirements of manned spaceflight simply because the expense is too great. The additional development time and cost for man rating and demonstration is one of the most significant, but most

easily forgotten, considerations in hypothetical mission studies. The only alternative to delaying application of a system until it is adequately developed is use of brute force redundancy and the consequent acceptance of weight increases on the order of perhaps several hundred percent. Because of the effect of this consideration, some systems which are touted as competitive alternatives for near future manned missions by some of their sponsors should be rejected as unrealistic.

2.2 Preliminary Selections

Those space power systems which are presently available or under development are discussed in relation to their suitability for the MOL mission in the following paragraphs. Detailed discussion of the theoretical aspects of the basic devices used in these systems cannot be included in a paper of this length and scope.* The discussion is concerned primarily with system characteristics as they apply to the mission in question. Primary batteries and hydrogen-oxygen auxiliary power units are not included as it is universally agreed that these systems are of no interest once the mission length exceeds a few days.[75, 79]

2.2.1 Solar Cells/Secondary Battery

Since 1958 solar cells used with rechargeable batteries have been the standard of space power. Both the cells and the batteries are well developed and flight experience is far more extensive than with any other system. Indeed, the state of development and experience are such that most designs flown today probably are sufficiently reliable for a 60 day manned application.

---

*The interested reader will find an overall summary of the physics and chemistry of solar cells, fuel cells, and thermoelectric and thermionic devices in Chang, S. L., Energy Conversion, Prentice Hall, 1963. More detailed discussions of specific problems and phenomena associated with solar cells will be found in Energy Conversion for Space Power, edited by N. W. Snyder, Academic Press, 1961, pp 221-383. A useful collection of papers on fuel cell research appears in volumes 1 and 2 of Fuel Cells, edited by G. J. Young, Reinhold Co., 1960 and 1963.

The principal disadvantage to using solar cells is that typical solar panels have outputs of only about 10 watts per square foot. The resulting large arrays contribute significantly to orbital drag at low altitudes and impose orientation requirements on the spacecraft. In addition, such large arrays are difficult to store inside the vehicle and erect in space. The resolution of these problems depends on the mission and the spacecraft configuration; in most, if not all, cases a solution can be found by accepting some weight penalty.

Neither solar cells nor batteries present any special hazard to the crew. In view of availability, reliability and experience, solar cells and secondary battery systems must be considered as prime candidates for the MOL mission.

2.2.2 Fuel Cells

Of all the space power systems available or under development only the fuel cell has been initially designed for manned applications. Such devices have already flown in the Gemini program and will be used for Apollo.

The principal disadvantage of fuel cells is that the system is energy limited. That is, for each kilowatt-hour of energy required, about one pound of hydrogen and oxygen must be used. As power levels and mission durations grow the point is finally reached at which the weight of reactants and tankage equal the allowable weight of the vehicle. On the other hand, if the weight problem is not extreme, credits can be applied to the water produced in the fuel cell. This by-product may be used for drinking and washing, as a monopropellant for attitude stabilization and control or orbit keeping, or for heat rejection through use of a water boiler.

Because it is the only system applied to manned spaceflight to date, fuel cells must also be intensively studied for MOL, keeping in mind possible credits for the water.

2.2.3 Thermoelectric Generators

A thermoelectric generator is a device for the direct conversion of heat to electrical power. Its operation is identical to the familiar thermal couple, the fundamental difference between the two being that the thermoelectric devices of today are composed of semiconductors which allow achievement of useful efficiencies. These devices are under development for use with solar, nuclear reactor and radioisotope heat sources. Each of these is considered below.

2.2.3.1 Isotope Systems

Radioisotope thermoelectric generators (RTG's) have been in use for years. Snap-3 devices were used in the Navy Transit 4A and 4B satellites. Snap-9A is a 25 watt device for Transit 5. Snap 11 is also a 25 watt device but is designed for Surveyor.[9] Snap-17 is a 30 watt unit for a medium altitude communications satellite. Snap 19 is also rated at 30 watts and is being developed for Nimbus B.[24] These devices with very low power outputs are well understood and have been developed on short notice in some cases.

RTG units for manned spacecraft requiring 3 to 5 kw have been reported as feasible.[78] However, in a recent study by Douglas Aircraft Company, an RTG analyzed specifically for the MOL mission was found to weight 6050 pounds including shield and radiator for a net output of 4.2 kw.[84] At 0.7 watts per pound this system cannot be considered competitive with solar cell/secondary battery systems which can readily achieve 2.0 to 2.5 watts per pound.[16]

2.2.3.2 Reactor Systems

The only thermoelectric-reactor system under development is the Snap-10A. The nominal output of this system is 500 watts for a weight of 950 pounds, including a shield adequate for selected unmanned payloads.[1] By adding three more thermoelectric converters weighing 200 pounds each,

the output can be raised to 1.25 kw.[1] Even with this improvement the specific power would be only 0.8 watts per pound, little better than an RTG. But even this weight does not include a simple conical shadow shield adequate for manned applications. For a manned 10 foot diameter station, the shield weight is estimated to be between 4000 and 7000 pounds.[78] In addition, the design goal reliability of 80% probability for mission success over a 90 day period is inadequate for manned applications.[1] Because of these reliability and weight considerations, the Snap-10A can be eliminated from consideration.

2.2.3.3 Solar Systems

Thermoelectric generators using Solar energy as a heat source have been studied. These are similar to solar cell systems in that a secondary power source is required when the spacecraft is in the Earth's shadow. The most successful flat plate generator using unconcentrated sunlight has demonstrated a capability of 2 watts output per square foot of collector area.[78] This contrasts sharply with the 10 watts per square foot available from solar arrays. And since solar array weight is limited principally by structural requirements for launch, thermoelectric panels should not weigh significantly less per unit area. Thus it may be concluded that all the thermoelectric power systems currently under development or in the hardware stage are significantly heavier than a comparable solar cell/ secondary battery system, when suitably configured for manned operations. Therefore, thermoelectric systems can be dropped from further consideration.

2.2.4 Thermionic Generators

The best thermionic devices to date are cesium diodes with reported efficiencies falling in the neighborhood of 10%.[24, 78] These devices are being studied for use with solar, isotope, and reactor energy sources. The only program thus far committed to hardware development is Snap 13 which is a 1 volt, 25 watt unit for Surveyor.[78] Feasibility of most large thermionic

systems is still uncertain and any large systems are considered to be several years from availability for any application, much less manned operations.[78]

2.2.5 Dynamic Engines

Heat engines using Brayton, Rankine, and Stirling cycles have been studied for use with reactor, isotope, and solar energy sources. The Stirling cycle systems are not receiving much attention as it is felt that their potential is far more limited than the other two.[43, 75] The Brayton cycle systems have received sporadic attention over the last eight years and so have not progressed very far. Even if full scale development programs were initiated today, it is unlikely that a solar Brayton system could be developed before 1969, or a reactor Brayton system before 1971.[73, 78] The only remaining alternative is the Rankine cycle; and even in this case, a mercury working fluid is the only choice until at least 1970.[78]

The mercury Rankine system has been the subject of much study and an impressive amount of development. The Snap 2 (now $Snap_{SI}$) and Snap 8 reactor programs as well as the Sunflower solar program are all designed for use with mercury Rankine cycles.[78]

The Snap 2 system was originally designed to provide 3000 watts of 120 volt AC power for a system weight of 1500 pounds including a shield adequate for unmanned missions. Shield weight for manned missions is about 4000 to 7000 pounds as the reactor is the same as in Snap 10A.[78] The system reliability goal is also about 80% for a 90 day mission as with the Snap 10A.[1] On these weight and reliability grounds alone, the Snap 2 system can be dropped from consideration.

The Snap 8 program has been stretched and is expected to complete the ground development phase by 1970. Conceptual studies of isotope-Rankine systems have been made, but these systems are limited by isotope availability and shielding weights.[24] Since development of isotope dynamic systems has been at only a very low level, it is doubtful at best whether a man rated unit could be produced by 1968.

Of all the solar dynamic systems under study, the Sunflower system is probably the most advanced. This power system utilizes a mercury-Rankine cycle with a solar heat source. Lithium hydridide is used to store heat energy for the shadow period of the orbit. This program had progressed to ground demonstration of major components when it was cancelled in 1964 in favor of a Brayton cycle system.[24, 78] At that time, about two years of development effort to initial-availability were remaining. The system design goals were 3 kw of AC output for a weight of about 700 pounds.[78] Even if system weight had to be increased by 50% for man rating, this system would be at least competitive with solar cell battery systems. However, because the program was cancelled and at least two years of development effort were remaining, this system cannot be considered as able to fulfill present MOL development deadlines.

2.3 Final Selection

Based upon availability, reliability, and weight considerations as presented above, the only power systems that can be seriously considered for the MOL program are solar cells, secondary batteries, and fuel cells. Solar cells need to be supplemented by a secondary system because solar energy is unavailable when the spacecraft is eclipsed by the Earth. In the past only rechargeable batteries have been employed with solar cells. However, this selection has been more a matter of necessity than choice. In this study, the novel combination of primary fuel cells and solar cells will also be explored. In most instances such a system would be rejected because the weights of fuel cells and reactants exceed the weights of secondary batteries and the solar cells needed for charging. But, in a manned system the fuel cell product water can be used in a variety of ways and generate credits by eliminating the need for other equipment. The particular combination of fuel cells and solar cells employed depends on the extent of credits which can be applied, the power level, and the mission duration. For instance,

fuel cells might be used for only the darktime loads or they might also be used to supplement the solar array output when power consuming experiments are performed.

In summary, the power systems considered in this study will be:

1. Solar cells with secondary batteries
2. Solar cells with primary fuel cells
3. Primary fuel cells alone.

3. SOLAR CELLS

3.1 Solar Cell Selection

Many different materials possessing photovoltaic characteristics have been investigated for use as solar cells; but for most missions silicon cells have no equal. The only close competitors are gallium-arsenide and cadmium-sulfide. All other materials are in such a primitive state of development that they can be eliminated from consideration.[16]

3.1.1 Gallium-Arsenide

Gallium-arsenide cells are a recent development of RCA as the result of NASA programs. Development has proceeded to the point that pilot production lines have been set up and some cells have been experimentally flown on satellites. At the present state of the art, gallium-arsenide cells in production lots would be about 65% as efficient and cost an estimated 5 to 10 times as much as silicon cells.[57] Gallium-arsenide cells have superior radiation resistance characteristics;[78] however, the new 10 ohm-cm N on P type silicon cells are just as resistant and much more efficient.[57] The only mission on which these cells are likely to outperform silicon cells are those which encounter severe radiation and temperature environments such as in the case of a probe to Mercury. The superiority of gallium-arsenide cells at higher temperatures is a result of the low degradiation factor for cell efficiency versus temperature. For silicon, efficiency declines at a rate of 0.06% per ^{o}C while the factor for gallium arsenide is only 0.02.[26a] Thus, if panel equilibrium temperatures exceed 125^{o}C, the gallium-arsenide cells will be superior to the silicon cells, assuming that the cells are 7% and 11% efficient, respectively, at 25^{o}C and AMO* conditions. Such temperatures are not to be expected in

*Air Mass zero or space conditions as opposed to Air Mass one (AM1) or sea level conditions. A cell tested at AM1 will have a higher apparent efficiency than at AMO conditions because of atmospheric filtering of radiation the cell cannot use anyway.

the vicinity of the earth and so there is no advantage to be gained by using gallium-arsenide cells on such missions.

3.1.2 Cadmium-Sulfide

Cadmium-sulfide single crystal cells of usable efficiencies were reported at about the same time as the first silicon cells.[26a] But rather than produce a cadmium-sulfide cell which is the twin of the small rigid single-crystal silicon cells, the research effort has been aimed at developing flexible, thin film polycrystalline cells of fairly large areas (10 to 50 square incles). Because of the polycrystalline structure, there are considerable resistance losses across crystal interfaces and efficiency is quite low. Small laboratory cells have achieved 3 to 4% efficiencies, but production arrays for space use would not likely exceed 1½%.[16] In spite of low efficiencies, flight panels are anticipated to weigh less per unit power output than comparable silicon panels. A typical array is expected to consist of a plastic substrate several mils thick on which the cadmium-sulfide has been deposited. The entire unit would be very flexible allowing storage and erection techniques to be much simpler than those necessary for rigid panels. However, cadmium-sulfide cells are still in the research and development stage.[16] Flight hardware must be considered as at least two years in the future. While not considered suitable for projects under current development, the cadmium-sulfide cell will probably be an important option for second generation space stations.

3.1.3 Silicon

The silicon solar cell has been the workhorse of spacecraft power. On almost every spacecraft with a useful life of more than a few days, it has been the primary source of electrical power. When silicon cells were first used in 1958 maximum efficiencies were about 5%, production was on a laboratory scale, and quality control was an immense problem. Today,

cells are routinely manufactured in mass production lots with most cells falling between 10.5 and 11.5% AMO efficiency at 25°C.[78]

There are two basically distinct types of silicon cells. One is the P on N type which is produced by diffusing N type silicon with BCl_3 to form a P type layer.* The other is the N on P type which is formed by diffusing P type silicon with P_2O_5.[1] The first silicon cells were the P on N type and are considered the standard of solar cells. The N on P type is a more recent development and is equal in performance to the P on N type, but with markedly superior resistance to the degrading effects of space radiation.

Available sizes and price data** currently applicable to 1 ohm-cm P on N cells are shown in Table 3.1.[57]

SIZE	COST PER CELL	RELATIVE COST	
		PER CELL	PER UNIT AREA
1 x 2 cm	$2.60	1	1
2 x 2 cm	$4.00	1.54	.77
3 x 3 cm	$5.00-$5.50	1.92-2.12	.213-.236

TABLE 3.1, PRICE DATA

The N on P cells are available in the same sizes at about 10% greater cost.

The 1 x 2 cm cell is considered to be the standard. The first cells were of this size and even today most designs specify the 1 x 2 cell. Handling techniques have been greatly improved and breakage losses are very low. As a result, cell thicknesses are being reduced from 18 mils to 12 mils with weight per cell being reduced from 0.25 gr. to 0.19 gr. including

---

*P and N type materials are so called because the majority carriers are "holes" and electrons respectively.

**Based on a production run of about one million cells.

solder contacts. No loss in performance has been experienced as a result of the reduction in thickness. It is thought by at least one cell vendor that the 12 mil cell is the optimum trade off between weight and structural integrity (or ease of handling).[57]

The 2 x 2 cell is a recent development and has been used on the Nimbus satellite.[16] Cell efficiency is equal to that of the 1 x 2 cell and handling problems have not proven to be any more severe.[57] A 12 mil thick 2 x 2 cell weighs 0.38 grs. with solder contacts.[57] Since the 2 x 2 cell is cheaper than the 1 x 2 cell per unit area, or per unit output, and equal in all other respects, there should be increased use of this size. Additionally, use of the 2 x 2 cell reduces the number of array components and interconnections by a factor of two which should reduce assembly times and costs while improving reliability.

The 3 x 3 cell has never been used in space. In spite of the very significant cost advantage noted in Table 3.1, there are some substantial disadvantages. First, the 3 x 3 cell is not as efficient as the smaller types and so results in larger and heavier arrays. Second, a 12 mil thick 3 x 3 cell is almost impossible to handle without incurring unacceptable breakage rates and a high demand for replacement cells.[57] Thus thicker cells should be used to attain the necessary structural integrity resulting in still heavier panels. Improvements in handling and assembling techniques as well as in efficiency are to be expected. However, for the present the 3 x 3 cell is the poorest alternative of the three.

All of the cells described above are made with integral grid lines sintered to the exposed face of the cell. These grids act as current collectors and reduce sheet resistance thus improving cell efficiency.[41] On 2 x 2 cells six grid lines are standard.

In the past, the grid lines terminated at a bus bar which covered about 10% of the cell's exposed surface. Now cells are available on which the grid lines "wrap around" to a contact on the reverse of the cell. This

seemingly very small development allows an increase in cell output of more than 10% because of the increased active area.[57]

From the description of solar cells given above, the 12 mil, 2 x 2 cm silicon cell with wrap around grid lines incorporates the most desirable properties of available cells. However, the decision on whether to use N on P or P on N cells must be predicated on an analysis of the radiation environment, which is presented below.

3.2 Radiation Damage

The radiation environment anticipated in a 250 NM orbit with a 90^{o} inclination is given in Table 3.2.[49, 74]

PARTICLE	ENERGY, MEV	PARTICLE FLUX PARTICLE/cm^2/DAY
ELECTRONS	0.2 - 4	10^{10}
PROTONS	4 - 12	10^{7}

TABLE 3.2, RADIATION ENVIRONMENT

The flux of both particles falls off rapidly with increasing energy.[74] As a result, the figures given in Table 3.2 represent almost the entire population of damaging particles.

The power system designer must compensate for the losses expected in the solar array output so that sufficient power is available to supply all demands, even at the end of the mission when the array has been degraded to the maximum extent. For this purpose, three principal techniques are available: overdesign, use of radiation resistant cells, and shielding of cells. In most designs, a combination of these three is employed. These techniques are discussed in turn below.

3.2.1 Overdesign

The simplest method of insuring that the solar array has sufficient capacity at the end of the mission is to provide an excess of solar cells. For example, if it is anticipated that the power output will degrade by 20%, the array should be 125% the size of an array designed without consideration of degradation effects. In the early stages of the mission, there will be excess capacity; but toward the end of the mission the array will just meet the demands. If the loads can be programmed so that demands decline as capacity drops, the overdesign approach is excellent.

3.2.2 Use of Radiation Resistant Cells

As noted above, the N on P cell has superior radiation resistance characteristics. If one is willing to sacrifice performance, N on P cells with base resistivities up to 25 ohm-cm will give even greater improvements. However, the gains above 10 ohm-cm are small and hardly justifiable in view of the power loss due to increased resistance.[14,45] In the present case, the mission length is relatively short and the radiation environment is not severe (since the vehicle never enters either Van Allen Belt) so that only 1 ohm-cm cells need be considered.

The significant parameter used in comparing P on N and N on P cells is the critical flux, the particle flux which results in a 25% reduction in output. The value of critical flux is dependent on the particle type and energy as shown in Table 3.3.[14,78]

PARTICLE	ENERGY MEV	CRITICAL FLUX, PARTICLES/cm^2	
		N on P	P on N
ELECTRONS	0.8	1.3×10^{15}	4×10^{13}
	5.6	3.0×10^{13}	2×10^{12}
PROTONS	1.8	1.3×10^{11}	4×10^{10}
	17.6	4×10^{11}	7×10^{10}
	95.5	7×10^{11}	2×10^{11}

TABLE 3.3, CRITICAL FLUXES, 1 ohm-cm CELLS

For all particle types and energies, the N on P cell is superior to the P on N.

The energies given in Table 3.3 do not directly correspond to the actual incident radiation as given in Table 3.2. Hence, it is necessary to interpola.e in order to find values of critical flux for the actual radiation environment. The resultant values given in Table 3.4 below are those used in this study and may be considered conservative since the greatest concentration of particles is at low energies.

PARTICLE	CRITICAL FLUX, PARTICLES/cm^2	
	N on P	P on N
ELECTRONS	1.5×10^{14}	1.0×10^{13}
PROTONS	3.5×10^{11}	6.0×10^{10}

TABLE 3.4, ASSUMED CRITICAL FLUXES

Comparison of Tables 3.2 and 3.4 shows that electrons have much greater effects than protons and that the time to 25% degradation from electron damage is much higher for the N on P cells, 830 days as opposed to 55 days for the P on N cells. While it may appear that the N on P cell is vastly superior to the P on N cell, selection of one cell type or the other must be postponed until cell shielding is considered, as in the following section.

3.2.3 Shielding of Cells

Protective cover slips of quartz, sapphire, glass, or fused silica are a common feature of solar arrays. The space environment is a hostile one to solar cells and such shields are necessary to protect the cell from micrometeorites and to control the cell operating temperature as well as to moderate incident radiation. Among the various possible materials, fused silica and sapphire have been found to be very useful as they do not brown in response to the severe ultraviolet (UV) radiation, a characteristic of other types of glass covers.[16] Because of expense, fused silica with a density of 2.65 gr/cm^3 will be considered here rather than sapphire.

The practical minimum thickness of cover slips is about 6 mils.[15,57] Below this value handling losses result in markedly increased expense. It has been reported that 3.5 mils of 2.2 gr/cm^3 glass will protect a P on N solar cell from the effects of 3 Mev protons.[26b] With six mils of denser material, it is then reasonable to assume that protons with incident energies of 4 Mev or less will be stopped or reduced to energies which do not affect the solar cell. With respect to electrons, 6 mils of cover slip will protect against particles with energies up to only 0.2 Mev.[26b] These values are identical to the minimum energies quoted in Table 3.2.

Use of cover slips has an effect identical to increasing the value of critical flux. The thickness of 2.2 gr/cm^3 glass cover slips necessary to increase the critical flux by a factor of 10 has been shown to be about 40 mils or less.[74] Since fused silica is to be used in this design, a correction factor of 1.2 is indicated to account for the higher density. Thus

$$\log_{10} \frac{\varphi_c^{cov}}{\varphi_c^{unc}} = \frac{1.2T}{40} = 0.03T \qquad (3\text{-}1)$$

where

φ_c^{cov} = the critical flux of the covered cell

φ_c^{unc} = the critical flux of an uncovered cell

T = cover slip thickness in mils.

3.2.4 Degradation Analysis

The degradation due to each type of particle may be expressed as[23]

$$Q = 1 - \left[0.785 \left(\frac{\varphi_t}{\varphi_c}\right)^{\frac{1}{2}} + 1\right]^{-\frac{1}{2}} \qquad (3\text{-}2)$$

where

Q = fractional degradation

φ_t = total flux

φ_c = critical flux .

Using equations (3-1) and (3-2) and the information in Tables 3.2 and 3.4, the fractional degradation may be calculated for any mission length and any cover thickness. The resulting fractional degradation suffered in the 30 and 60 day missions using 6 mil cover clips is shown in Table 3.5 for both types of cell.

PARTICLE	FRACTIONAL DEGRADATION			
	30 DAY MISSION		60 DAY MISSION	
	N on P	P on N	N on P	P on N
ELECTRONS	0.0140	0.0511	0.0196	0.0700
PROTONS	0.0092	0.0218	0.0124	0.0304
BOTH	0.0230	0.0718	0.0317	0.0982

TABLE 3.5, FRACTIONAL DEGRADATION WITH 6 MIL COVER SLIPS

It is readily apparent from Table 3.5 that for both mission lengths the N on P cell is superior. By using the N on P cell fewer cells will be needed, but the cost per cell is still 10% more than the P on N. Assuming that assembled arrays weigh one pound per square foot and launch costs are $1000 per pound, the added cost of N on P cells just balances the cost of a slightly larger array with P on N cells so that there is no significant total cost difference between the two. But a smaller array will weigh less and require less volume thus allowing more equipment of other types in the spacecraft. Hence, N on P cells are selected for this mission.

It still remains to be seen whether the 6 mil cover slip is optimum for this mission. The fractional degradation suffered by cells with 8 mil cover slips is shown in Table 3.6.

PARTICLE	FRACTIONAL DEGRADATION	
	30 DAY MISSION	60 DAY MISSION
ELECTRONS	0.0131	0.0183
PROTONS	0.0086	0.0121
BOTH	0.0215	0.0300

TABLE 3.6, FRACTIONAL DEGRADATION, N on P CELLS WITH 8 MIL COVERS

The weight of the complete array (less cover slips) per square foot which makes the 8 mil thickness configuration lighter in weight may be found from

$$(W + 6\rho)\frac{1}{1 - Q_6} > (W + 8\rho)\frac{1}{1 - Q_8} \qquad (3\text{-}3)$$

where

W = weight of complete array less cover slips, lbs/ft^2

ρ = weight of coverslips per square foot per mil thickness

= 0.0138 $lbs/ft^2/mil$

Q = fractional degradation anticipated with the cover slip.

The 8 mil configuration will be lighter in weight if the value of W is greater than 18.3 for the 30 day mission or 16.15 for the 60 day mission. Values of W for solar arrays which have been flown recently are very close to 1.0.[15] Thus the optimum design, weightwise, probably involves using less than 6 mils of protective material; but other considerations require that 6 mils be the minimum.

Thus, the solar cells selected in this study are of the 12 mil thick, 2 x 2 cm, N on P silicon type with six "wrap around" grid lines and 6 mil fused silica cover slips. To allow for radiation degradation, the array must be overdesigned by 2.3% for the 30 day mission and 3.17% for the 60 day mission.

3.3 Module Design

Solar cells equipped with current collector grids and cover slips already assembled into modules are available from the vendors. A module consists of up to 10 closely matched cells which are fully interconnected and is the basic unit mounted on the solar array.

3.3.1 Shingled Modules

Shingled modules of 2 x 2 cells can consist of any number of cells, but usually only three are used as shown in Figure 3.1.

FIGURE 3.1, SHINGLED MODULE OF 2 x 2 cm. CELLS

In the shingled configuration cells are connected negative to positive and so are in series. Disadvantages of this arrangement are that part of the useful cell area is lost in the overlap and if one cell breaks in assembly the entire module must be discarded.

3.3.2 Flat-Mounted Modules

As in the case of the shingled module any number of cells can be used, but the standard figure is ten cells as shown in Figure 3.2.

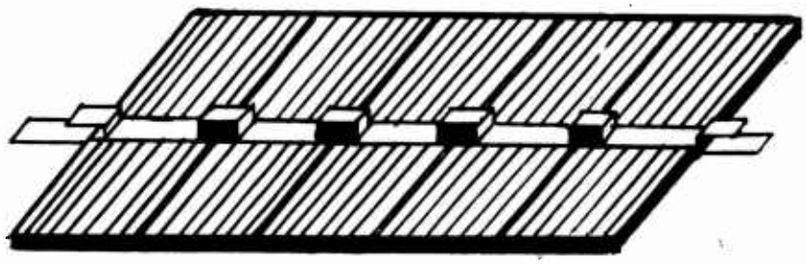

FIGURE 3.2, FLAT MOUNTED MODULE OF 2 x 2 cm. CELLS

Between the two rows of cells are two bus bars, only one of which is shown above. Between each pair of cells there is a stress loop to allow thermal expansion and contraction without damaging the cells.[57, 62] The configuration in Figure 3.2 is for all ten cells in parallel and is the simplest wiring arrangement, though series connections are also possible. This design allows high packing factors, stronger bonding of cells to the substate and simple replacement of broken cells.[16] In addition, the flat-mounted module can be supplied already mounted on 3 to 4 mil thick epoxy filled fiber-glass (printed circuit board) which is excellent for insulating the solar cells from the substrate; modules assembled in this manner are easily mounted on the substrate and reduce handling problems.[16, 57]

3.3.3 Cell Failures and Module Design

Silicon solar cell technology has advanced to the point that the reliability of single cells is very high.[61] However, about 20,000 2 x 2 cm cells are required to give one kilowatt and so some failures must be expected. It has been found through experience that open circuit failures are many times more common than shorts and that reliability can be increased through paralleling within modules.[62]

If one cell in a parallel module fails in the open mode, the current carried by other cells in the module increases slightly while the current through modules in series with the partially failed module decreases

slightly until all currents are equalized. The power loss in a series string of parallel type modules depends on the number of cells per module and the number of failures in the worst module. These power losses are shown in Figure 3.3.[62]

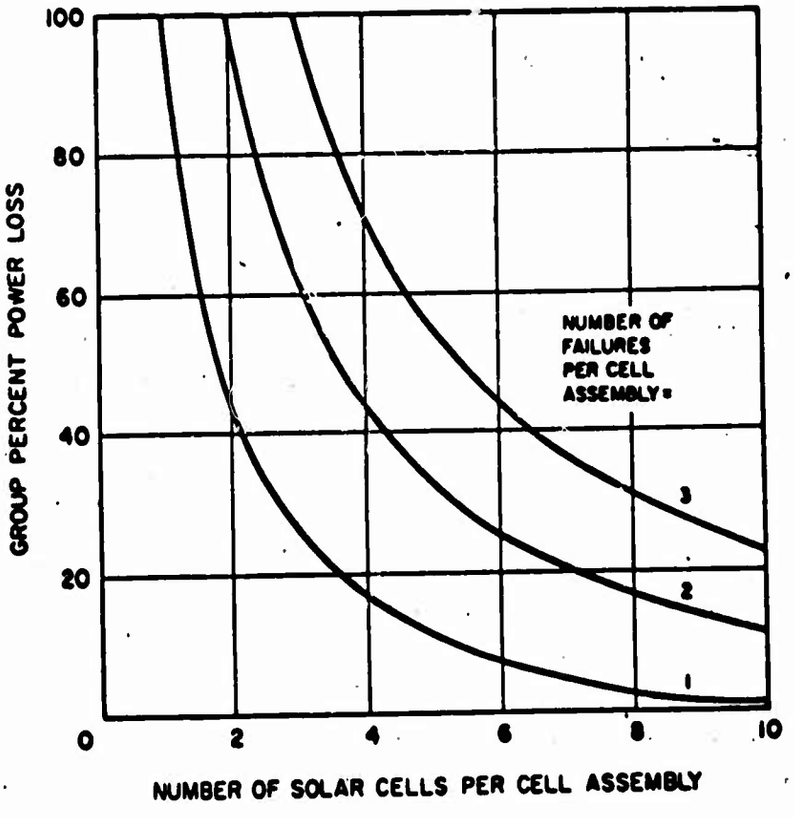

FIGURE 3.3, POWER LOSS IN PARALLEL TYPE MODULES*

For one failure in a module, little improvement can be expected beyond paralleling 10 cells. The two and three failure cases are unlikely for missions of even one year in length and so are very remote possibilities in the case of the relatively short missions considered in this study. A nominal 1% degradation per 30 days due to cell failures will be used here and may be considered quite conservative.

---

*Reproduced from "A Large Area Solar Array," by K. A. Ray and D. H. Winicur, AIAA Paper No. 64-739.

The ten cell, flat-mounted parallel module is readily available; and because of the desireable property of minimizing power losses due to open circuits it will be selected for use in this design. Such modules are available directly from vendors with a minimum efficiency of 11% in AMO sunlight at 25°C. All losses due to cell mismatch, wiring resistance and light attenuation by covers and filters are taken into account in arriving at the 11% figure.[57]

Each module consists of the cells and their accessories plus two bus bars. The bus bars are nominally 70 mils wide and 10 mils thick. Spacing between cells and modules is nominally 33 mils. A complete module is then 4.10 inches by 1.68 inches. The total area covered by a module is 6.89 in^2 which corresponds to 20.9 modules/ft^2 of array.

3.3.4 Spectrally Selective Coatings

As noted in section 3.1.1 the performance of silicon solar cells is very temperature dependent, the efficiency declining by 0.06% for each degree centigrade increase in temperature. The importance of maintaining low equilibrium cell temperatures was recognized at an early stage and spectrally selective coatings for cover slips were developed.

The response region of a silicon solar cell is from about 0.4μ to 1.1μ while the incident solar energy falls in the range of 0.2μ to a little beyond 2μ.[5] The cell coating is then designed to reject as much as possible of the incident energy falling outside the cell response region while absorbing the remainder and providing high emissivity in the infra-red. The absorptivity (or emissivity) of an ideal coating is shown in Figure 3.4.

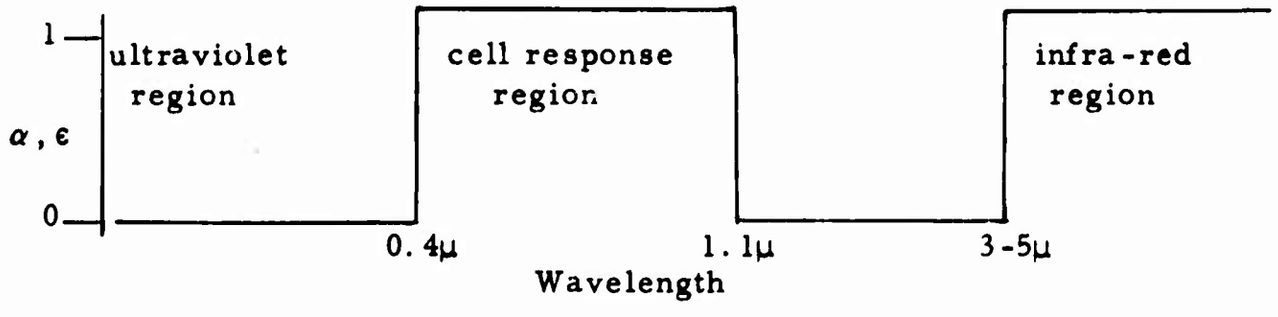

FIGURE 3.4, IDEAL COATING RESPONSE

From the viewpoint of minimizing the cell temperature, the ultraviolet (UV) energy is not very important. However, the adhesive used to bond the cover slips to the solar cells tends to brown under UV radiation and can cause a significant performance degradation unless properly protected by a UV filter.

Idealized filters such as that described above are not available and probably never will be. The coatings presently available do give very satisfactory performance however. A typical value of absorptivity for a coated cover slip and cell is 0.835 (based on all incident solar energy) while the effective emissivity is[16]

$$\epsilon_c = 1.64 \times 10^{-4} T(^{\circ}K) + 0.804. \qquad (3\text{-}4)$$

3.3.5 Equilibrium Temperature Calculation

Assuming that the front and back surfaces of the solar array stabilize at the same temperature,* the panel equilibrium temperature is

$$T = \left(\frac{L}{\sigma}\right)^{1/4} \left[\frac{p\alpha_c + (1-p)\alpha_s - \eta}{p\epsilon_c + (1-p)\epsilon_s + \epsilon_b}\right]^{1/4} \qquad (3\text{-}5)$$

where

L = solar illumination intensity = 0.140 watt/cm^2

σ = Stephan-Boltzmann constant = 5.735×10^{-12} watt/cm^2 - $^{\circ}K^4$

p = fraction of front surface covered by solar cells

α = effective absorptivity

ϵ = effective emissivity

and the subscripts c, s, and b correspond to cells, substrate and back surface of the array respectively. At one astronomical unit from the Sun,

$$\left(\frac{L}{\sigma}\right)^{1/4} = 395^{\circ}K. \qquad (3\text{-}6)$$

---

*A reasonable assumption since thermal paths are short.

If the back surface of the array is pained with black paint,[16] the value of ϵ_b is then

$$\epsilon_b = 3.46 \times 10^{-4} T\ (^{\circ}K) + 0.685. \qquad (3\text{-}7)$$

The exposed area of the substrate is very small since a value of p = 0.90 is readily achieved. The properties of this small area will not greatly affect the equilibrium temperature and may be taken as $\alpha_s = 0.20$ and $\epsilon_s = 0.40$ independently of ten perature.

The value of cell efficiency used in this calculation must be that achieved at the end of the mission when the performance degradation is maximum. This value is used because the array operates at this efficiency throughout the mission, leaving the initial excess power on the array. With an initial efficiency of 11% at 25°C and a temperature degradation factor of 0.06% per degree centigrade, the end-of-mission efficiency is

$$\eta_{em} = (1 - Q_t)\,[11.0 - 0.06\,(T - 298^{\circ}K)]\,\%\,. \qquad (3\text{-}8)$$

Assuming that the radiation and cell failure degradation factors increase linearly between 30 and 60 days,*

$$1 - Q_t = 0.9857 - 2.90 \times 10^{-4} M \qquad (3\text{-}9)$$

where M is the mission length in days. Using equations (3-4) through (3-9) and other information presented above, the equilibrium temperature is 330°K (57°C) for missions anywhere between 30 and 60 days.

3.6 Efficiency and Array Size

Using equations (3-8) and (3-9) and the equilibrium cell temperature of 330°K, the cell efficiency at end of mission is

$$\eta_{em} = 8.950 - 2.63 \times 10^{-3} M\%\,. \qquad (3\text{-}10)$$

*Equation (3-2) is very nearly linear over a range as short as 30 days.

Since the array is only 90% covered with solar cells, the efficiency based on array area ia

$$\eta_a = 8.055 - 2.37 \times 10^{-3} M\% \ . \qquad (3\text{-}11)$$

The average Sun illumination at Earth is 0.140 watts/cm^2 or 130 watts/ft^2. The array area as a function of array output power in watts is then

$$A_a = \frac{P_a}{10.47 - 3.08 \times 10^{-3} M} \ ft^2 . \qquad (3\text{-}12)$$

However, the output of the array should be at voltage of at least 31.5 volts at the maximum power point because the inherent voltage regulation of a solar array is usually no better than ±20%. The load power, P_L, is based on 25 volts minimum voltage. In order to provide the current demanded, the array output power, P_a, should be related to the load power, P_L, by the equation

$$P_a = \frac{V_a}{25} P_L, \ V_a \geq 31.5V \ . \qquad (3\text{-}13)$$

Using equations (3-12) and (3-13) the array area required may be found for any load power.

3.7 Block Configuration

In Figure 3.5, the current voltage characteristics of a new module at 25°C and modules degraded for 30 and 60 day missions at 57°C are shown. Most of the degradation is a result of the temperature increase from 25°C to 57°C and the greatest effect is on the current. Figure 3.5 has been derived from the characteristics of single cells at the indicated conditions. The basic curves for making such determinations are found in Reference 16.

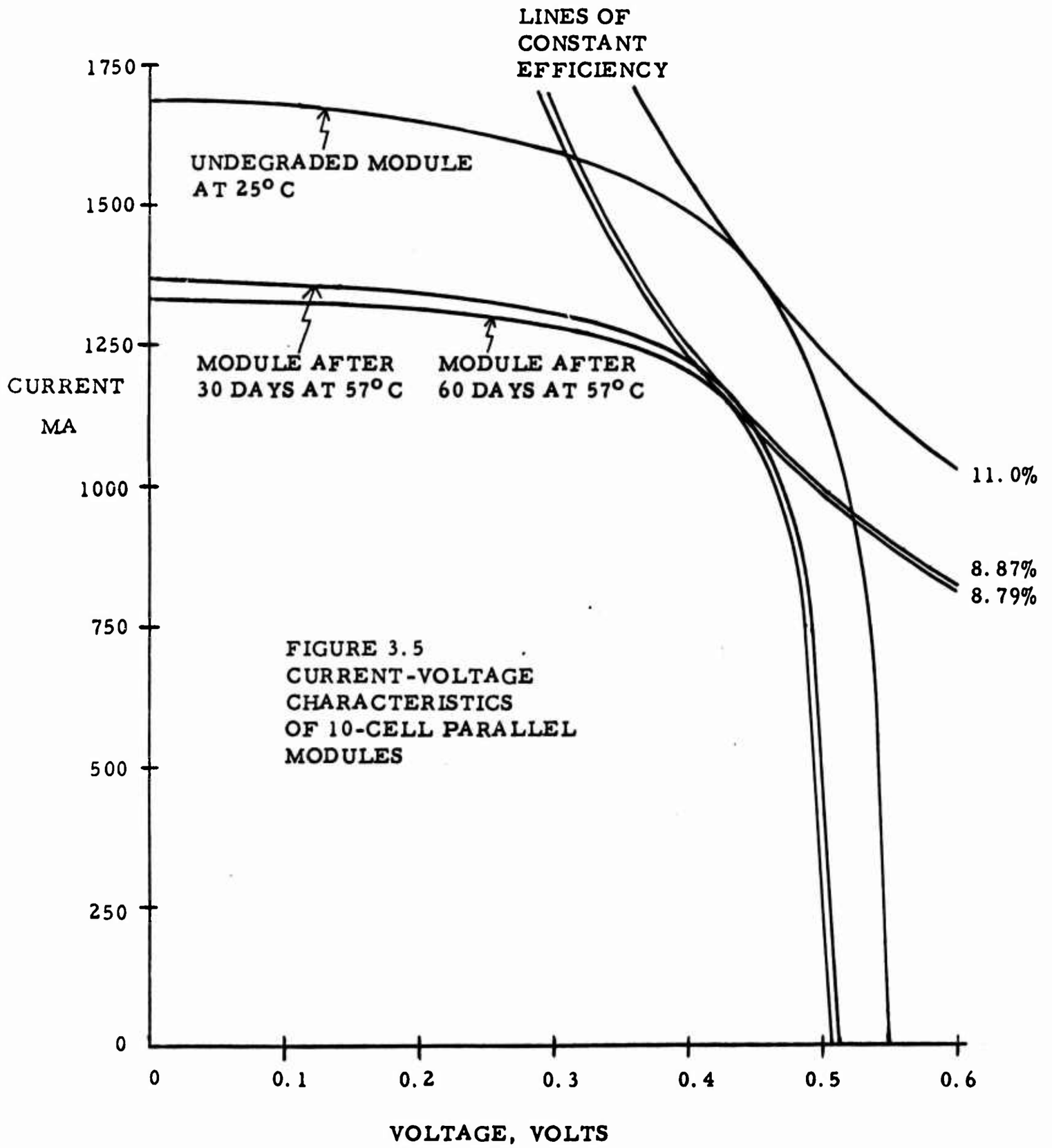

FIGURE 3.5
CURRENT-VOLTAGE CHARACTERISTICS OF 10-CELL PARALLEL MODULES

The maximum power point occurs where the characteristic is tangent to the associated line of constant efficiency. Because of temperature and radiation degradation, the maximum power point voltage is reduced from 0.45 volts to a little more than 0.42 volts. To achieve a minimum of 31.5 volts at the maximum power point, 75 modules in series are required. Henceforth a unit of 75 modules (750 cells) will be called a block and the array will consist of an integral number of these blocks.

3.8 Array Configuration

A wide variety of array configurations have been suggested, but most have serious drawbacks. For instance, circular arrays which are closed and opened like an umbrella or a fan could be used.[8a] Such designs are complex and exhibit poor packing factors; it is doubtful whether 90% cell coverage could be achieved with such designs. Another approach is to use flexible substrates so that a one-piece array can be rolled up for launch and subsequently unrolled in space. Such flexibility can be achieved by use of plastic substrates or many very small rigid sections hinged together. The first approach would probably not have sufficient rigidity to adequately protect the cells during launch while the second involves use of many precision hinges which would be costly and make the array unduly complicated.

In this study, a simple accordion array consisting of a small number of rigid rectangular panels is proposed and will be used. Erection will be by means of a scissors mechanism similar to that used to erect the meteoroid detection panels on the Pegasus spacecraft.

For symmetry, the array consists of two sub-arrays placed on opposite sides of the vehicle. Each sub-array is made up of a number of panels which in turn consist of an integral number of blocks. The panel configuration is constrained by the requirement that both sub-arrays must be stored in the 240 inch equipment and experiment section and should require a minimum of volume for storage. A 6 inch allowance for the

erection mechanism and adequate clearances should be substracted from the 240 inches of useable length in determining the panel size. Panels should also be as near the resulting 234 inch maximum length so as to keep the extended length to a minimum and thus minimize the erection mechanism weight.

In section 3.3.3, the dimensions of individual modules were given as 4.10 inches by 1.68 inches. Using these dimensions and the requirement that a panel consist of an integral number of 75 module blocks, any number of panel sizes may be constructed. Of the possibilities, only three configurations or multiples thereof come close to the 234 inch available space. These are:

9 Blocks	20.5 x 226.8 inches
11 Blocks	25.2 x 225.5 inches
19 Blocks	42.0 x 233.7 inches

The 19 block configuration comes closest to 234 inches. However, storing a rectangular object in a circular space results in a volume penalty which increases with width as shown in Figure 3.6.

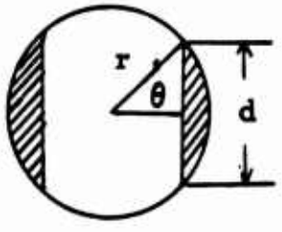

FIGURE 3.6, WASTED AREA

The shaded area is the area wasted by use of panels d feet wide. No other equipment can be stored there as this area must be clear to allow array erection. The volume penalty is the wasted area times 240 inches. From geometrical considerations, the volume penalty is then

$$V_p = 20\,\pi\, r^2 \frac{4\theta}{360^\circ} - dr\cos\theta \text{ ft}^3 \qquad (3\text{-}14)$$

where

$$\theta = \sin^{-1} \frac{d}{2r} . \qquad (3\text{-}15)$$

The value of r is taken to be 4.9 feet to allow space for the vehicle skin and structural stringers. The volume penalty for various panel sizes are shown in Table 3.7.

BLOCKS PER PANEL	d, FEET	VOLUME PENALTY CUBIC FEET
9	1.71	3.6
11	2.10	6.6
18	3.42	28.4
19	3.50	30.2
22	4.20	53.0

TABLE 3.7, VOLUME PENALTY

More than 28 cubic feet is considered to be a significant penalty and so the choice is narrowed to the 9 and 11 block panels. The 9 block panel is slightly longer and so makes better use of available space. Further, the total number of panels used is not likely to be greatly affected by whether 9 or 11 block panels are used. Hence, the 9 block panel will be specified. Its dimensions are 20.5 by 226.8 inches. Using equations (3-12) and (3-13) the output of a panel at the end of 30 days is 268 watts and at the end of 60 days 263 watts. It is not desireable to increase the output in such large steps. Hence, the outboard panel of each sub array may consist of one to nine blocks. With this specification, the system can be tailored to within 30 watts of the power requirement.

3.9 Array Weight

With the array configuration determined, it is now possible to find the weight of the solar cell power system. The weight will be found as a continuous function of array area which can easily be translated into a function of peak power loads by use of equation (3-12). Actually, the array weight increases in increments equal to the weight of a 75 module block. However, it will be shown that the increment is small and the continuous formulation is sufficiently accurate.

A 2 x 2 cm, 12 mil thick solar cell with grids and contacts weighs 0.38 grams.[57] Using the conversion factor 1 gr/cm^2 = 2.05 lbs/ft^2, the weight of solar cells is 0.1950 lbs/ft^2. Since only 90% of the panel is covered with solar cells, the weight is 0.1750 lbs/ft^2 of panel. The fused silica coverslips have a density of 2.65 gr/cm^3 which for 6 mil covers is 0.0829 lbs/ft^2. For 90% coverage, the weight of cover slips is 0.0745 lbs/ft^2 of panel. The epoxy-filled fiber glass on which the modules are mounted is 3 to 4 mils thick and weighs 0.110 lbs/ft^2 of panel. The weight of all adhesives and black paint on the back surface of the panel has been estimated in one study as 1 pound per 90 square feet or 0.0111 lbs/ft of panel.[8] Each module has two bus bars, each nominally 0.010 x 0.070 x 4.10 inches (see section 3.3.3). The total volume of bus bar material per module is 0.00574 in^3/module. With 20.9 modules per square foot and a density of 0.320 lbs/in^3, the weight of copper bus bars is 0.0384 lbs/ft^2 of panel. The support structure consists of an aluminum honeycomb core with aluminum facing sheets braized to it. The weight of a hexcel core is

$$W_c = \frac{144\ Tw\rho}{D}\ \frac{\text{lbs}}{\text{ft}^2} \qquad (3\text{-}16)$$

where

T = thickness of foil used to make core, inches

w = distance between facing sheets, inches

D = distance between parallel sides of a cell, inches

ρ = density of aluminum = 0.10 lbs/in^3.

Typically,[80]

$T = 0.002$ in

$w = 0.750$ in

$D = 0.125$ in

The weight of the core is then 0.1728 lbs/ft^2. The back facing sheet is 30 gage (10 mils) aluminum sheet which weighs 0.1410 lbs/ft^2. The front facing sheet need be only 36 gage (5 mils) aluminum sheet weighing 0.0705 lbs/ft^2 because of the structural properties of the epoxy filled fiber glass. If satisfactory techniques can be found for attaching the fiber glass to the honeycomb core, the thin front facing sheet could be eliminated.

In summary, the weight of all array components is then:

solar cells	0.1750 lbs/ft^2
coverslips	0.0745
fiber glass	0.1100
adhesives and paint	0.0111
bus bars	0.0384
honeycomb core	0.1728
front facing sheet	0.1410
back facing sheet	0.0705
Total	0.7933 lbs/ft^2

The weight of the array is then

$$W_a = 0.7933 A_a \quad . \tag{3-17}$$

The panel thickness is 0.775 inches.

A 75 module block has an area of 3.52 ft^2 and so weighs 2.79 pounds. The assumption that the array weight can be expressed as a continuous function is seen to be justified since a maximum error of 2.79 pounds is small when speaking of arrays weighing several hundred pounds.

3.10 Concentrated Panels

Several panel designs which use reflectors to increase the intensity of solar illumination on the solar cells have been advanced.[62] The obvious

advantage of such schemes is that the number of solar cells required can be reduced. Since the solar cells are the most expensive portion of the array, the cost of an array can be correspondingly reduced.

In spite of this advantage, concentrated arrays suffer from a number of disadvantages. Because the illumination intensity is increased (by perhaps a factor of two or more)[16] the cell operating temperature is increased and so efficiency is reduced. Also the reflectors cannot be 100% efficient at the beginning of the mission and are expected to degrade from micrometeorite erosion and exposure to intense ultraviolet radiation. The net effect is that a concentrated array must have a larger area than the conventional array described in the preceding sections. And since array weights are limited primarily by substrate and support structures of adequate strength to withstand the launch environment, it is difficult to imagine that concentrated arrays would have lower weights per square foot than conventional arrays of the same construction. The requirement for reflectors may very well result in higher array weights. The reflectors will certainly result in thicker arrays; one complete design put the panel thickness at 2.342 inches, 3.02 times the thickness of the conventional panel described in this paper.[8b] For the 60 day mission, this concentrated array would require a storage volume of 30.3 ft^3/kw as opposed to 10.0 ft^3/kw for the conventional array assuming that the power output per square foot is the same in both cases. Because of these weight and volume considerations, the concentrated panel has been dropped from consideration for this mission.

3.11 Array Erection

The erection sequence, using a four panel sub-array for illustration, is shown schematically in Figure 3.7. A small piece of a panel is shown attached to the panel mounts in Figure 3.8.

The rotation shaft is a piece of hollow aluminum tubing which connects the two sub arrays and rotates them for sun orientation. At each end of the rotation shaft is a small telescoping shaft which is used to accomplish

FIGURE 3.7, ARRAY ERECTION SEQUENCE

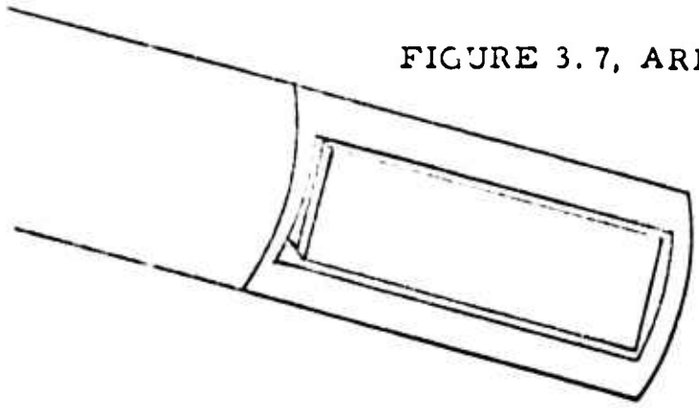

A. PANEL COVER EJECTED AND ARRAY EXPOSED

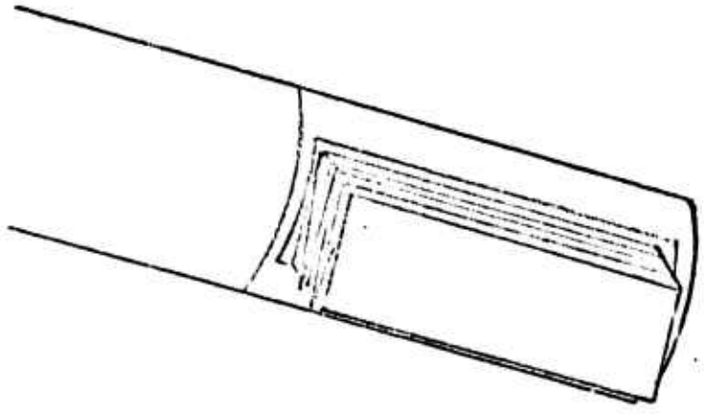

B. ARRAY PUSHED CLEAR OF THE SPACECRAFT

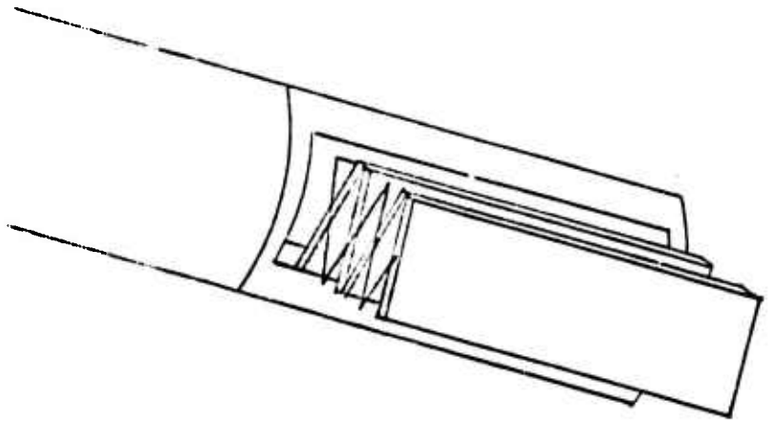

C. ARRAY PARTIALLY UNFOLDED

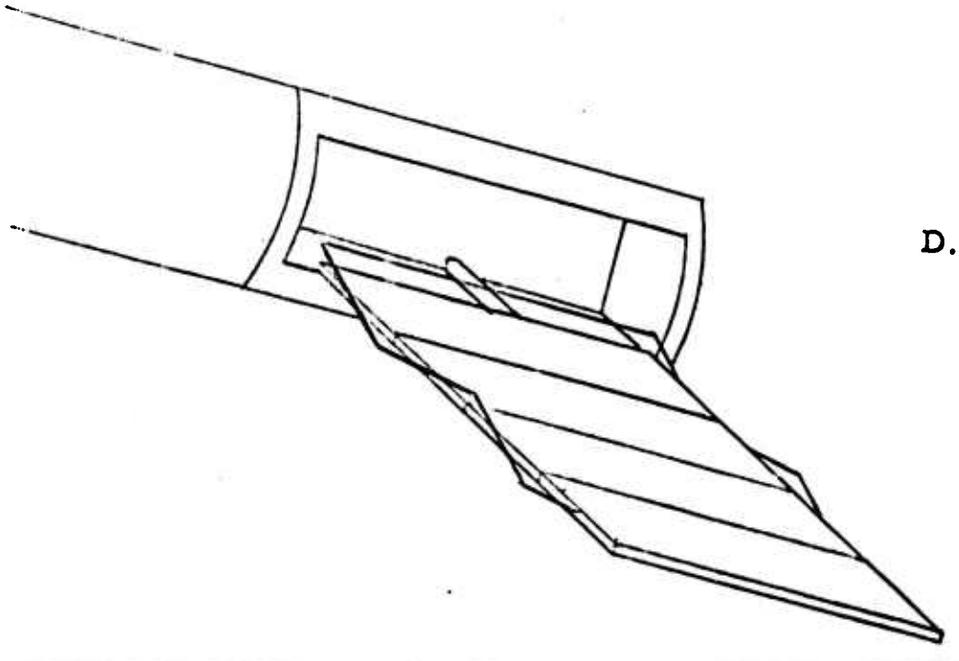

D. ARRAY COMPLETELY ERECTED

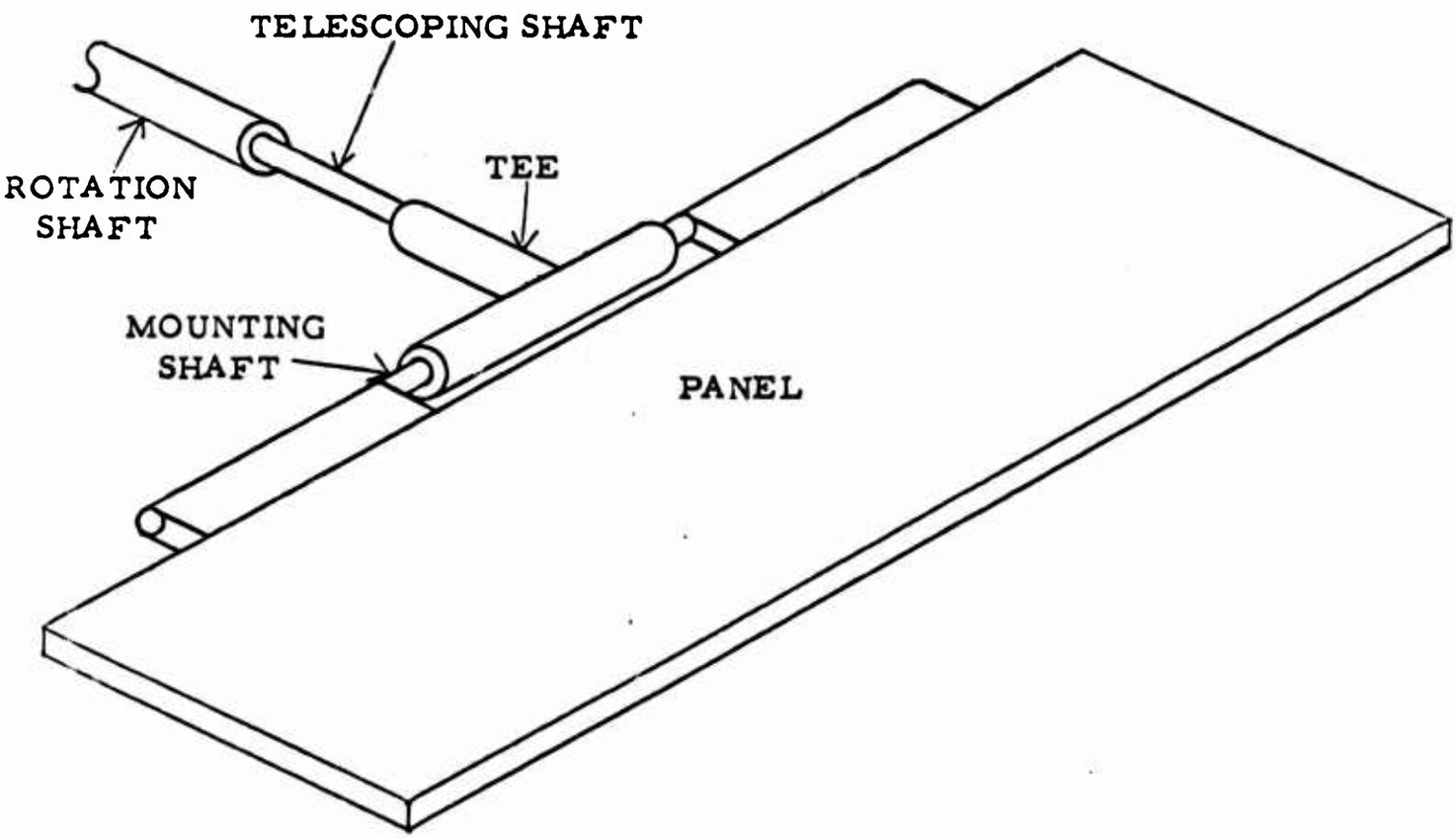

FIGURE 3.8, VIEW OF ARRAY ERECTION MECHANISM

step B in the erection sequence. The space between these two shafts is sealed with an "O" ring which allows extension of the telescoping shafts by use of pressure from a CO_2 cartridge. The telescoping shaft is prevented from rotating, relative to the rotation shaft, by a spline which runs its full length. At the end of the telescoping shaft is a tee joint supporting the hollow mounting shaft which is attached to the panel nearest the vehicle. This shaft rotates within the tee as the panel is extended in step C. as seen in the schematic of step D, the two scissors linkages are connected by a hollow shaft. For erection, this connecting shaft is pulled into place by a simple cable and pulley mechanism which in turn closes the scissors.

3.12 Erection Mechanism Weight

The tee, scissors arms and all shafts are made of aluminum. The dimensions and weight of each part are shown below in Table 3.8.

PART	DIMENSIONS	WEIGHT, POUNDS	NUMBER USED
Rotation Shaft	Length: 72 in ID: 1.75 in, OD: 2.00 in	5.15	1
Telescoping Shaft	Length: 30 in ID: 1.50 in, OD: 1.70 in	1.56	2
Tee	Bar: 9 in, Stem: 5 in ID: 1.70 in, OD: 2.00 in	1.22	2
Mounting Shaft	Length: 33 in ID: 1.50 in, OD: 1.65 in	1.27	2
Connecting Shaft	Length: 228 in ID: 0.4 in, OD: 0.6 in	1.14	2
Scissors Arm	23 x 0.6 x 0.2 in	0.274	2n - 1*

TABLE 3.8, WEIGHT OF ERECTION MECHANISM PARTS

* n = the number of panels in each sub array

The dimensions of these parts are large enough to accomodate sub arrays of up to 20 panels.

In addition to the parts listed in Table 3.8, the following are required:

1. 2 pieces of cable, each 8 feet long and consisting of 4 strands of No. 10 A.W.G. aluminum wire. Total weight: 0.61 pounds.
2. 4 aluminum pulleys each 1½ inches in diameter and ⅛ inch thick. Total weight: 0.35 pounds.
3. A small windlass and supports. Total weight: 0.500 pounds.
4. 2 servo motors with independent drive trains to drive the windlass. Total weight: 4.50 pounds.[8c]

Only one servo motor is required to erect the array but two are provided so that there will be a backup.

The total weight of the erection mechanism is then

$$W_{em} = 21.2 + 0.550n \text{ pounds} \qquad (3\text{-}18)$$

where

n = the number of panels in each sub array.

3.13 Array Orientation

The array has only a single degree of freedom, motion about the rotation shaft. The other degree of freedom required for orientation is achieved by rotating the entire spacecraft about the yaw axis which is parallel to the local vertical. Both of these motions are at the orbit rate.

If the array was continuously rotated in the same direction throughout the mission, electrical connections would have to be through slip rings. However, during the shadow period the array can be turned back through the angle it traversed in the preceding sunlight period and the motion can thus be constrained to the limits of $\pm 130^{\circ}$. By specifying this retrograde rotation requirement, the electrical connections between the spacecraft and the array can be made using continuous wires rather than unreliable slip rings.

To orient the array, sun sensors and control circuitry are required to command a servo motor which turns the rotation shaft through a reduction

gear box. The total weight of sensors, motor, drive train, and circuitry has been estimated in one study as 16 pounds.[8d] The weight penalty and effects of requiring the entire spacecraft to rotate about the yaw axis at a controlled rate are discussed in parts 5 and 7 of this study which deal with integration of a solar array with battery and fuel cell systems.

3.14 Drag Penalty

At 250 NM the atmosphere is still present though in a very thin condition. As a result, short term drag effects are negligible; but over the space of several weeks the integrated drag effect can be significant. A particularly useful and lucid analysis of orbital drag effects appears in NASA TN D-1995 and is the basis of the particular analysis used here.[44]

The spacecraft itself is continuously Earth oriented which means that it always presents the maximum possible area perpendicular to the air stream. The frontal area of the MOL is 41 x 10 = 410 ft^2. The frontal area of the Gemini capsule is about 45 ft^2 for a total of 455 ft^2. The weight of the entire spacecraft will be taken as 25,000 pounds. The solar array used for this example will have an area of 1250 ft^2, which corresponds to about 10 kw. This array is larger than any that are required for the given loads, even including capacity to recharge a battery. When the sun lies in the orbital plane, the array is perpendicular to that plane and so presents the largest drag area. However, the array is oriented to the sun so that its full area is perpendicular to the air stream at only two points in the orbit. The average drag area is then $2A_a / \pi$ where A_a is the array area.

To use the above cited reference for analysis, the weight and areas should be in the metric system. The weight of the entire spacecraft is then 11,350 kg and the average drag area approximately 116 $meters^2$. A drag coefficient of 2.75 is recommended for cylinders and flat plates. The ratio $W / C_D A$ is then 34.5. For a 250 nm (464 km) orbit and this ratio, the corresponding lifetime (time to re-entry) is found to be 131 days from a graph in reference 44. Because of the combined effects of nodal regression, loss

from the dirunal bulge, and the expected peak in the atmospheric density in 1968, this figure should be reduced by about 20%[44] The lifetime is then 105 days. Using the same procedure in reverse, the altitude of the circular orbit after 60 days is then about 395 km or about 213 nm.

Thus, for the worst possible case, the spacecraft has 45 days of life remaining at the end of a 60 day mission and its orbit has decayed approximately 37 nm. The first five MOL vehicles will not be equipped for rendezvous and so this orbit decay should be acceptable. Use of a propulsion system for orbit maintenance therefore is not indicated. Hence, there is no weight penalty chargeable to the solar array as a result of drag effects at least for the initial phases of the MOL program.

3.15 Solar System Storage Volume

Figure 3.9 shows a schematic cross section of the MOL with one sub array stored.

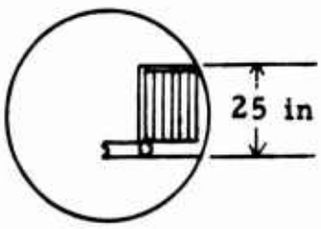

FIGURE 3.9, VIEW OF STORED ARRAY

Each panel is 0.775 inches thick and the space between folded panels 0.10 inches. The storage cavity is 25 x 240 inches. The wasted volume is found from Table 3.7 as 6.6 ft^3. The volume of motors, gear trains, windlass, and control circuits is estimated as 2 ft^3. The solar system volume is then

$$V_{ss} = 8.6 + 6.08n \text{ ft}^3 \qquad (3\text{-}19)$$

where n = the number of panels in each sub array.

3.16 Structural Alterations

To erect the array, two exterior panels must be ejected. These panels may be of the same construction as the rest of the outer hull and so can support structural loads during launch. The only penalty for this alteration is use of explosive rather than ordinary rivets. However, once the array is erected, other equipment inside the vehicle should not be exposed to the space environment and so a thin structural shell conforming to the array storage cavity is used. For this purpose, a single sheet of 24 gage (20 mils) aluminum weighing 0.2834 lbs/ft^2 is adequate. The sheet is bent in a U shape to conform to the storage cavity. The weight of two such sheets as a function of the number of panels per sub array is

$$W_s = 27.4 + 0.825\,n \text{ pounds} \qquad (3\text{-}20)$$

3.17 Solar System Summary

The basic unit of the array is a module of 10 parallel connected N on P type silicon solar cells. The cells in the module are nominally 12 mils thick, have 6 line current collector grids, and are covered with 6 mils of fused silica which offers protection against radiation damage and serves as a mounting surface for spectrally selective coatings. The modules are mounted on epoxy filled fiber glass which also insulates the cells from the panel structure.

Seventy-five such modules are series connected to make a block. Each panel consists of nine blocks and n panels are in each sub-array. The entire system consists of two sub-arrays.

The two sub-arrays are internally stored for launch and are erected by use of a scissors mechanism similar to that employed with the Pegasus spacecraft. Orientation is accomplished by rotating the array and the vehicle at the orbit rate. During shadow time, the array rotation is reversed so that all electrical connections can be made by continuous wiring.

The area of each 9 block panel, A_p, is 32.3 ft^2. Since there are n panels per sub-array, the value of n may be found from

$$n = \frac{A_a}{2A_p} = \frac{A_a}{64.6} \quad . \tag{3-21}$$

From equations (3-19) and (3-21), the solar system volume as a function of array area is

$$V_{ss} = 8.60 + 0.094\, A_a \ ft^3. \tag{3-22}$$

Combining equations (3-17), (3-18), and (3-20) and adding 16 pounds for the weight of the orientation mechanism, the system weight is found to be

$$W_{ss} = 64.6 + 0.8146 A_a \text{ pounds}. \tag{3-23}$$

Finally, the array area to be used in equations (3-22) and (3-23) is found from equations (3-12) and (3-13) as

$$A_a = \frac{P_L}{8.309 - 2.44 \times 10^{-3} M} \ ft^2 \tag{3-24}$$

where

P_L = the power required at 25 volts, watts

M = mission duration, days .

Thus, the system weight and volume for a 30 day mission are

$$V_{ss} = 8.60 + 0.0114\, P_L \ ft^3 \quad \text{and} \tag{3-25}$$

$$W_{ss} = 64.6 + 0.0981\, P_L \text{ pounds}. \tag{3-26}$$

For a 60 day mission

$$V_{ss} = 8.60 + 0.0115\, P_L \ ft^3 \quad \text{and} \tag{3-27}$$

$$W_{ss} = 64.6 + 0.0998\, P_L \text{ pounds}. \tag{3-28}$$

In both cases, the maximum power point voltage is 31.5 volts.

4. SECONDARY BATTERIES

4.1 Introduction

Any planetary satellite is periodically eclipsed from the sun. For many types of power systems, this event is of little consequence. But for those which rely on the sun as the source of energy, the primary electrical power system is useless during the shadow period. To maintain the spacecraft functions, a secondary system which can operate in the dark is required. In the case of solar cells, rechargeable batteries have been used as the secondary system exclusively. Other sources, such as regenerative fuel cells, have been proposed but none other than batteries have actually flown.

4.2 Available Battery Types

There are many couples which may be used for secondary batteries but only three have been developed for space use. These are nickel-cadmium, silver-cadmium, and silver-zinc. Of the three, the silver-zinc couple has the highest energy density (watt-hours per pound). Unfortunately, the silver-zinc system is also the least reliable of the three. The charge-discharge cycle life of silver-zinc batteries is only about 3% of that achieved with the other two types under comparable conditions.[78] Both the nickel-cadmium and silver-cadmium batteries have been used in space and may be considered as reliable, off-the-shelf items.

4.3 General Battery Characteristics

While the nickel-cadmium and silver-cadmium couples differ in many respects, there are some characteristics which the two have in common. The similarities of these two battery types are considered below.

4.3.1 Cell Construction and Overcharge Characteristics

Internally, both cells consist of a cadmium anode, a cathode of the other metal making up the couple, nylon felt separators, and a KOH

electrolyte. Externally, the case is stainless steel and forms one of electrical contacts. The other contact comes through the case and is insulated by a ceramic to metal seal which also insures that the cell retains its electrolyte in the hard vacuum of space.

If cells were made with anodes and cathodes of equal capacity, H_2 and O_2 would be generated at the respective plates as the cell neared full charge. Besides being a dangerous (explosive) mixture, the gases build up pressure rapidly and may cause a catastrophic failure. Consequently, in cells designed for use in space, the anode is made with a capacity sufficiently in excess of that of the cathode so it does not fully charge and generate H_2. Of course the cathode still generates O_2 near the end of charge and on overcharge. However, the O_2 is electrochemically reduced at the anode at a rate proportional to its partial pressure. The rate of generation is proportional to the charge current. Thus by limiting the charge current after the onset of gas generation, any desired maximum cell pressure can be maintained.[54] To keep the weight of cell cases reasonable, a maximum equilibrium pressure of 50 psia is usually specified.[67] This pressure then corresponds to a unique maximum overcharge current, for a given temperature. The allowable overcharge current increases with temperature because the rate of O_2 reduction is increased.

4.3.2 Charge Control

After about 100% of the energy withdrawn in the previous discharge has been returned to the battery, the internal pressure rises as described above. However, the charging process is not 100% efficient as heat is generated, and at later stages O_2. As a result it is necessary to overcharge the battery.

To keep the pressure limited while overcharging there are two principal methods available. One is through limiting the current as described above. The signal for reducing charge current to the safe overcharge level may be provided by the rather sharp increase in voltage

across the battery terminals which occurs as full charge is neared. This method has been widely used and has proven to be very satisfactory.

A second technique for limiting the internal pressure is to accelerate O_2 reabsorption. Cells with so called "auxiliary electrodes" which promote reduction of O_2 have been recently developed.[10,11,63] The auxiliary electrode is simply a fuel cell electrode placed inside the cell and externally connected to the cadmium anode through a suitable resistance. With such an arrangement, O_2 is reduced through the following reactions:[63]

$$O_2 + 2H_2O + 4e^- \longrightarrow 4OH^- \quad \text{(auxiliary electrode)} \qquad (4\text{-}1)$$

$$2Cd + 4OH^- \longrightarrow 2Cd(OH)_2 + 4e^- \quad \text{(anode)} \qquad (4\text{-}2)$$

The rate of O_2 reduction is limited only by the area of the auxiliary electrode. The energy passing through the external circuit may be used in lieu of voltage sensing as the signal for current reduction. However, this device is much more interesting as a means of reducing pressure and allowing higher overcharge currents.

A battery equipped with auxiliary electrodes would require much less time for overcharge and so allow a longer period of high rate charging. Since the time available for high rate charging is increased, the current required, and consequently the solar panel area to charge the battery may be decreased. Unfortunately, a high acceptable overcharge rate requires a very large auxiliary electrode which increases both the volume and weight of the cell. Severe mechanical problems have been encountered in designing such cells which will allow overcharge rates in excess of C/5. A C/10 rate can be achieved with a small increase in the cell volume and weight.[63] Since ordinary nickel-cadmium batteries can accept the C/10 overcharge rate at 25°C, the auxiliary electrode does not offer any substantial advantage in this case. However, ordinary silver-cadmium batteries can be overcharged at only the C/200 rate at 25°C.[66] Thus, the allowable overcharge rate can be increased by a factor of 20, an almost revolutionary improvement. There

appears to be no reason to expect that use of auxiliary electrodes will have any detrimental effect on cell life.

4.3.3 Cycle Life

Many figures on cycle life appear in the literature and must be treated with caution. Such data is the result of cycling a small sample of cells to failure. Some researchers report only the longest lived cell of a sample while others report the cycle number at which some percentage of the sample has failed. Since test programs which used large enough samples to establish interesting statistical confidence levels have not appeared in the literature, the results of any one test program should be viewed cautiously. However, there are a number of factors which mitigate against the low confidence level which can be ascribed to a single small sample test program. First, many such test programs have been run and the results obtained show a high degree of consistency. Second, battery systems designed for reliability on the basis of life cycle figures have had a remarkable degree of success. Third, under conditions expected in close earth orbits and at low discharge depths, cell life exceeds 10,000 cycles. If the cycling program is designed to simulate a 90 minute orbit, 625 days are required to demonstrate 10,000 cycles. Thus most available data based on actual tests are for cells that are several years old and so are not reflective of the current state of the art. The cycle life data used in this study will be a compilation of reported results from sources which are considered to be the most reliable.

4.3.4 Factors Affecting Cycle Life

It has been conclusively determined that the operating temperature, the depth of discharge and the orbit which the cycling program is intended to simulate are the significant parameters which affect cycle life.[42] Cell size has not been reported as having a distinguishable influence.

In a comprehensive testing program on nickel-cadmium cells and batteries, it was found that cycle life goes through a broad maximum in the

vicinity of 25°C, regardless of discharge depth. It was also found that battery life increases exponentially for decreasing discharge depth.[42] The data on silver-cadmium cells point to the same conclusion.[78]

A few years ago silver-cadmium cells had cycle life characteristics much inferior to those of nickel-cadmium. Recent developments in silver-cadmium technology have been impressive and it can now be said that for any given set of conditions the cycle lives of the two systems are equal, for use in close earth orbits.[42, 78] Drawing on information from many sources, a conservative estimate of the cycle life capabilities for the two battery types is given in Figure 4.1 as a function of discharge depth. The data are for a temperature of 25°C and failure of one half the sample. Since experience at discharge depths of 50% or more is extremely limited, no cycle life data are given for deeper discharges and the maximum allowable discharge depth will be specified as 50% for purposes of this study.

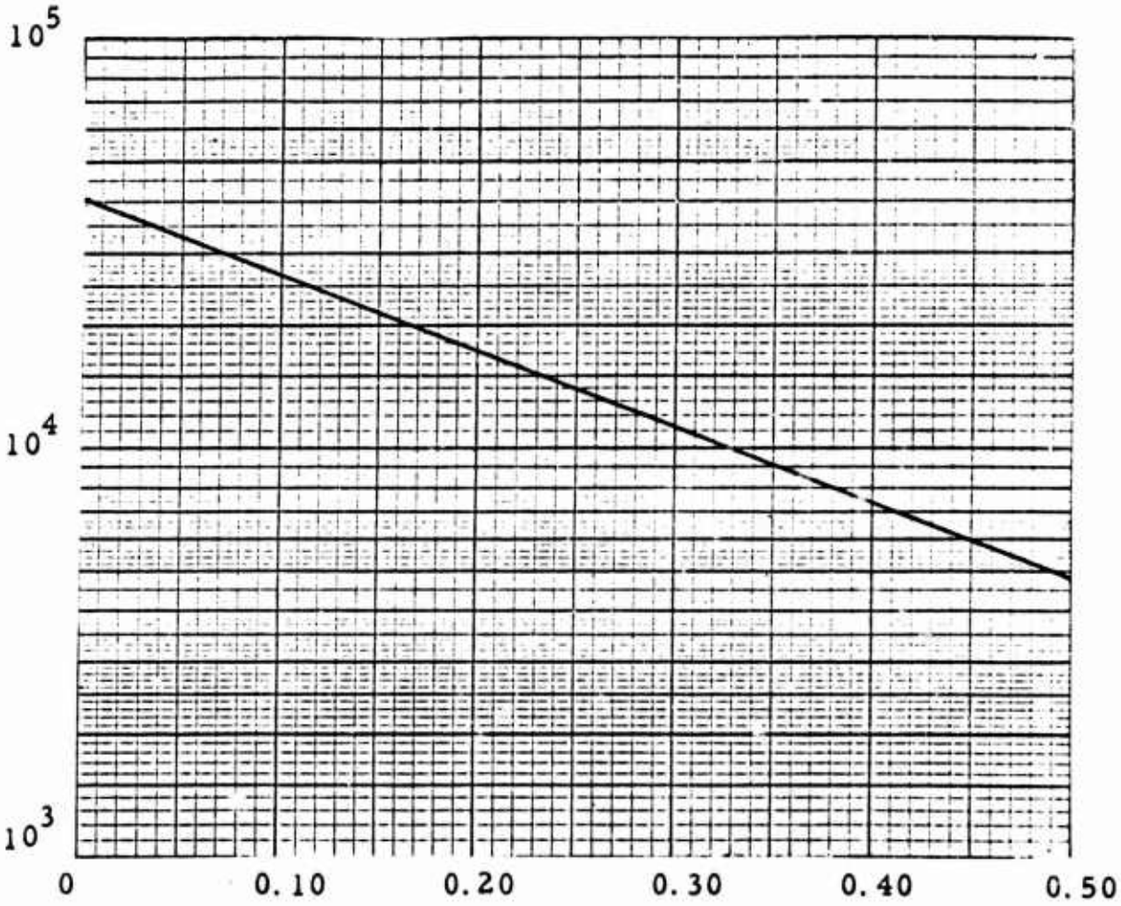

FIGURE 4.1, SINGLE CELL CYCLE LIFE AS A FUNCTION OF DISCHARGE DEPTH

4.4 Battery Reliability

Using cycle life figures based on failure of one-half the sample, it is possible to determine a mean time to failure (MTF) for a given set of conditions by assuming some failure distribution. The more or less standard exponential distribution will be used here. For a constant failure rate the reliability of an individual cell may be expressed as

$$R_c = e^{-(\frac{t}{\theta})} \tag{4-3}$$

where

R_c = reliability of a single cell

t = required service life, cycles

θ = MTF, cycles

By letting t equal the demonstrated cycle life and R_c equal 0.50, a MTF can be determined for any discharge depth from the data in Figure 4.1 as 1.443 times the cycle life.

The potential of a single cell is only about one volt and so a number of cells must be connected in series to supply the load voltage. Fortunately, design for reliability requires series redundancy. It has been found that the most important mode of cell failure is the internal short circuit. About the only way a cell can fail and create an open circuit is through leakage of all its electrolyte. However, seals are very well developed and a short period of testing will reveal any "leakers." Three years ago Bell Telephone Laboratories tested a group of cells which had been rejected for leaks and found that these cells operated satisfactorily for up to nine months.[85] As a result open circuit cell failures can be largely neglected.

The number of cells in a series string equals the number required to give 25 volts at the end of discharge plus as many as three redundant cells. The number of extra cells per string usually does not exceed three because with the high reliability of individual cells, two or three redundant

cells are usually adequate to achieve probabilities of 0.95 or more that a string will deliver at least 25 volts for the entire mission. Also, use of redundant cells results in high string voltages at the beginning of the mission and consequently high thermal loads on the voltage regulators.

The reliability of a string of n cells, three of which are redundant is

$$R_s = \binom{n}{0}R_c^n + \binom{n}{1}R_c^{n-1}(1-R_c) + \binom{n}{2}R_c^{n-2}(1-R_c)^2 + \binom{n}{3}R_c^{n-3}(1-R_c)^3 \qquad (4-4)$$

where $\binom{n}{k}$ is the binomial coefficient which is expressed as

$$\binom{n}{k} = \frac{n(n-1)(n-2)\ \ldots\ (n-k+1)}{k(k-1)(k-2)\ \ldots\ 3\cdot 2\cdot 1}\ ,\ \binom{n}{0} = 1\ . \qquad (4-5)$$

The entire battery package is never designed as a single string. Even in unmanned satellites the practice has been to use at least two or three fully independent strings. One reason for being so conservative is that a total failure can originate at points in the system other than in the cells themselves. For instance, if the charge control circuit fails to reduce the current at the onset of gas evolution, one or more cells in the affected string will burst leaving an open circuit. Hence, more than one string is provided and each string is completely independent of the others.

Providing redundant parallel strings in the battery package has a double effect. Of course the primary effect is that of maintaining the required capacity even if some number of strings should fail. A secondary effect is a reduction of the required service life of individual cells. For instance, if the battery package has 2 strings, either of which can satisfy all loads, the strings can be used alternately so that the required service life of each cell is only half the mission length and the cell reliability found from equation (4-3) is accordingly improved.

Virtually any number of strings in parallel may be used in the battery package. However, there are advantages to keeping the number

small. First, as the number of strings increases, the battery package becomes more complex. Second, if the design is such that a large number of strings in parallel is required to satisfy the electrical demands, the cell size will be small. If cell capacity in nickel-cadmium batteries goes below about 40 ampere-hours, the energy density (ampere hours per pound) decreases significantly and so results in a heavier system for the given required capacity.[66]

The reliability of a battery package which consists of q strings, r of which are redundant is

$$R_p = \binom{q}{0} R_s^q + \binom{q}{1} R_s^{q-1}(1-R_s) + \cdots + \binom{q}{r} R_s^{q-r}(1-R_s)^r \qquad (4\text{-}6)$$

where $\binom{q}{k}$ is found from equation (4-5), R_s is found from equation (4-4), and R_c is found from equation (4-3) by letting

$$t = \frac{q-r}{q} T, \qquad (4\text{-}7)$$

T being the number of orbits in the entire mission.

The battery package will be designed for mission success reliability of 0.995 and a crew safety reliability of 0.9999 as specified in section 1.4.

4.5 Orbital Period and Charge-Discharge Cycles

In order to determine the reliability of the battery package, it is necessary to know how many charge-discharge cycles are experienced. Each cycle coincides with one orbital revolution. The period of a circular orbit may be expressed as

$$P = 2\pi\sqrt{\frac{R_{cs}^3}{K}} \qquad (4\text{-}8)$$

where

K = gravitational constant

R_{cs} = orbit radius.

In section 1.1 the orbital altitude was given as 250 NM, a radius of 3695 NM. The corresponding orbital period is then 93.5 minutes. Thus, there are 15.38 orbits per day and a 30 day mission consists of 462 orbits, a 60 day mission 923 orbits.

The electrical power system must be designed to meet the worst set of conditions which will occur in the mission. In the case of secondary batteries, the worst condition is when the shadow time (discharge period) is a maximum and the light time (charge period) is a minimum. This condition occurs when the sun lies in the orbit plane.

The ratio of maximum shadow time to orbital period for a circular orbit is[82]

$$\left(\frac{T_s}{P}\right)_{max} = \frac{\sin^{-1} R_e / R_{cs}}{\pi} \qquad (4\text{-}9)$$

where R_e is the radius of the earth. For a 250 NM orbit,

$$\left(\frac{T_s}{P}\right)_{max} = 0.382 .$$

This figure corresponds to a shadow time of 35.6 minutes and a light time of 57.7 minutes.

When the vehicle emerges from the earth's shadow, the solar array is cold and misoriented so that batteries must continue to supply power for a few minutes of daylight. For purposes of this analysis, the time for sun acquisition and array warm up will be taken as 2.2 minutes. An additional one minute is allowed for other contingencies. Thus, in the worst case, the battery will discharge for 39 minutes and be charged for 54.5 minutes.

4.6 Battery Loads

Since the battery capacity and the size of the solar array needed for charging are directly determined by the magnitude of the shadow time loads, it is desirable to keep these loads to a minimum. Hence, all experiments

and telemetry are locked out during the shadow time. Additionally, periodic and transient life support loads are programmed to occur during the illuminated portion of the orbit. Thus, the battery loads consist of only:

1. Life support — 1 to 2.5 KW continuous
2. Voice — 20 W continuous
3. Biomedical monitors — 25 W continuous

At the minimum bus bar voltage of 25 volts, these power requirements correspond to total current requirements of 41.8 to 101.8 amperes.

4.7 Battery Sizing

The nominal capacity of a battery, C, is conventionally expressed in ampere-hours since the nominal watt-hour capacity depends on the end of discharge voltage which declines with increasing depth of discharge. Use of the ampere-hour capacity avoids any such variations which cloud the analysis.

The total energy which the battery must deliver in the worst orbit is the product of the shadow load current, I_s, and the maximum shadow time, T_s minutes. The discharge efficiency of a battery, η_d, is less than 100% so that the energy removed from the battery is greater than that actually used by the load. Also, in section 4.2.3 it was pointed out that the discharge depth, D, has a significant effect on cycle life and should be limited to achieve high reliability. Thus, taking into account the effects of discharge efficiency and discharge depth, the required battery capacity is

$$C = \frac{I_s}{\eta_d D} \frac{T_s}{60} \text{ amp-hrs.} \qquad (4\text{-}10)$$

Since the battery package is designed with q parallel strings, r of which are redundant, equation (4-10) gives the required capacity of q - r strings combined.

4.8 General Battery Weight Analysis

For a portion of the charge period the battery is charged at a high rate until the internal cell pressure rises. At this point, the charge current is reduced to the maximum allowable overcharge rate. At the overcharge rate, a certain fraction of the energy removed during the previous discharge must be put back into the battery to insure a full charge. Thus, as the discharge depth increases, the total ampere hour overcharge increases while the overcharge rate remains constant. As a result, the overcharge time increases and the time for high rate charging decreases thus requiring a higher charge rate and a larger solar panel. To obtain the minimum weight secondary battery system, the discharge depth must then be optimized so as to obtain the lowest total weight of batteries and solar panel necessary for recharging. The optimization analysis is given below.

4.8.1 Battery and Panel Optimization

The weight of the cells and their cases is

$$W_b = \frac{q}{q-r} CV_b w_b \text{ pounds} \qquad (4\text{-}11)$$

where

q = the total number of strings in the battery

r = the number of redundant strings

C = capacity of $q-r$ strings as given by equation (4-10)

w_b = battery specific weight, lbs/watt-hour

V_b = end of discharge voltage of a string of n cells.

The weight of the solar panel required to charge the battery is

$$W_p = I_{ch} V_p w_p \text{ pounds} \qquad (4\text{-}12)$$

where

I_{ch} = the high charge rate, amperes

V_p = solar panel voltage at maximum power point, volts

w_p = solar panel specific weight, lbs/watt.

The high charge rate is

$$I_{ch} = \frac{DC}{\eta_{ch}} \frac{60}{T_{ch}} \text{ amps} \tag{4-13}$$

where

D = discharge depth

T_{ch} = available time for high rate charging, minutes

η_{ch} = efficiency of the battery charger.

The available time for high rate charging is

$$T_{ch} = 54.5 - T_{och} \text{ minutes} \tag{4-14}$$

where

54.5 minutes is the total available charge time found in section 4.5

and T_{och} = time required for overcharging.

The time required for overcharging is

$$T_{och} = \frac{60 \epsilon DC}{I_{och}} \text{ minutes} \tag{4-15}$$

where

ϵ = required overcharge as a fraction of the capacity used in the previous discharge,

I_{och} = maximum allowable overcharge rate, or

I_{och} = C/ number of hours to fully charge at this rate.

Combining equations (4-12) through (4-15), the solar array weight is

$$W_p = \frac{60DC}{54.5 - \frac{60 \epsilon CD}{I_{och}}} \frac{1}{\eta_{ch}} V_p w_p . \tag{4-16}$$

Combining equations (4-10), (4-11), and (4-16), the total weight of batteries and associated solar array is

$$W_{tot} = \frac{I_s T_s}{60 \eta_d} \left[\frac{q}{q-r} \frac{V_b w_b}{D} + \frac{60}{54.5 - \frac{60 \epsilon CD}{I_{och}}} \frac{V_p w_p}{\eta_{ch}} \right] . \tag{4-17}$$

Differentiating W_{tot} with respect to D and setting the result equal to zero gives the discharge depth at which the system weight is minimized. Thus,

$$\frac{dW_{tot}}{dD} = \frac{I_s T_s}{60 \eta_d} \left[- \frac{q}{q-r} \frac{V_b w_b}{D^2} + \frac{3600 \frac{\epsilon C}{I_{och}}}{(54.5 - \frac{60 \epsilon CD}{I_{och}})^2} \frac{V_p w_p}{\eta_{ch}} \right] . \qquad (4\text{-}18)$$

Equating to zero and rearranging, the optimum discharge depth is

$$D_{opt} = \frac{54.5}{60 \left[\frac{\epsilon C}{I_{och}} + \sqrt{\frac{q-r}{q} \frac{\epsilon C}{I_{och}} \frac{1}{\eta_{ch}} \frac{V_p w_p}{V_b w_b}} \right]} . \qquad (4\text{-}19)$$

The capacity, C, need not be known to solve equation (4-19) since I_{och} is expressed as a fraction of capacity and C is eliminated when values for I_{och} are substituted. Actually, V_b is a very weak function of D. But, the maximum error in D_{opt} due to V_b is less than 1%, and this error can be reduced to zero by iteration.

Thus, the only remaining variables in equation (4-19) are q and r which are varied in order to achieve the system reliability goal. By assuming values for q and r, a value of D_{opt} is determined. Knowing D_{opt} and T_s the discharge rate as a function of capacity is

$$I_d = \frac{60}{T_s} CD_{opt} \text{ amps} . \qquad (4\text{-}20)$$

It is necessary to know the discharge rate as it influences the current-voltage characteristic of the battery.[66,67] Knowing I_d and D, the end of discharge voltage can be determined and in turn the number of series cells per string and number of redundant cells can be found. Then using equations (4-3) through (4-7) the reliability of the battery package can be determined and compared with the specified design goal. Convergence is rapid and only a few iterations of q and r are recessary.

After q, r, and D_{opt} are determined, I_{ch} can be found from equation (4-13) which in turn determines the current-voltage charge characteristics. The ratio of the end of discharge voltage, V_b, and the maximum charge voltage, V_c, is the discharge efficiency. Thus,

$$\eta_d = \frac{V_b}{V_c} . \tag{4-21}$$

Using equations (4-10) and (4-11), the battery weight may be found as

$$W_b = \frac{q}{q-r} \frac{V_b w_b}{\eta_d D_{opt}} \frac{T_s}{60} I_s . \tag{4-22}$$

The shadow time load in watts is

$$P_s = I_s \ (25 \text{ volts}) . \tag{4-23}$$

Thus, W_b may be alternately expressed as

$$W_b = \frac{q}{q-r} \frac{V_b w_b}{\eta_d D_{opt}} \frac{T_s}{60} \frac{P_s}{25} . \tag{4-24}$$

The weight of the panel required to recharge the battery is given by equation (4-16). Substituting equations (4-10) and (4-23) into (4-16), the panel weight may be alternately expressed as

$$W_p = \frac{T_s}{54.5 - \frac{60 \epsilon C}{I_{och}} D_{opt}} \frac{V_p w_p}{\eta_{ch} \eta_d} \frac{P_s}{25} . \tag{4-25}$$

4.8.2 Battery Charger and Control Circuits

The weights of the battery charger and the control circuits are only weakly dependent on the discharge depth and are very small in comparison to the weights of the batteries and solar panels. As a result, their weights were not included in the preceding analysis since the analytical relationship

is very indirect and does not significantly influence the value of D_{opt} obtained from equation (4-19).

The battery charger is essentially a regulator operated as a DC to DC converter which controls the charge voltage to maintain a constant charge current. The charging is conducted in two steps, one at the high charge rate and the other at the overcharge rate. The control circuit causes the charge rate to be reduced when the pressure rises due to gas generation. In the nickel-cadmium battery the sharp voltage increase near end of charge is used as a signal for rate reduction. In the silver-cadmium system, the current or voltage through the anode-auxiliary electrode circuit may be used as a signal.

As the battery is charged, the back EMF increases so that the charging voltage also must increase to maintain the constant current charging. With such a scheme, the charge voltage is less than the panel voltage at the beginning of charge and higher than the panel voltage at the end of charge. Thus a "buck-boost" type of regulator is required.

The efficiency of a "buck-boost" regulator is at least 83% for inputs exceeding 100 watts.[77] The weight of such a regulator may be approximately expressed as

$$W_r = 2.0 + 4.75 \times 10^{-3} P_r, \quad 400 \leq P_r \leq 900 \text{ watts} \tag{4-26a}$$

$$W_r = \frac{P_r}{150}, \quad P_r \geq 900 \text{ watts} \tag{4-26b}$$

where P_r is the input power.[77] The value of P_r can be found from

$$P_r = \frac{I_{ch} V_p}{q - r} \text{ watts} \tag{4-27}$$

where

I_{ch} is found from equation (4-13),

V_p is the panel voltage which is approximately the average charge voltage,

$q - r$ is the number of parallel strings needed to satisfy normal loads, hence the number being charged.

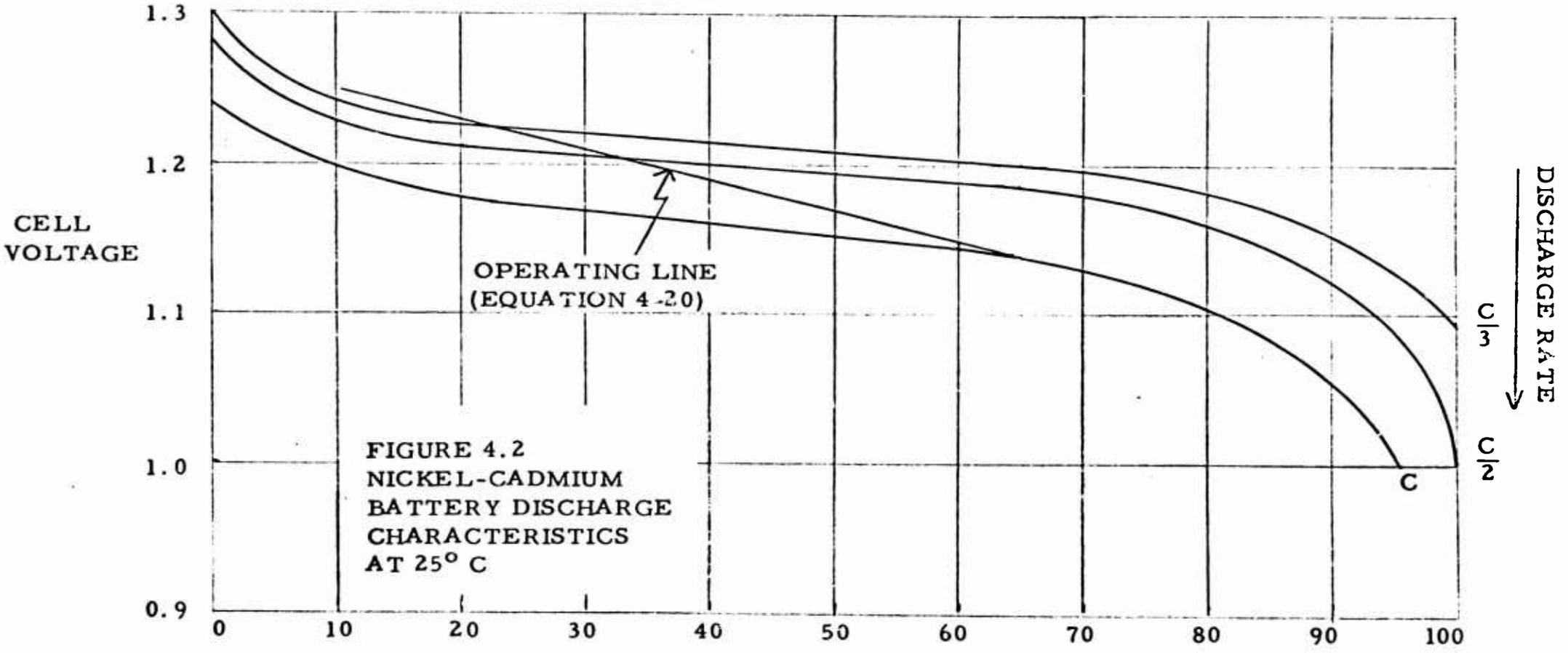

FIGURE 4.2
NICKEL-CADMIUM
BATTERY DISCHARGE
CHARACTERISTICS
AT 25° C

The weights and efficiency quoted above are for a regulator accepting input power with ± 30% regulation and providing an output of ± 5% regulation.[77]

The weight of control circuits is nearly constant at 1.5 pounds per string.[8, 19] Thus, the weight of the battery charger is

$$W_{bc} = q[W_r + 1.5] \text{ pounds.} \tag{4-28}$$

4.9 Nickel-Cadmium Battery Evaluation

Sealed nickel-cadmium batteries were first used in the Vanguard program and have dominated the field of secondary power systems ever since. Wide use has produced a large fund of operational experience and contributed to the development of a most reliable system.

4.9.1 Characteristics of Nickel-Cadmium Batteries

The chemical reaction in the cell is[54]

$$Cd + 2\ NiOOH + 2H_2O \underset{\text{charge}}{\overset{\text{discharge}}{\rightleftharpoons}} Cd(OH)_2 + 2Ni(OH)_2 . \tag{4-29}$$

The voltage generated by this reaction is a function of temperature and discharge rate. The discharge characteristics of a typical nickel-cadmium cell at 25°C are shown in Figure 4.2. Also plotted in Figure 4.2 is equation (4-20) which relates the discharge rate to the optimum discharge depth. At a discharge depth of 40%, the cell voltage is 1.19 volts so that 21 cells will provide 25 volts if the discharge depth is less than 40%. If the discharge depth is more than 40%, 22 series cells are required. Adding three cells for redundancy, either 24 or 25 cells are needed per string depending on the discharge depth.

At 25°C, nickel cadmium cells require an 18% overcharge. The maximum recommended overcharge rate at 25°C is C/10.[66] In mid-1966, cells with energy densities of 20 watt hours per pound will be available for cell sizes of 40 ampere hours or greater.[66]

4.9.2 30 Day Mission

In section 3.17, the solar array voltage is given as 31.5 volts and the panel specific weight is given as 0.0981 pounds per watt based on loads at 25 volts. The voltage difference between the battery and solar panel is taken into account in the analysis of section 4.7 so that the panel specific weight used in evaluating the batteries should be based on the output at 31.5 volts. The value of w_p is then 0.0805 lbs/watt based on 31.5 volt output.

Using the values of the various parameters, as quoted above, the optimum discharge depth is found from equation (4-19). Knowing the discharge depth, the discharge rate is found from equation (4-20). Then with the discharge depth and discharge rate, the number of cells per string and the cell voltage is found from the discharge characteristics in Figure 4.2. The value of the battery voltage can then be checked against the value assumed in solving equation (4-19) and any corrections can be made by iteration. If the assumed and calculated values of the battery voltage at the end of discharge are within about one volt of each other, the value of D_{opt} will be the same for both voltages, to slide rule accuracy.

Knowing the optimum discharge depth, the cell cycle life can be found from Figure 4.1. Then using 463 cycles as the mission length, the cell, string, and battery package reliabilities are found by using equations (4-3) through (4-7).

Again using the known discharge depth, the high charge rate is found by combining equations (4-13) through (4-15). Knowing the charge rate, the maximum charge voltage, V_c, can be found. For nickel-cadmium batteries at 25°C,[67]

$$V_c \cong n \left[1.42 + \frac{0.11}{C} I_{ch}\right] \text{ volts} . \qquad (4\text{-}30)$$

The discharge efficiency may then be found from equation (4-21). Thus, the discharge efficiency and the discharge depth can be used to find the

required capacity of q-r strings from equation (4-10) as a function of the load current.

Finally, the weights of the battery package, extra solar array for charging, and the battery charger are found by using equations (4-24) through (4-28). A summary of the results of these calculations, and the parameters used, is presented in Table 4.1 for the 30 day mission using several values of q and r. The data are arranged according to increasing redundancy in the battery package.

The configuration with the lowest weight uses only one string. The reliability of this single string condiguration is found to exceed the design goal reliability for mission success (0.995) but falls short of that required for crew safety (0.9999). In addition, the single string configuration does not provide any back-up for failure in the battery charger, a component which is believed to be very reliable, but whose numerical reliability is unknown.

The next lightest configuration requires only three out of four strings to survive the mission and has a mission success reliability in excess of that required for crew safety. The cell size used in each string is given in the c/(q-r) column as $1.04I_s$. At the minimum load of 41.5 amperes, the required capacity of each cell is over 43 ampere hours and so the cell is large enough to have the assumed energy density of 20 watt hours per pound. The other configurations are thus of no interest as the one with three out of four strings surviving meets all requirements and weighs less than the more redundant designs.

4.9.3 60 Day Mission

For a 60 day mission, the solar array voltage is still 31.5 volts. The panel specific weight was given as 0.0998 pounds per watt in section 3.17. Adjusting this value for the voltage difference as discussed in section 4.9.2, the panel specific weight is then 0.0818 pounds per watt. All other parameters associated with the battery and the solar array are

Battery: Nickel-Cadmium

Mission Duration: 30 days (462 cycles)

Parameters:

$\epsilon = 0.18$

$I_{och} = C/10$ amperes

$w_b = 0.05$ pounds/watt hours

$\eta_{ch} = 0.83$

$V_p = 31.5$ volts

$w_p = 0.0805$ pounds/watt

q	r	D_{opt}	I_d	V_b	Cycle Life	R_c	R_s	R_p	I_{ch}	η_d
1	0	0.240	0.369C	29.2	14,800	0.9786	0.9984	0.9984	0.605C	0.818
4	1	0.258	0.397C	29.1	13,700	0.9826	0.9993	>0.9999	0.700C	0.810
3	1	0.266	0.410C	29.1	13,100	0.9838	0.9994	>0.9999	0.748C	0.806
2	1	0.284	0.437C	29.0	12,100	0.9869	0.9997	>0.9999	0.863C	0.797

q	r	$\frac{C}{q-r}$	W_b	W_p	P_r	W_{bc}	W_{tot}
1	0	$3.32I_s$	$4.85I_s$	$4.95I_s$	$63.2I_s$	$1.5 + 0.42I_s$	$1.5 + 10.22I_s$
4	1	$1.04I_s$	$6.05I_s$	$5.54I_s$	$22.9I_s$	$6.0 + 0.61I_s$	$6.0 + 12.20I_s$
3	1	$1.515I_s$	$6.61I_s$	$5.75I_s$	$35.7I_s$	$4.5 + 0.74I_s$	$4.5 + 13.10I_s$
2	1	$2.87I_s$	$8.83I_s$	$6.28I_s$	$78.1I_s$	$3.0 + 1.04I_s$	$3.0 + 15.65I_s$

TABLE 4.1, SUMMARY OF NICKEL-CADMIUM BATTERY PERFORMANCE FOR A 30 DAY MISSION

unchanged. A summary of the results obtained for a 60 day mission of 923 cycles is presented in Table 4.2.

Any of the three configurations shown in Table 4.2 has sufficient reliability for mission success; but only the one with two strings has a mission success reliability in excess of that required for crew safety. However, in section 1.2 it was stated that crew safety was dependent on the power system having the capability of supplying at least half the life support. Both the four string and three string configurations have probabilities in excess of 0.9999 that no more than two strings will fail; and even if two should fail the remaining strings can provide more than one half the life support power. Thus, all three configurations satisfy the reliability requirements. Of the three, the one with four strings is the lightest and has already been shown to require cells large enough to satisfy the assumed energy density.

Thus, the four string configuration is the lightest of the alternatives presented here for both the 30 and 60 day missions. Configurations using larger numbers of strings, only one of which is redundant, will also meet the reliability requirements in both cases. But any weight improvement will be very small because by increasing the number of strings, the cell size and energy density will decrease and the weight of battery charger will increase. Hence, there is little or no weight advantage to be gained by increasing the complexity of the battery package.

4.10 Silver-Cadmium Battery Evaluation

Sealed silver-cadmium batteries have only recently attained the cycle lives necessary for long missions. These batteries are not considered as highly refined as the nickel-cadmium type but are enjoying increasing use because of their high energy density and reliability. With the recent development of the auxiliary electrode to improve the overcharge characteristics, the silver-cadmium battery may all but completely replace nickel-cadmium batteries in future space uses.

Battery: Nickel-Cadmium

Mission Duration: 60 days (923 cycles)

Parameters: same as for 30 day mission but for $w_p = 0.0818$

q	r	D_{opt}	I_d	V_b	Cycle Life	R_c	R_s	R_p	I_{ch}	d
4	1	0.258	0.397C	29.1	13,700	0.9656	0.9914	0.9996	0.700C	0.810
3	1	0.265	0.408C	29.1	13,100	0.9680	0.9933	0.99987	0.748C	0.806
2	1	0.283	0.435C	29.0	12,100	0.9739	0.9968	>0.9999	0.863C	0.797

q	r	$\frac{C}{q-r}$	W_b	W_p	P_r	W_{bc}	W_{tot}
4	1	$1.04I_s$	$6.05I_s$	$5.63I_s$	$22.9I_s$	$6.0 + 0.61I_s$	$6.0 + 12.29I_s$
3	1	$1.515I_s$	$6.61I_s$	$5.85I_s$	$35.7I_s$	$4.5 + 0.74I_s$	$4\ 5 + 13.20I_s$
2	1	$2.87I_s$	$8.33I_s$	$6.38I_s$	$78.1I_s$	$3.0 + 1.04I_s$	$3.0 + 15.65I_s$

TABLE 4.2, SUMMARY OF NICKEL-CADMIUM PERFORMANCE FOR A 60 DAY MISSION

4.10.1 Characteristics of Silver-Cadmium Batteries

There are two reactions which occur in silver-cadmium cells:[54]

$$Cd + 2AgO + H_2O \underset{\text{charge}}{\overset{\text{discharge}}{\rightleftharpoons}} Cd(OH)_2 + Ag_2O \qquad (4\text{-}31a)$$

$$Cd + Ag_2O + H_2O \underset{\text{charge}}{\overset{\text{discharge}}{\rightleftharpoons}} Cd(OH)_2 + 2Ag. \qquad (4\text{-}31b)$$

On discharge, reaction (4-31a) occurs first and generates a higher voltage than reaction (4-31b). Consequently, the discharge characteristic has two plateaus as shown in Figure 4.3.

The upper plateau can be totally suppressed by using a pasted type of silver electrode. The characteristics of such a cell are shown by the dashed lines in Figure 4.3. If it is desired to use the upper plateau, sintered carbonyl nickel plaques of the type employed in nickel-cadmium cells are impregnated with silver and used as electrodes.[31,54] In evaluating silver-cadmium batteries, it is of interest to consider using only the upper plateau or the lower plateau. There is no point in using both voltages as the extra energy available from the upper plateau is only dissipated in the voltage regulators.

Also plotted in Figure 4.3 are the operating lines for both plateaus as given by equation (4-20). For the lower plateau, 23 cells are required to give 25 volts at the end of discharge if the discharge depth is less than 18%. If the discharge depth is greater than 18%, 24 cells are required. Adding three cells for redundancy, each string will consist of either 26 or 27 cells.

For the upper plateau, 19 cells are required if the discharge depth is greater than 10%. Adding three cells for redundancy, each string will then consist of 22 cells. Because the operating line is just tangent to the

C/2 discharge curve, the maximum discharge rate is C/2 and the maximum discharge depth which may be used, if the upper plateau is employed, is 32.5%.

In distinction to nickel-cadmium cells, silver-cadmium cells require a 5% overcharge at 25°C, but can be overcharged at only the C/200 rate.[66] The analysis presented here will be for cells equipped with auxiliary electrodes which allow the overcharge rate to be increased to C/10.[63]

Because of the disparity in voltages at the two plateaus, the effective energy density achieved is very dependent on voltage. The energy density of a silver-cadmium battery discharged at the C/2 rate and exhibiting both plateaus is reported to be 25 watt-hours per pound for cells available in mid-1966.[66,69] The average cell voltage in a C/2 discharge is 1.16 volts. Hence, the specific weight of the battery may be simply expressed as

$$w_b = \frac{1.16}{25 V_{cell}} \text{ lbs/watt-hr} \qquad (4-32)$$

where V_{cell} is the cell voltage on the particular plateau being used. This value of specific weight is relatively insensitive to cell size.[66,69]

4.10.2 Upper Plateau Evaluation

Using equation (4-19) the optimum discharge depth for silver-cadmium cells, using the upper plateau, is over 50% for both mission durations. However, the maximum allowable discharge depth using the upper plateau is only 32.5% as discussed above. Hence, all upper plateau configurations will be analyzed at this discharge depth as it is the closest to the optimum which can be achieved.

Because only one discharge depth is used, the following quantities are independent of mission length and battery package configuration:

$D = 0.325$	$V_p = 31.5$ volts
$\epsilon = 0.05$	$V_b = 29.5$ volts
$I_d = C/2$	$V_c = 33.4$ volts

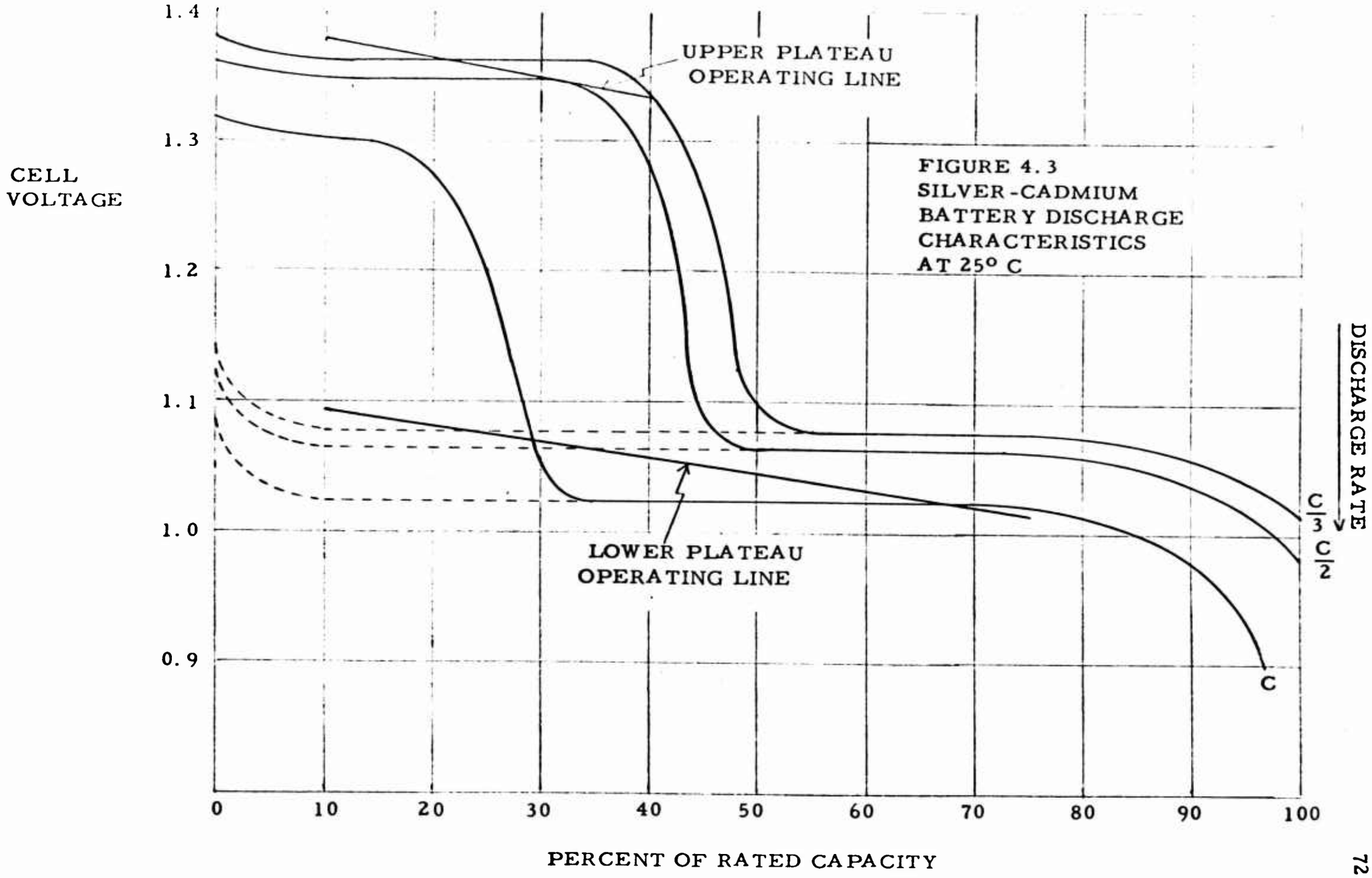
CELL VOLTAGE
1.4
1.3
1.2
1.1
1.0
0.9
UPPER PLATEAU OPERATING LINE
LOWER PLATEAU OPERATING LINE
FIGURE 4.3
SILVER-CADMIUM BATTERY DISCHARGE CHARACTERISTICS AT 25° C
DISCHARGE RATE
C/3
C/2
C
0
10
20
30
40
50
60
70
80
90
100
PERCENT OF RATED CAPACITY

q	r	R_c	R_s	R_p	$\frac{C}{q-r}$	W_b	W_p	P_r	W_{bc}	W_{tot}
1	0	0.9691	9.9958	0.9958	$2.26I_s$	$2.31I_s$	$3.01I_s$	$37.4I_s$	$1.5 + 0.25I_s$	$1.5 + 5.57I_s$
4	1	0.9768	0.9987	>0.9999	$0.754I_s$	$3.08I_s$	$3.01I_s$	$12.5I_s$	$14 + 0.23I_s$	$14 + 6.32I_s$, $I_s < 72$
									$6 + 0.33I_s$	$6 + 6.42I_s$, $I_s > 72$
3	1	0.9793	0.9990	>0.9999	$1.31I_s$	$3.47I_s$	$3.01I_s$	$18.7I_s$	$10.5 + 0.27I_s$	$10.5 + 6.75I_s$, $I_s < 48$
									$4.5 + 0.37I_s$	$4.5 + 6.85I_s$, $I_s > 48$

A. MISSION DURATION: 30 DAYS (462 CYCLES)

q	r	R_c	R_s	R_p	$\frac{C}{q-r}$	W_b	W_p	P_r	W_{bc}	W_{tot}
4	1	0.9541	0.9833	0.9984	$0.754I_s$	$3.08I_s$	$3.06I_s$	$12.5I_s$	$14 + 0.23I_s$	$14 + 6.37I_s$, $I_s < 72$
									$6 + 0.33I_s$	$6 + 6.47I_s$, $I_s > 72$
3	1	0.9591	0.9887	>0.9999	$1.13I_s$	$3.47I_s$	$3.06I_s$	$18.7I_s$	$10.5 + 0.26I_s$	$10.5 + 6.80I_s$, $I_s < 48$
									$4.5 + 0.37I_s$	$4.5 + 6.90I_s$, $I_s > 48$
2	1	0.9692	0.9958	>0.9999	$2.26I_s$	$4.62I_s$	$3.06I_s$	$37.4I_s$	$3 + 0.50I_s$	$3 + 8.18I_s$

B. MISSION DURATION: 60 DAYS (923 CYCLES)

TABLE 4.3, SUMMARY OF SILVER-CADMIUM BATTERY PERFORMANCE AT THE UPPER VOLTAGE LEVEL

$I_{ch} = 0.525C$

$I_{och} = C/10$ $\qquad$ $\eta_d = 0.885$

$n = 22$ cells $\qquad$ $\eta_{ch} = 0.83$

cycle life = 10,200 cycles $\qquad$ $w_b = 0.0348$ pounds/watt-hour.

The solar panel specific weights are 0.0805 and 0.0818 pounds per watt for the 30 and 60 day missions respectively. A summary of the reliabilities and weights achieved using these results is given in Tables 4.3A and 4.3B.

Taking the 30 day mission first, the single string configuration is inadequate for crew safety. The other two configurations have mission success reliabilities in excess of that required for crew safety and so more than meet the reliability requirements. Of these two, the four string configuration is the lightest and so the best of the alternatives.

For the 60 day mission, all three alternatives presented in Table 4.6B exceed the mission success reliability requirements and the two and three string configurations exceed the crew safety requirements. In the four string configuration two out of four strings will provide more than two-thirds of the life support power with a probability greater than 0.9999. Thus, all three choices will meet reliability goals; and of the three, the four string configuration has the least weight.

4.10.3 Lower Plateau Evaluation

Using equation (4-19), the optimum discharge depth for a silver-cadmium cell, using the lower plateau, is greater than 55% for both the 30 and 60 day missions. However, in section 4.3.4 it was specified that discharge depths greater than 50% would not be allowed because of the lack of experience in this operating regime. All battery configurations using the lower plateau will be analyzed at a discharge depth of 0.500 as this is the closest to the optimum which can be achieved.

Because only one discharge depth is used, the following quantities are independent of mission length and battery package configuration:

q	r	R_c	R_s	R_p	$\frac{C}{q-r}$	W_b	W_p	P_r	W_{bc}	W_{tot}
4	1	0.9512	0.9544	0.9883	$0.514I_s$	$2.68I_s$	$3.57I_s$	$14.8I_s$	$14 + 0.28I_s$ $6 + 0.40I_s$	$14 + 6.53I_s$, $I_s < 61$ $6 + 6.65I_s$, $I_s > 61$
3	1	0.9565	0.9682	0.9970	$0.771I_s$	$3.02I_s$	$3.57I_s$	$22.3I_s$	$4.5 + 0.45I_s$	$4.5 + 7.04I_s$
2	1	0.9672	0.9876	0.99986	$1.54I_s$	$4.10I_s$	$3.57I_s$	$44.5I_s$	$3.0 + 0.58I_s$	$3.0 + 8.25I_s$

A. MISSION DURATION: 30 DAYS (462 CYCLES)

q	r	R_c	R_s	R_p	$\frac{C}{q-r}$	W_b	W_p	P_r	W_{bc}	W_{tot}
2	1	0.9355	0.8977	0.9896	$1.54I_s$	$4.10I_s$	$3.63I_s$	$44.5I_s$	$3 + 0.58I_s$	$3 + 8.31I_s$
3	2	0.9565	0.9682	>0.9999	$0.771I_s$	$6.15I_s$	$3.63I_s$	$44.5I_s$	$4.5 + 0.87I_s$	$4.5 + 10.65I_s$

B. MISSION DURATION: 60 DAYS (923 CYCLES)

TABLE 4.4, SUMMARY OF SILVER-CADMIUM BATTERY PERFORMANCE AT THE LOWER VOLTAGE LEVEL

$D = 0.500$	$V_p = 31\ 5$ volts
$\epsilon = 0.05$	$V_b = 29.0$ volts
$I_d = 0.790C$	$V_c = 34.4$ volts[17]
$I_{och} = C/10$	$\eta_d = 0.844$
$I_{ch} = 0.915C$	$\eta_{ch} = 0.83$
$n = 28$ cells	$w_b = 0.0348$ pounds/watt-hour

cycle life = 4800 cycles.

The solar panel specific weights are 0.0805 and 0.0818 pounds per watt for the respective mission durations of 30 and 60 days. A summary of the reliabilities and weights achieved using these results is given in Tables 4.4A and 4.4B.

Taking the 30 day mission first, the four string configuration does not meet the design reliability goal for mission success and so can be discarded. The three string configuration exceeds the mission success reliability. In addition, the probability that at least one of the three strings will survive is greater than 0.9999. Since one string can supply more than one-half the life support load, the three string configuration meets all reliability requirements. The two string configuration requires one out of two strings to survive for mission success and so the mission success reliability equals the crew safety reliability. Thus, the two string configuration cannot meet the crew safety reliability goal. Hence, only the three string configuration meets all reliability requirements.

For the 60 day mission, only the three string configuration meets the reliability requirements.

4.11 Comparisons and Selection

In Tables 4.5A and 4.5B the reliability and weight data for the best configuration of each battery type are summarized.

BATTERY TYPE	q	r	R_p		W_{tot}
			ms*	cs	
Nickel-Cadmium	4	1	>0.9999	>0.9999	$6 + 12.20I_s$
Silver-Cadmium Upper Plateau	4	1	>0.9999	>0.9999	$14 + 6.32I_s$, $I_s < 72$ $6 + 4.42I_s$, $I_s > 72$
Silver-Cadmium Lower Plateau	3	1	0.9970	$>0.9999(\frac{1}{3})$	$4.5 + 7.04I_s$

A. MISSION DURATION 30 DAYS

BATTERY TYPE	q	r	R_p		W_{tot}
			ms	cs	
Nickel-Cadmium	4	1	0.9996	$>0.9999(\frac{2}{4})$	$6 + 12.29I_s$
Silver-Cadmium Upper Plateau	4	1	0.9984	$>0.9999(\frac{2}{4})$	$14 + 6.37I_s$, $I_s < 72$ $6 + 6.47I_s$, $I_s > 72$
Silver-Cadmium Lower Plateau	3	2	>0.9999	>0.9999	$4.5 + 10.65I_s$

B. MISSION DURATION 60 DAYS

*ms = mission success
cs = crew safety

TABLE 4.5

WEIGHT AND RELIABILITY COMPARISONS OF THE BEST CONFIGURATION OF EACH BATTERY TYPE

All configurations exceed the design reliability goals by a comfortable margin. In three of the six cases, the mission success reliability is less than the specified crew safety reliability goal. The proportion of the battery package which must survive to meet crew safety requirements is given in parentheses for these cases.

The silver-cadmium battery utilizing the upper voltage plateau has the lowest weight of any of the alternatives. This result is very much dependent upon use of an auxiliary electrode in each cell If auxiliary electrodes were not used, the optimum depth of discharge found from equation (4-19) would be less than 8% in which case the nickel-cadmium battery would be the lowest weight alternative. However, the auxiliary electrodes are now part of the state of the art and so the substantial weight savings as a result of using the silver-cadmium battery may be realized.

4.12 Thermal Control

The preceding analysis of the battery has been based on maintaining the operating temperature in a narrow range around 25°C. To validate this assumption it is necessary to provide some means of controlling the battery temperature

In Appendix A a cold plate scheme for radiating excess heat is described and analyzed. It is found that by using such a device, the battery temperature varies between 297°K and 300.8°K (23.8 to 27.6°C). The weight penalty for using the plate is only $0.0408I_s$ pounds. It is also found in the appendix that the volume of the battery and cold plate is $31.3I_s$ cubic inches.

4.13 Battery Summary

For both the 30 and 60 day missions, silver-cadmium cells utilizing the high voltage discharge plateau are selected. The battery package consists of four parallel strings, any three of which can satisfy the load. Each string has 22 series cells, each cell being equipped with an auxiliary electrode to improve the overcharge characteristics. This configuration exceeds all reliability requirements by a comfortable margin.

The battery package weight including the battery charger, the thermal control device, and the solar array directly associated with charging the battery is shown below as a function of shadow time current, I_s.

MISSION DURATION	SYSTEM WEIGHT
30 Days	$14 + 6.36I_s$, $I_s < 72$
	$6 + 6.46I_s$, $I_s > 72$
60 Days	$14 + 6.41I_s$, $I_s < 72$
	$6 + 6.51I_s$, $I_s > 72$

TABLE 4.6

BATTERY WEIGHT SUMMARY

The volume of the battery and radiating plate is 31.31_s cubic inches. To allow for the volume of the battery charger, the figure is increased to $40I_s$ cubic inches. The volume of the solar array is 0.3521_s cubic feet for both durations. The battery system volume is then $0.354I_s$ cubic feet. These weight and volume figures may alternately be expressed as functions of shadow time power load, P_s, by simply using the conversion factor

$$I_s = \frac{P_s}{25} . \qquad (4\text{-}33)$$

5. BATTERY/SOLAR CELL SYSTEM INTEGRATION

5.1 Load Sharing and Programming

In part 4 the battery subsystem weight and volume were found inclusive of the solar array needed for recharging. In part 3 the solar array weight and volume were found as functions of all loads but battery charging. This artifice is convenient as it allows a direct assessment of the weight and volume penalties associated with use of secondary batteries. In spite of this analytical division of the array into two parts, there is only one solar array and it has a uniform output which goes to an unregulated bus and then to the various loads. No specific portion of the array is allotted to the battery or any other load. As a result, the battery charger is just one of many loads which may be put on or taken off the bus bar at will.

In the course of the mission transient peaks occur during the sunlit portion of the orbit. These transients last only a few seconds total per orbit so that it is hardly worthwhile to add array capacity just to meet their demands. Instead, battery charging can be interrupted momentarily and the full power of the array can be brought to bear. If necessary, the battery could be used as well. These interruptions in the charging sequence will have an insignificant effect on the battery because of the very short durations. On the other hand, this technique of load sharing cannot be used with sustained loads because the battery would be insufficiently charged at the end of sunlight.

By properly programming the loads which occur in sunlight and satisfying peak loads as described above, the required array area can be minimized. In light or shadow, the continuous life support load, the biomedical monitors, and voice communications require a minimum level of power designated P_s. For the shadow portion of the orbit, P_s is also the maximum demanded and all other loads are programmed to occur in sunlight. The maximum single sunlight load in excess of P_s is that

associated with the high load experiments, P_{eh} (see Table 1.2). Further, there is no reason why any other of the periodic or occasional loads should occur simultaneously with P_{eh}. If these loads cannot be delayed until the next orbit, then they can be satisfied when the battery is on overcharge and drawing a reduced current. Thus, the solar array only needs the capacity to satisfy the sum of P_s, P_{eh}, and the battery charging power. The value of P_{eh} to be used in sizing the array is the average power as charging is interrupted to meet peak demands. When high load experiments are not in progress, the array will be able to satisfy all other peaks without affecting the charge sequence as there will be a large excess of generating capacity.

5.2 Orientation System

Discussion of the vehicle orientation system has been purposely delayed to this point because the specific effects of the solar array cannot be analyzed independently of the shadow time power source. The spacecraft is oriented in an earth-pointing mode which is both stable and conducive to reconnaissance experiments (see section 1.3). Because the solar array has only one degree of freedom the spacecraft must rotate about the yaw axis (parallel to local vertical) to give the array the second degree of freedom necessary for sun orientation (see section 3.13). The vehicle motions are thus defined by these two requirements.

First order estimates of torque and momentum requirements are presented in Appendix B along with weight and power estimates of the required attitude control systems for vehicles with and without solar arrays. It is concluded in that Appendix that the gravity gradient torque is of sufficient magnitude to maintain the earth-pointing orientation well within $\pm$ 0.001 radian in the presence of aerodynamic and solar radiation torques. However, an attitude control system is still necessary to serve the needs for command reorientations to obtain fixes on ground targets.

If magnetic torquers are used as the attitude control system, high current transients are imposed on the power system. Since these demands

are of short duration they may be satisfied by interruption of the charging sequence as with the transients due to the high load experiments. The added current available from the solar array, using this technique is simply the charge current or 0.525C (see section 4.10.2). Using equation (4-10) to find C as a function of I_s, the shadow time load current, the current available for transients is then $2.28I_s$. The value of I_s is between 41.8 and 101.8 amperes depending on the magnitude of the continuous life support loads. The available current then ranges between 95.5 and 232 amperes.

Referring to section B.8.2 in the appendix, it was found that a magnetic torquer will be the lightest weight system for the 30 day mission if more than about 45 amperes are available. For the 60 day mission the corresponding current is about 29 amperes. Comparing these break even values to the available currents, the magnetic torquer system should obviously be used.

Using equations (B-41) and (B-42) in the Appendix, and allowing the nominal current used by the magnetic torquers to be a maximum of $2.0I_s$, the weight of the attitude control system is approximately

$$W_{acc} = \frac{1.2X10^5}{P_s} \text{ pounds} \qquad (5-1)$$

where P_s is the shadow time load in watts. This weight is independent of the mission duration.

5.3 System Weight and Volume

The weight of the attitude control system will not be added into the weight of the power system at this point as it will be useful to directly assess the effect of attitude control requirements when comparing the alternative power systems. Using the results of parts 3 and 4 of this study, the sum of the battery and array weights for an integrated system are given in Table 5.1 for both the 30 and 60 day missions.

MISSION DURATION	BATTERY/SOLAR CELL SYSTEM WEIGHT	VALUE OF P_s	
30 Days	$78.6 + 0.352P_s + 0.0981P_{eh}$,	$P_s < 1800$	(5-2a)
	$70.6 + 0.356P_s + 0.0981P_{eh}$,	$P_s > 1800$	(5-2b)
60 Days	$78.6 + 0.356P_s + 0.0998P_{eh}$,	$P_s < 1800$	(5-3a)
	$70.6 + 0.360P_s + 0.0998P_{eh}$.	$P_s > 1800$	(5-3b)

TABLE 5.1, BATTERY/SOLAR CELL SYSTEM WEIGHT

The system volume is nearly independent of duration and is given as

$$V_{B/sc} = 8.60 + 0.0255P_s + 0.0115P_{eh} \text{ ft}^3 . \quad (5-4)$$

6. PRIMARY FUEL CELLS

6.1 Introduction

A fuel cell is basically a cathode and anode separated by a suitable electrolyte in which an oxidizer and a reducing agent are allowed to react without ever coming in physical contact with each other. In the reaction, energy is released in the form of electricity. Efficiency is not constrained by the Carnot limitation since heat generation is not an intermediate step in the energy conversion process. The electrical characteristic may be described as a source of constant voltage in series with a fixed resistance. In all these respects, the fuel cell is similar or identical to a primary battery.

But the fuel cell is not a primary battery. In fuel cells, designed for space use, the reactants are hydrogen and oxygen stored in cryogenic tankage whereas in a battery the reactants are the electrodes themselves. In contrast, the electrodes of a fuel cell must be inert and not change during the reaction if long life and reliability are to be achieved. The reaction products of a battery remain in the cells; but in a fuel cell, the reaction product is potable water which is removed and may be used for astronaut consumption or other purposes. In addition, the fuel cell is a much more complex device than a battery. The basic cells are quite simple, but the control devices, valves, pumps, cryogenic tankage, and radiator complicate the system.

In Figure 6.1 there is shown a schematic of a fuel cell in operation.

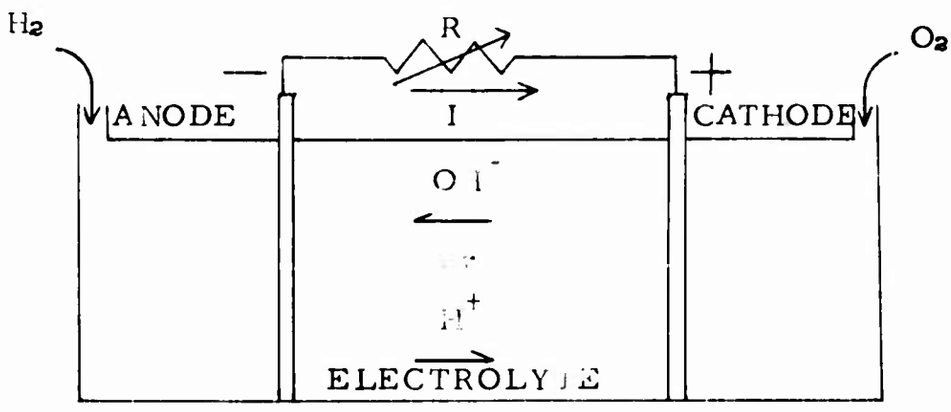

FIGURE 6.1, FUEL CELL SCHEMATIC

The reactions in an H_2-O_2 cell are

1. With acidic electrolyte.

$$\text{Anode: } 2H_2 \longrightarrow 4H^+ + 4e^- . \tag{6-1a}$$

$$\text{Cathode: } 4e^- + 4H^+ + O_2 \longrightarrow 2H_2O . \tag{6-1b}$$

2. With a basic electrolyte:

$$\text{Cathode: } O_2 + 2H_2O + 4e^- \longrightarrow 4(OH^-) \tag{6-2a}$$

$$\text{Anode: } 2H_2 + 4(OH^-) \longrightarrow 4H_2O + 4e^- . \tag{6-2b}$$

Overall:

$$2H_2 + O_2 \longrightarrow 2H_2O + 4eE + Q - 3kT . \tag{6-3}$$

The last three terms on the right side of equation (6-3) represent the electrical energy generated, the heat released, and the mechanical energy absorbed, respectively.

The thermal efficiency of a fuel cell is directly proportional to the cell voltage and may be expressed as

$$\eta = \frac{V}{E_h} \tag{6-4}$$

where E_h = 1.48 volts, the potential which would result if all the energy of the reaction was converted to electrical energy. This figure is quite insensitive to temperature between 100 and 500°F, the present operating limits of fuel cells designed for use in space.

6.2 Space Fuel Cells

General Electric fuel cells have flown in Geminis 2 and 5 and will be used in the remainder of the Gemini program. The GE fuel cell has also been selected for 21 and 30 day biosatellite missions.[32]

Pratt and Whitney is developing two fuel cells, one for the Apollo Command and Service Module and the other for the Lunar Excursion Module (LEM). The fate of the LEM fuel cell is in some doubt since NASA's Manned Spacecraft Center in Houston has recommended that the

power supply be converted to primary batteries.[53] The justification is that for the short two day mission primary batteries will give 50% more power and greater reliability than fuel cells for the same weight. Such batteries were not developed at the time that the fuel cell was selected for LEM.[4,53]

In spite of the developments in the LEM program, fuel cells are still considered to be competitive, if not superior, for missions with moderate power requirements and durations ranging from a few days to a few weeks. Longer missions are certainly possible with fuel cells, but the weight of reactants becomes prohibitive unless very substantial credits can be applied to the water by-product.

Unlike solar cell and battery systems, the mission analyst cannot simply begin with basic off the shelf components and design a fuel cell system tailored to his needs. At present, design and development of fuel cell systems may be described as more of an art than a science which incorporates an unusual degree of trial and error as compared to solar cell and battery systems. For this reason, the fuel cell portion of this study will be based upon the existing technology of Gemini and Apollo fuel cells. As such, the analysis will be simply an investigation into the possibilities of using existing fuel cell hardware on a mission for which it originally was not designed. This approach is justifiable in that the maximum time between power system selection and first launch of MOL is less than 3 years leaving a probable development time of only about 18 months. Considering that the Gemini and Apollo fuel cells have required development times of about 5 years, a MOL fuel cell system could only be a modification of existing hardware.

6.3 Comparison of Apollo and Gemini Fuel Cells

6.3.1 Apollo System

The Apollo fuel cell is a modified version of the Bacon fuel cell originally invented in the 1930's. The electrolyte is an aqueous solution of 70-85% KOH by weight and is pressurized through a diaphragm by nitrogen gas. The reactant gas pressure is maintained at 50 to 60 psia, about 5 to

10 psi greater than the electrolyte pressure. These pressures are necessary in order to keep the electrolyte in a liquid state at the 400 to 500°F operating temperatures. The operating conditions of temperature, pressure, and electrolyte concentration are allowed to vary within the ranges indicated so that the system can be self adaptive to changes in load conditions and radiator heat sink temperatures.[20, 70]

The hydrogen and oxygen electrodes are porous sintered nickel and nickel oxide respectively. The pores on the electrolyte side are much smaller than those on the gas side. This biporous electrode structure in conjunction with the pressure differential between the gas and electrolyte maintains the location of the interface between the two media in the pores.[13]

In the Apollo system 31 cells are series connected to make a module or "stack." Three such stacks are placed in parallel to form a complete system and all three stacks are connected to the load throughout the mission.[20] However, two stacks are adequate for mission success and one stack is adequate for crew safety. System reliability for crew safety has been reported as 0.9999 for a 14 day (332 hour) mission.[59] Assuming an exponential failure distribution, the reliability of each stack is calculated to be at least 0.9536. Mission success requires two out of three stacks to operate satisfactorily for only the first 147 hours.[60] The mission success probability is then 0.9987. The stack reliability figure is obviously based on designing the system so that if all stacks survive, the nominal load on each is only 1/3 to 2/3 of maximum rating.

In both the Gemini and Apollo systems, potable water and heat are byproducts of the reaction and must be removed for the operating conditions to remain within limits. In the Apollo system, heat and water removal is achieved by circulation of an excess of hydrogen gas through each cell. The hydrogen flow picks up both water and heat, transporting them to a heat exchanger/condenser where the excess heat is transferred to a secondary loop. The water/hydrogen mixture then enters a pump where the water is separated by centrifugal action. The secondary loop uses a water-glycol

mixture as the coolant fluid which carries heat to the radiator. The system is designed to operate at any load condition with the radiator facing sink temperatures between -460°F and +180°F. Heaters are provided in the stacks to maintain the operating temperature when the electrical loads and the sink temperature are low.[20]

6.3.2 Gemini System

The Gemini fuel cell uses an acidic ion exchange membrane in place of the electrolyte. Fine wire screens are used as electrodes in order to allow adequate access to the membrane by the reactant gases. The membrane itself is coated with catalysts because at the operating temperature of 100°F and pressure of 20 psia the reactions are very slow.[15] In the Apollo design no such catalysts are needed because of the higher temperature.

The Gemini system consists of two modules, each module made up of 3 stacks of 32 series cells. The normal operating mode is for all three stacks in a module to share the load (or half the load); but any stack can be shut down without affecting the others in the module. Mission success is based on 5 out of 6 stacks operating satisfactorily for 14 days and the associated reliability is 0.995.[5,47] Crew safety is based on 2 out of 6 stacks surviving and the associated reliability is calculated to be greater than 0.99999. The probability that any given stack will survive 14 days is 0.9815 (calculated).

Water removal is accomplished by use of a series of wicks in the O_2 chamber of each cell. Such a simple method is possible since the product water is in the condensed phase at normal operating conditions.

In the Gemini spacecraft a single heat removal system is used for environmental control, fuel cell temperature control, and cooling of electrical equipment mounted on cold plates. The system consists of two independent loops which follow parallel paths. When heat loads are low only one loop is used and when loads are high, both loops are in operation. Each

loop goes directly to the radiator which is also the vehicle skin. Structural stingers double as flow passages. This arrangement results in a very low weight penalty for heat rejection. At very high heat loadings the radiator is inadequate even with both coolant loops working. As a result, a small boiler using water from the fuel cell supplements the radiator. This device is also used for about 30 minutes after launching because the radiator temperature is too high for effective cooling.[7]

6.3.3 Comparison of the Two Systems

Unfortunately, some of the most interesting and useful performance data on these fuel cell systems is proprietary or classified.[56, 51, 78] The Apollo system is especially notable in this respect. However, sufficient data exists in the open literature on the two systems to make some reasonably good estimates. Drawing on information in references 2, 5, 13, 20, 32, 35, 47, 59, 51, 70, 75, estimates of the weight, volume, and electrical characteristics of the two systems are shown in Table 6.1 along with a summary of operating conditions and system configuration. The module weights and volumes shown include pumps, water separators, and other auxiliaries, but not the radiator which is listed separately. The radiator area is estimated on the basis of the radiator chargeable to the fuel cell in the Gemini. The weight estimates are for a radiator integral with the spacecraft exterior structure. For the Apollo system, these figures have been scaled downward because of the higher heat rejection temperature.

Just quickly glancing at the comparative data, one sees that neither system is clearly superior to the other for all conditions. The Gemini module weighs less per kilowatt and is more reliable while the Apollo module is more efficient (hence has lower fuel consumption rates) and requires a smaller radiator. Valid comparisons can only be made if mission length, power levels, and design goal reliabilities are clearly specified.

ITEM	GEMINI	APOLLO
Operating Temperature, ^{o}F	100	400-500
Operating Pressure, psia	30	50-60
Electrolyte	membrane	70-85% KOH
Series cells per stack	32	31
Stacks per module	3	1
Modules per system	2	3
Stack reliability (14 days)	0.9815	0.9536
Maximum current density, amps per square foot	40	141
Watts per module	$\leq$ 1150	$\leq$ 2000
Volts per module	$\geq$ 25.6	$\geq$ 26.0
Amps per module	$\leq$ 45.0	$\leq$ 77.0
Module current-voltage characteristics	V = 29.44-0.8543I	V = 33.52-0.0975I
Module efficiency, percent	η = 62.16-0.180I	η = 73.06-0.213I
Module weight, pounds	68	190
Module volume, ft^3	1.8	8.8
Radiator area, ft^2/ kw peak	40	4.6
Radiator weight, lbs/ kw peak	40	4.6

TABLE 6.1, SUMMARY OF APOLLO AND GEMINI FUEL CELL CHARACTERISTICS

6.4 Analytical Fuel Cell Reliability Model

The required system reliability will be 0.9999 for crew safety and 0.995 for mission success. As noted in section 1.2 crew safety is dependent, on supplying only half of the continuous life support power.

Reliability figures are given above for both systems as used on 14 day missions. To compute the system reliability for the MOL missions, the procedure of section 4.4 will be used. Stack failures will be assumed to follow an exponential distribution so that stack reliability is

$$R_s = e^{-\frac{t}{\theta}} \qquad (6\text{-}5)$$

where

t = required service life

θ = mean time to failure as calculated from 14 day reliability figures.

System reliability will be achieved by paralleling stacks and will be calculated from equation (4-6).

This analytical approach is valid only so long as the required service life is such that the equipment does not begin to wear out, in which case the failure rate increases. Failures in fuel cell systems can occur in the dynamic equipment (pumps, water separator, etc.), the control circuits or the fuel cells themselves. Even if there is no complete failure in any part of the system, the fuel cells themselves tend to degrade in performance as the electrolyte and electrodes become contaminated. Seals also tend to degrade markedly and so appear to wear out.

6.4.1 Apollo Wear Out Data

In early 1965, one stack of the Apollo type completed 1000 hours of continuous operation in a qualification test.[59] However, the test conditions and failure criteria are unknown so that little can be said about the significance of this single success.

In 1964 representatives of North American Aviation's Space and Information Systems Division, the Apollo prime contractor, reported on some mission studies of satellites using the Apollo fuel cell.[18] It was their conclusion that, for the 45 day mission considered in the study, the average Apollo type stack would probably not operate continuously for 45 days (1080 hours) under mission conditions, much less provide power at useful voltages and reasonable efficiencies.

As already noted, the design goal of the Apollo fuel cell is a stack reliability of at least 0.9536 for 14 days (336 hours) of continuous operation. With the available data, it can only be said that wear out failures do not occur for at least 400 hours of continuous operation, but probably at less than 1000 hours. Since 30 days corresponds to 720 hours, it is doubtful whether the life of the Apollo system is adequate for a 30 day mission. However, for comparison with the Gemini system, it will be assumed that wear out does not occur in 30 days. If the Apollo type system turns out to have the lower weight, a separate analysis for some shorter time to wear out should also be performed in order to give an estimate of the effects of uncertainty in the system life.

6.4.2 Gemini Wear Out Data

By early 1964, complete Gemini stacks had run for more than 1000 hours and individual cells for more than 5000 hours.[79] Once again, the test conditions were not reported. However, in the second half of 1964 an extensive testing program was conducted using 3 complete modules (3 stacks each) and 15 single stacks. Each stack was run at loads varying from 10 to 15 amps, the maximum current rating of a Gemini stack. The results of that program are shown below in Table 6.2.[32] In all cases, the highest load was run first. After some number of days the load was reduced except in the case of stacks B, F, L, N, and O which were run at constant load for the duration. In modules A and B, all stacks were run at the same conditions. Apparently, the stacks in module C were operated independently.

STACK	DAYS AT 10.0-15.0 Amps	DAYS AT 4.6-9.9 Amps	DAYS AT 1-4.5 Amps	TOTAL DAYS
A	58	----	48	106
B	----	----	155	155
C	42	44	----	86
D	59	6	----	65
E	35	67	----	102
F	----	93	----	93
G	48	19	39	106
H	22	----	18	40
I	35	2	----	37
J	30	3	----	33
K	18	12	----	30
L	19	----	----	19
M	20	14	----	34
N	19	----	----	19
O	28	----	----	28

MODULE	STACK	DAYS AT 10.0-15.0 Amps	DAYS AT 4.6-9.9 Amps	DAYS AT 1-4.5 Amps	TOTAL DAYS
A	All	----	46	----	46
B	All	4	29	----	33
C	1	12	8	----	20
	2	2	7	4	13
	3	15	6	----	21

TABLE 6.2, GEMINI FUEL CELL LIFE DATA

Some of the data on individual stacks is truly spectacular, especially that for stacks B and G. However, maximum accomplishments are not nearly as important as these minimum conclusions:

1. Even when operated at the maximum rated load, none of the individual stacks failed before 19 days.
2. When operated at variable loads, failure did not come before 30 days.
3. When half or less of the test was conducted at the maximum rated load, the earliest failure was 86 days.

In the Gemini vehicle, peak loads are about 70 amps, sustained loads which continue for hours at a time are about 60 amps, and during relatively inactive periods the load is only 18 amps or less. All six stacks share these loads.[5] Thus, considering that there are only two men on board, individual modules will probably be called upon to deliver no more than 3 amps for 80% of the mission, 10 amps for about 20% of the time, and more than 10 amps for only a few minutes total of the 14 days. Hence, the data on the individual stacks are representative of much worse conditions than will ever be encountered in a Gemini flight.

The data on the three stack modules are especially interesting when compared to that for single modules. The shorter lives reported are almost certainly a result of failure in auxiliary equipment rather than the fuel cells. Such a conclusion is strongly supported by the fact that for both modules A and B all stacks in the module were reported to have identical lives on test. The results of module C were not explained; but it might be inferred that stack 2 was in some way defective and its failure damaged the system. Of the three modules, the test program for module B was probably the most representative of the Gemini mission.

From these test results it is reasonable to conclude that:

1. A stack operated at two thirds to full rating for less than half the mission can be expected to survive for 60 days or more.
2. A module operated at one-third to two-thirds of rating can be expected to survive 30 days or more.

3. The module life is less than the stack life because of failures in auxiliary equipment.

Thus, for purposes of this study, the wear out time for a Gemini type module can be taken as at least 30 days and the exponential failure distribution of equation (6-5) will be considered controlling to that duration. Because of the apparent effects of auxiliary equipment on system reliability, and the lack of quantitative data for separating out these effects, the design of Gemini type systems for MOL will be based upon using 3 stack modules as building blocks rather than single stacks.

As for restarts, the Gemini fuel cell has an apparently unlimited capability. The ion exchange membrane does not deteriorate while it is idle. There are no special precautions which must be taken in the start up procedure and the system is ready to serve as soon as a load is put on it.

6.5 Fuel Cell Weight for a 30 Day Mission

In this section, the weight of all equipment but the reactants and the cryogenic storage system are found as a function of peak power. Because additions to capacity are made in increments of one or two kilowatts, weight cannot be expressed as a continuous function of power but is constant over various intervals and increases by significant amounts when passing from one interval to another.

The reliability goals are:

1. The probability that the number of modules in operation is adequate to satisfy the peak load should be at least 0.995 at all times.
2. The probability that the number of modules in operation is adequate to satisfy half the life support load should be at least 0.9999 at all times.

For mission success, the fuel cell is required to deliver a minimum continuous load for life support and biomedical monitors. At various times the fuel cell will also be required to satisfy higher loads. The peak will come when the voice communication load and the high experimental load are coincident. This peak load is then the sum of P_s, the minimum continuous load

including voice communication, and P_{ehp}, the peak demand of the high load experiments.

Implicit in the stack reliability figures given in Table 6.1 for the two fuel cell systems are the natures of the demand schedules for the Gemini and Apollo missions. To use these figures in evaluating fuel cell systems for the MOL mission, it is necessary to insure that the demands made on the fuel cell do not exceed those of the other missions. For both the Apollo and Gemini missions, the fully operative fuel cell system is required to deliver less than two-thirds its capacity for about 80 to 85% of the mission. Referring to Table 1.2, the MOL loads will be at or near the minimum (P_s) for over 89% of the mission. Further, these low loads are always less than two-thirds of the peak load, even assuming the worst possible combination of demand (P_s a maximum, P_{ehp} a minimum). Thus the MOL demands do not qualitatively exceed those of the other two missions.

6.5.1 Gemini-Type System Weight

Using equation (6-5), the probability that a single stack will function for 30 days (720 hours) is 0.9608. The maximum rating of each module is 45 amperes so that a single module can satisfy as much as 1125 watts of the peak load. As noted previously, the Gemini type system capacity must be increased in increments of modules of three stacks rather than single stacks. The weight of a module is 68 pounds. The range of possible peak demand is

$$2545 \leq P_s + P_{ehp} \leq 6545 \text{ watts.}$$

Using these specifications, the characteristics of a Gemini type system are tabulated in Table 6.3

$P_s + P_{ehp}$	N_L	N_{ms}	N_{cs}	WEIGHT, LBS
≤1500	4	2	3	136
≤2625	7	3	4	204
≤3375	9	4	8	272
≤4500	12	5	10	340
≤5625	15	6	13	408
≤6375	17	7	16	476
≤6750	18	8	18	544

TABLE 6.3, GEMINI BASIC HARDWARE CONFIGURATION AND WEIGHT SUMMARY

In the first column of Table 6.3 are values of the peak load in watts. These loads increase stepwise in multiples of 375 watts, the capacity of a single stack. In the second column is shown N_L, the number of stacks required to satisfy the peak load in the first column. In the third column is shown N_{ms}, the number of modules of three stacks each required to give a probabiliby of 0.995 or greater that N_L stacks will survive the mission. In the fourth column is N_{cs}, the number of stacks available throughout the mission for a probability of 0.9999 or greater. Or put another way, N_{ms} is the minimum number of modules required to meet the mission success requirements while N_{cs} is the maximum number of stacks that may be required for crew safety given the value of N_{ms}. Comparing the values of N_{cs} and N_L, we see that in the very worst case, there is a 0.9999 probability that the system will be able to supply at least 4/7 (57.1%) of the peak load power which is more than adequate for crew safety. The final column shows the weight of N_{ms} modules. The weight of the radiator is simply

$$W_r^G = 4.0X\ 10^{-2}(P_s + P_{ehp})\ \text{pounds.} \qquad (6\text{-}6)$$

The weight of reactants is found in section 6.6 and the weight of the cryogenic storage system is found in section 6.7.

6.5.2 Apollo Type System Weight

If it can be assumed that the Apollo system does not wear out before the end of the 30 day mission,* equation (6-5) gives the module (or stack) reliability as 0.9033 for a 30 day mission. The maximum rating of each module is 77 amperes so that a single module can satisfy as much as 1925 watts of the peak load. The weight of a module including accessories is 190 pounds. Using these specifications, the characteristics of an Apollo type system are tabulated in Table 6.4.

$P_s + P_{ehp}$	N_L	N_{ms}	N_{cs}	WEIGHT, LBS
≤ 3850	2	4	1	760
≤ 5775	3	6	2	1140
≤ 7700	4	7	2	1330

TABLE 6.4, APOLLO TYPE SYSTEM CONFIGURATION AND WEIGHT SUMMARY

The symbols N_L, N_{ms}, and N_{cs} all have the same meaning as was given in section 6.5.1 except that the word "stack" should be replaced by the word "module" when applying those definitions in this section. Comparing N_{cs} and N_L, there is 0.9999 probability that the power system will be able to supply at least 50% of the peak power for the full mission duration. This capability is more than adequate for crew safety. The weight of the radiator is

$$W_r^A = 4.6 \times 10^{-3}(P_s + P_{ehp}) \qquad (6\text{-}7)$$

*See section 6.4.1.

If the weight of the Apollo and Gemini type systems including radiators are compared, the Apollo-type system is found to weight between 157% and 252% of the Gemini type system depending on the peak power chosen. This significant difference indicates that the Gemini system is superior. However, such a conclusion cannot be validly drawn without considering the weight of reactants and storage required because the efficiencies of the two systems vary.

6.6 Weight of Reactants

The reliability calculations of section 6.5 were based on the assumption that all operational stacks are on line at all times. As failures occur, the load on the remaining stacks increases and efficiency is reduced. Since the failure rate is constant, the efficiency may be thought of as degrading linearly. Then, the average efficiency may be found by using the average number of stacks on line throughout the mission. In 99.5% of the cases, the minimum number of stacks in use at the end of the mission will be equal to or greater than N_L. Thus a conservative estimate of the mean number of stacks is the average of the total number of stacks provided and N_L. The current to be used in the expression for efficiency is then

$$I = \frac{P}{\frac{25(N_L + aN_{ms})}{2}} \qquad (6\text{-}8)$$

where

a = the number of stacks per module

P = a weighted average of the various levels of demand encountered.

Using Table 1.2, the various levels of demand and their durations are as given in Table 6.5 below.

POWER LEVEL, WATTS	DURATION, MIN/DAY
P_s	1158.72
$P_s + 20$	120.00
$P_s + 100$	10.00
$P_s + 500$	1.28
$P_s + \frac{1}{2}P_{eh}$	60.00
$P_s + P_{eh}$	90.00

TABLE 6.5, SCHEDULE OF LOAD LEVELS AND DURATIONS

The quantity P_{eh} is the average load due to the high load experiments. The medium and low load experiments were defined as having an average demand half that of the high load experiments. The quantity P_s is defined as the sum of the continuous life support, biomedical monitor, and voice communication loads. In developing Table 6.5, voice communication has been taken as continuous since it may occur at any time. The weighted average demand is then

$$P = 2.8 + P_s + \frac{P_{eh}}{12} \text{ watts.} \tag{6-9}$$

The total watt-hours of energy required to satisfy the anticipated loads is then 720P. There should also be a small reserve for contingencies and an allowance for residual fluid in the tanks. Hence, the quantity of reactants stored will be taken as that necessary to supply 800P watt hours.

The energy released by a stoichiometric reaction of hydrogen and oxygen is 136.5 k-cal per mole. There are 36 grams of reactants per mole and 860 k-cal equals 1000 watt-hours. The energy content of one pound of reactants is then 2000 watt-hours per pound. Thus the total weight of reactants required is

$$W_{O+H} = \frac{800P}{2000\eta} = 0.40\,\frac{P}{\eta} \qquad (6\text{-}10)$$

where **P** is given by equation (6-9).

The efficiency functions given in Figure 6.1 are of the form

$$\eta = \eta_o - GI. \qquad (6\text{-}11)$$

By combining equations (6-10) and (6-11), the weight of reactants is found as

$$W_{O+H} = \frac{0.40}{\eta_o}\ \frac{P}{1-ZP} \text{ pounds} \qquad (6\text{-}12)$$

where

$ZP = \frac{G}{\eta_o} I$ and I is given by equation (6-8).

The value of $0.40/\eta_o$ is 0.644 and 0.548 for the Gemini and Apollo type systems respectively. The minimum steady flow rate of reactants is similarly found as

$$W_{O+H} = \frac{1.2X10^{-2}}{\eta_o}\ \frac{P_s}{1-ZP_s}\ \frac{\text{pounds}}{\text{day}}. \qquad (6\text{-}13)$$

The value of $1.2X10^{-2}/\eta_o$ is $1.93X10^{-2}$ and $1.64X10^{-2}$ for Gemini and Apollo type systems respectively. Values of Z are tabulated in Table 6.6 for both systems.

$P_s + P_{ehp}$	Z
≤ 2625	$1.45X10^{-5}$
≤ 3375	$1.105X10^{-5}$
≤ 4500	$8.60X10^{-6}$
≤ 5625	$7.03X10^{-6}$
≤ 6375	$6.10X10^{-6}$
≤ 6750	$5.63X10^{-6}$

GEMINI

$P_s + P_{ehp}$	Z
≤ 3850	$3.90X10^{-5}$
≤ 5775	$2.59X10^{-5}$
≤ 7700	$2.12X10^{-5}$

APOLLO

TABLE 6.6, VALUES OF Z

6.7 Cryogenic Storage System

Beech Aircraft Corporation, the contractor for the Apollo cryogenic storage system, has prepared a study entitled "Cryogenic Storage Systems for the Manned Orbiting Laboratory."[22] In this study, a system which uses new pressure vessels and the existing Apollo hardware for all other components is analyzed. Also considered are subcritical storage and 100% use of Apollo hardware. The former approach is rejected because of cost and lead time requirements while the latter is rejected because the insulation is not sufficient for 30 days. The selected system uses only state of the art techniques and hardware thus requiring very little development. Beech emphasizes that the design is very conservative.

Since cryogenic storage for MOL has already been analyzed by a competent firm, a separate analysis here would be only redundant. Hence, the Beech study will be used to estimate the volume and weight of cryogenic storage for MOL. Thanks are due to the Beech Aircraft Corporation for granting permission to use the information in the study.

6.7.1 Design Assumptions

The assumptions used in the analysis are:

1. Room temperature safety factors:
   1.33 on yield
   1.50 ultimate
2. Operating conditions:
   Temperature: 130°F continuous
   Delivery Pressure: 150 psia minimum
   Nominal Tank Pressure: H_2: 250 psia
   O_2: 900 psia
   Acceleration: 7 g's
   Vibration: 17 grms
3. Vessel heat leak at 130°F:
   H_2: 0.18BTU/ft^2-hr
   O_2: 0.55BTU/ft^2-hr

4. In addition to the reactants required for the fuel cell, the system also stores oxygen for the environmental control system (ECS) which amounts to 5.0 pounds per day for the two men. The weight of oxygen, tankage, and controls required for a separate ECS oxygen supply should be subtracted from the final weight to find the weight chargeable to the fuel cell system.

6.7.2 Recommended Configuration and Reliability

Because the mission is manned and all cryogenic oxygen storage is combined into a single system, at least two oxygen vessels should be used so that a single failure does not endanger the crew. However, as the number of tanks increase, the probability of mission success decreases. As a result, Beech has chosen two oxygen vessels as a compromise between these conflicting requirements.

Two hydrogen vessels were also chosen for the analysis even though one vessel would have been lighter and given a higher probability of mission success. Apparently, though not explicitly, the reason for choosing two vessels was that if one failed or became unusable, another would still be available and the mission could continue at full power for as much as half the duration remaining at the time of failure. The same point is also true of the oxygen system.

The mission success reliability of this four tank system was calculated by Beech as 0.9966 for 30 days by using known failure rates for all components. The reliability of a similar four tank system used in Apollo is 0.9987 for mission success (147 hours) and 0.9999 for crew safety (340 hours).[60] With a selective increase in redundancy, the mission success reliability can probably be raised to the Apollo value for a nearly insignificant weight penalty.

6.7.3 System Weight and Volume Results

Before determining the weight of the cryogenic storage system for a given set of requirements, it is necessary to determine if either oxygen or hydrogen or both will have to be vented during the mission. In substance,

the procedure described in the Beech report consists of finding the total weight of a given fluid required for the mission and then determining the flow rate due to heat leak alone in tanks sized for this quantity of fluid. Then, if this flow rate is less than the minimum flow rate demanded at any time during the mission, venting is not required. The Beech presentation is graphical; but most lines are nearly linear so that the following inequalities may be used as approximate tests for the venting requirement:

$$\frac{W_H}{\dot{w}_{Hmin}} \leq 32.2 + 0.104W_H, \quad 75 \leq W_H \leq 200 \tag{6-14}$$

and

$$\frac{W_O}{\dot{w}_{Omin}} \leq 37.0 + 0.0182W_O, \quad 700 \leq W_O \leq 1800 \tag{6-15}$$

The subscripts "O" and "H" refer to oxygen and hydrogen respectively. The sum of W_H and W_O is found from equation (6-12) and the sum of $\dot{w}_H$ and $\dot{w}_O$ is found from equation (6-13). Since the reactants are used in a stoichiometric ratio the values of these parameters can be found. If the inequalities (6-14) and (6-15) are satisfied, no venting is required. The worst case which results from the demand schedule used in this study occurs when P_s is a minimum and P_{eh} is a maximum. Even under these conditions, no venting is required as both inequalities are satisfied for both the Gemini and Apollo type systems.

The dry weight of a two tank oxygen system as a function of the weight of stored fluid is approximately

$$W_{dO} = 82.0 + 0.1614W_{SO} \text{ lbs}, \quad 700 \leq W_{SO} \leq 1800 \text{ lbs} \tag{6-16}$$

where W_{SO} is the sum of the oxygen required for ECS (150 pounds) and the oxygen required for the fuel cell as found from equation (6-12). The outside diameter of each tank is approximately

$$D_{tO} = 25.28 + 8.18X10^{-3}W_{SO} \text{ in, } 700 \leq W_{SO} \leq 1800 \text{ lbs.} \quad (6\text{-}17)$$

The dry weight of a two tank hydrogen system as a function of the weight of stored fluid is approximately

$$W_{dH} = 50.0 + 1.25W_{SH} \text{ lbs, } 75 \leq W_{SH} \leq 200 \text{ lbs} \quad (6\text{-}18)$$

where W_{SH} is found from equation (6-12). The outside diameter of each hydrogen tank is

$$D_{tH} = 27.4 + 0.108W_{SH} \text{ in, } 75 \leq W_{sh} \leq 200 \text{ lbs.} \quad (6\text{-}19)$$

The weights, W_{dO} and W_{SH}, include all controls and plumbing as well as the tanks. The indicated ranges of W_{SO} and W_{SH} include the maximum and minimum weights of stored fluid of interest in this study.

Combining equations (6-16) and (6-18), and adding the weight of hydrogen and oxygen, the total weight of stored fluids and the storage system is

$$W_{F+S}^{tot} = 156.2 + 1.282\ W_{H+O} . \quad (6\text{-}20)$$

where W_{H+O} is given by equation (6-12).

The weight of a separate oxygen storage system for ECS plus 150 pounds of oxygen must be subtracted from equation (6-20) to find the weight chargeable to the power system. The separate ECS oxygen system is assumed to consist of only one tank as this configuration is the lightest of the possibilities and so gives the most conservative estimate of the storage weight chargeable to the fuel cells. From a graph in the Beech study, the dry weight of a one tank oxygen system with a 150 pound storage capacity is approximately 66 pounds. The total weight of a separate one tank ECS oxygen system including fluid is then 216 pounds. Thus, the weight of fluids and storage chargeable to the fuel cells is

$$W_{F+S}^{fc} = 1.282W_{H+O} - 59.8 \text{ pounds.} \quad (6\text{-}21)$$

The diameter of the tanks in terms of the fluid required for the fuel cells are

$$D_{tO} = 26.5 + 7.27X10^{-3} W_{H+O} \qquad (6-22)$$

$$D_{tH} = 27.4 + 1.2X10^{-2} W_{H+O} . \qquad (6-23)$$

The diameter of the oxygen tanks includes capacity for the 150 pounds of ECS oxygen. A separate ECS oxygen tank with 150 pounds capacity has a volume of 4.7 ft^2. Using equations (6-22) and (6-23) and subtracting the volume of a separate ECS oxygen system, the volume of the cryogenic storage system chargeable to the fuel cell system may be found as a function of W_{H+O}. However, this exact expression involves W_{H+O} to the second and third powers. A much simpler linear approximation is

$$V_t^{fc} = 8.80 + 5.60X10^{-2} W_{H+O}, \quad 600 \leq W_{H+O} \leq 1850 . \qquad (6-24)$$

At the end points of the specified range of W_{H+O}, the value of V_t^{fc} is exact. Over the remainder of the range, the volume is overestimated, reaching a maximum error of only 7% near the center of the range.

6.8 Weight Comparison of Gemini and Apollo Systems

The weight functions for the components of these fuel cell systems do not readily lend themselves to being combined into a single analytic function expressing the system weight. However, piecemeal comparisons are possible by simply assuming a set of conditions and using the figures and equations to find the resulting weights.

It has already been determined that the basic hardware of the Apollo-type fuel cell system is at least 57% heavier than that of the Gemini type system for the conditions of this 30 day mission. Hence it is useful to determine whether the Apollo type system is superior under any combination of possible power demand conditions specified for the mission before attempting to outline the regions of optimality. From Table 6.4, one sees that the

basic Apollo type hardware has the lowest specific weight (pounds per watt) at peak power levels of 3850, 5775,and 6545 watts. Further, the superior efficiency of the Apollo type system has its greatest effect when P (equation 6-9) is a maximum because this condition corresponds to the maximum quantity of reactants. The value of P is a maximum when P_s is the maximum allowed by the peak demand condition of $P_s + P_{ehp}$.

The weights of the basic fuel cell hardware (W^G_{FC} and W^A_{FC}) are found from Tables 6.3 and 6.4. The radiator weights (W^G_r and W^A_r) are found from equations (6-6) and (6-7). The weights of fluid and storage (W^G_{F+S} and W^A_{F+S}) are found by combining equations (6-12) and (6-21) and using the values of Z given in Table 6.6. The peak and average demands of the high load experiments are related by

$$P_{eh} = -200 + 0.800P_{ehp}, \quad 1500 \leq P_{ehp} \leq 4000 . \tag{6-25}$$

The calculated results for the three cases most favorable to the Apollo-type fuel cell system are summarized in Table 6.7 below.

$P_s + P_{ehp}$	≤ 3850	≤ 5775	≤ 6545
P_s	2350	2545	2545
P_{eh}	1000	1580	3000
P	2436	2678	2798
W^G_{FC}	340	476	544
W^A_{FC}	760	1140	1330
W^G_r	154	231	258
W^A_r	17.5	26.6	29.7
W^G_{F+S}	1995	2190	2290
W^A_{F+S}	1840	1955	2035
W^G_{tot}	2389	2897	3092
W^A_{tot}	2617	3121	3395

TABLE 6.7, COMPARISON OF GEMINI AND APOLLO WEIGHTS

From the total system weights shown in the last two lines of Table 6.7, it is apparent that the Apollo system is the heavier of the two by at least 224 pounds, in even these most favorable cases. Further, this margin consists entirely of basic hardware and not reactants which make water that might be used in some way to generate weight credits for the fuel cell system. It may be concluded that the Gemini type fuel cell system is definitely superior for the 30 day mission.

6.9 Credits for Fuel Cell Water

The product of the fuel cell reaction is water which may be utilized for astronaut drinking and hygiene, as a propellant for a mass expulsion attitude control system, or in a water boiler to augment the radiator during periods of high thermal load. The total weight of water produced is equal to the weight of reactants consumed which is nominally

$$W_w = 0.90 W_{H+O} \qquad (6\text{-}26)$$

where W_{H+O} is total reactant supply, including the contingency reserve, as given by equation (6-12). The maximum and minimum quantities of water produced are then 1650 and 666 pounds respectively. The corresponding rates of production are 55.0 and 22.2 pounds per day.

6.9.1 Water for Astronaut Uses

Assuming that the crew will be eating dehydrated food, the drinking water requirement will be about five pounds per man per day (p.m.p.d.)[39, 87] Since the crew will not be wearing pressure suits and because of the mission length, there will be both the opportunity and necessity for frequent bathing. The very minimum requirement for wash water is about two pounds p.m.p.d.[39] For long missions a more reasonable figure is about four to five pounds p.m.p.d.[46] For purposes of this study the water requirement will be taken as 9.5 pounds p.m.p.d. or 19 pounds total per day.

The alternatives to using fuel cell product water are to include about 600 pounds of fresh water in the payload or provide a water recovery system which allows recycling of a small inventory of fluid. The first choice is obviously absurd and so the second will be used here to analyze the credits due to fuel cell water if used for life support purposes.

The following sources of water are available for reclamation.[39]

urine	3.2 pounds p.m.p.d.
feces	0.4 pounds p.m.p.d.
insensible	2.2 pounds p.m.p.d.
wash water	4.5 pounds p.m.p.d.

Processing of feces can be immediately rejected because of the complex treatment required and the relatively small recovery.[71] The insensible water consists of vapor excreted by perspiration and respiration and is recovered by the humidity control system. The only processing for this water is filtration and ultraviolet sterilization which would be required for fuel cell water as well.[39, 71]

In most practical schemes for recovery of urine and wash water, purification consists of simple distillation followed by absorption, dyalisis, or pyrolysis to remove bacteria and organic constituents remaining. Finally, the water is filtered and sterilized by ultraviolet light as with the humidity control system condensate. Only a simple still system with activated carbon absorption will be considered here as weight estimates for pyrolysis and dialysis systems do not appear in the literature. The weight of filters and the ultraviolet lamp will not be evaluated as such equipment is required regardless of the water source.

In a study for the Air Force, a simple still using a hand operated blower and piston with a capacity of 4.9 pounds per day was estimated to have the following weight breakdown:[87]

Evaporator-condenser	19.7 lbs
Blower	1.0 lbs
Centrifugal separator	1.0 lbs
Holder for activated carbon	0.1 lbs

Storage tank and piston	2.5 lbs
Piping and check valves	1.2 lbs
Expendables	0.17 lbs/day

Even though the crew needs exercise, it seems advisable to replace the hand operated blower by a small motor. The same study estimates the weight of a motor for this use as 2.8 pounds.

The nominal quantity of water to be processed in the still is the sum of urine and wash water or 15.4 pounds. A small excess capacity should be provided so that a batch failing to meet purity standards can be reprocessed without causing buildup of a permanent backlog of waiting fluid. Hence, a nominal capacity of 20 pounds per day is specified. Using the weights given above and scaling linearly, the weight of a simple still is 120.6 pounds. An initial inventory of water and additional tankage is required so that reprocessing of a batch does not force rationing. One day's supply of water and associated tankage for this purpose weigh about 30 pounds.

A simple still of this type will recover about 85% of the water it processes.[38] With an input of 15.4 pounds per day, about 13.85 pounds are recovered. With 4.4 pounds per day recovered from the himidity control system, the total output is 18.25 pounds per day, a deficit of 0.75 pounds per day. A supplemental supply of about 25 pounds of water is required to replenish the losses. Associated tankage will be about 10 pounds. The total system weight is then about 185 pounds. A two day emergency water supply should also be provided in case of a complete breakdown in purification.[87] However, this weight is not included as it will be necessary even if fuel cell water us used.

The requirement for water was given earlier as 19 pounds per day. Regardless of whether a still or the fuel cell water is used, the humidity control system will recover 4.4 pounds per day. The daily requirement from the fuel cells is only 14.6 pounds. Thus, if about 440 pounds of the fuel cell product water is diverted to life support uses, a 185 pound credit can be applied to the fuel cell system. The ratio of these numbers is 0.421 and will be used as an index of efficiency in comparing alternative uses for the water.

6.9.2 Water Boiler

If a water boiler is included in the spacecraft cooling systems, the size and weight of the radiator can be reduced by expelling water vapor during periods of high thermal loading. Based on the experience of the Gemini spacecraft, the fuel cell will be the largest single source of waste heat. The nominal minimum thermal load on the radiator from all heat sources but the fuel cell is about 2300 BTU/hr while the nominal maximum is about 5200 BTU/hr for Gemini.[5] Most of this thermal load is associated with life support equipment similar to that which will probably be used in the MOL. Hence, the Gemini thermal loads exclusive of the fuel cell, are reasonable estimates of the thermal loads encountered in the MOL. It is also assumed that the environmental control system and fuel cell coolant loops are combined into a single system as in Gemini.

If P_{FC} is the power level at which the fuel cell is operating and η is its conversion efficiency, the thermal load, P_T, is

$$P_T = \frac{1-\eta}{\eta} P_{FC} \text{ watts} . \tag{6-27}$$

And if the number of surviving stacks at the end of the mission is just sufficient to satisfy the peak load, the load on each stack is 15 amperes, the maximum capacity. Using the efficiency function of Table 6.1, the corresponding efficiency is 54.1%. The peak thermal load of the fuel cell is then

$$P_{TP}^{fc} = 0.847\,(P_s + P_{ehp}) \text{watts} = 2.9\,(P_s + P_{ehp}) \text{ BTU/hr.} \tag{6-28}$$

The peak for the whole system is then

$$P_{TP}^{sys} = 5200 + 2.9\,(P_s + P_{ehp}) \text{ BTU/hr.} \tag{6-29}$$

The nominal constant thermal load is

$$P_{TC}^{sys} = 2300 + 2.9\,P_s \text{ BTU/hr.} \tag{6-30}$$

The periodic excess heat load is the difference between equations (6-30) and (6-29),

$$P_{pe} = 2900 + 2.9\, P_{ehp} \text{ BTU/hr.} \tag{6-31}$$

Referring to equation (6-6) and converting the units there, the weight of the radiator required to handle the excess heat is

$$W_r = k(33.9 + 3.39X10^{-2}\, P_{ehp}) \text{ pounds} \tag{6-32}$$

where k is the proportion of P_{pe} dumped by the radiator. Using equation (6-25), the radiator weight in terms of P_{eh} is

$$W_r = k(42.4 + 4.24X10^{-2}\, P_{eh}) \text{ pounds.} \tag{6-33}$$

Assuming the environmental control system maximum heat loads have a duration of four hours per day and using the data of Table 6.5, with a minimum fuel cell efficiency of 54.1%, the excess heat generated by these periodic loads is

$$H = 11600 + 5.80\, P_{eh} \text{ BTU/day.} \tag{6-34}$$

Water has a heat of vaporization of 539.4 BTU/lb so the weight of water required to remove this heat in a water boiler is

$$W_w = (1-k)(21.5 + 1.07X10^{-2}\, P_{eh}) \text{ lb/day} \tag{6-35}$$

The water boiler only need be a small tank wrapped with the coolant loop coils. The weight of the water boiler is taken as

$$W_{wb} = 5 + 0.5W_w \text{ pounds} \tag{6-36}$$

With all the weights thus known, the credit which is gained for use of W_w pounds of water per day is

$$W_{cr} = \frac{1-k}{k} W_r - 0.5W_w - 5 \text{ pounds} \tag{6-37}$$

or

$$W_{cr} = (1-k)\,(31.6 + 3.70X10^{-2}\,P_{eh}) - 5 \text{ pounds} \qquad (6\text{-}38)$$

The ratio of the weight credit to the weight of water used increases slowly as P_{eh} increases and ranges from 0.070 to 0.081. A simple linear relationship for the water credit is then

$$W_{cr} = (6.45X10^{-2} + 5.5X10^{-6}\,P_{eh})\,W_{wa} \qquad (6\text{-}39)$$

where W_{wa} is the weight of water available for these uses. Since the ratio of weight credit to water used is 0.421 for water used by the crew, the water used in the water boiler should come last in the order of priority. Using equations (6-12) and (6-26), and noting that ZP has a maximum value of 0.04, the approximate total weight of water created in the mission less that used by the crew is

$$W_{wa} = 0.60P - 440 \text{ pounds} \qquad (6\text{-}40)$$

From this availability function it is easily shown that the value of k is 1.0 only when P_s is a maximum and P_{eh} is a minimum. Hence all the excess water may be used in the water boiler. The maximum possible weight credit is 98.0 pounds.

6.9.3 Attitude Control

In appendix B various attitude control systems are considered including a mass expulsion system using water. Unfortunately, it is found that the water system is inferior to a nitrogen gas system because of the water heating requirements. Hence, no credit can be applied to the fuel cell system by using water for attitude control.

The remaining alternatives for attitude control are the magnetic torquer and nitrogen gas attitude control systems. The magnetic torquer system requires substantial power levels if it is to be competitive, weightwise, with the mass expulsion system. However, the maneuvers analyzed

in Appendix B are conducted when the experiments are demanding power and so would require an increase in the capacity of the fuel cell system. For the 30 day mission at least 44.6 amperes are required if the magnetic torquer system is to be lighter in weight than the equivalent mass expulsion system. Referring to Table 6.1, a full module of three stacks can deliver a peak load of 45 amperes and weighs 196 pounds. Thus, the weight of the basic fuel cell hardware not to mention the additional radiator, reactants, and storage, is heavier than the simple nitrogen gas system which has a weight of about 175 pounds. Consequently, the mass expulsion system should be selected for attitude control if the fuel cell power system is employed.

6.10 Fuel Cell Summary for the 30 Day Mission

The Gemini-type fuel cell is selected as superior to the Apollo type system because it has a significantly lower weight and generates more water which can be used to create weight credits for the system. Further, the Apollo fuel cell system has a doubtful ability to survive the 30 day mission while the Gemini system has demonstrated adequate life on test.

The weight of the basic fuel cell hardware for a 30 day mission is given in Table 6.8 as a function of the peak power, $P_s + P_{ehp}$.

$P_s + P_{ehp}$, WATTS	2625	3375	4500	5625	6375	6750
WEIGHT, POUNDS	204	272	340	408	476	544

TABLE 6.8, FUEL CELL HARDWARE WEIGHT

Noting that the value of the quantity ZP in equation (6-12) is a maximum of 0.04 and combining equation (6-12) with equation (6-21), the weight of the cryogenic fluids and the supercritical storage system chargeable to the fuel cell is

$$W_{F+S}^{fc} = 0.860P - 59.8 \text{ pounds} \qquad (6-41)$$

where

$$P = 2.6 + P_s + \frac{P_{eh}}{12} \text{ watts,} \tag{6-42}$$

the weighted average power level. The relationship between the peak and average demands of the high load experiments is

$$P_{eh} = -200 + 0.800\, P_{ehp} \tag{6-43}$$

For any combination of the life support and experimental loads, the system generates an adequate quantity of water for drinking and washing uses. By allocating 440 pounds of the product water to astronaut uses, the need for a water reclamation system is eliminated and the power system is given a credit of 185 pounds.

Water may also be used in a water boiler to reduce or eliminate the peak thermal loads sustained by the radiator. The credit for this use is rather small, a maximum of 98.0 pounds for the maximum values of P_s and P_{eh}. The water available for this use is

$$W_{wa} = 0.60P - 440 \text{ pounds} \tag{6-44}$$

where P is given by equation (6-41). The credit for water used in the boiler is

$$W_{cr} = (6.45X10^{-2} + 5.50X10^{-6}\, P_{eh})W_{wa} \tag{6-45}$$

Water was found to be unsuitable as a propellant for the attitude control system as a result of the heating requirements. The magnetic torquer system was also rejected because of the high power requirements. A nitrogen gas mass expulsion system weighing 175 pounds was finally selected for use with the fuel cell power source.

The volume required for the basic fuel cell hardware is given in Table 6.9.

$P_s + P_{ehp}$, WATTS	2625	3375	4500	5625	6375	6750
VOLUME, FT^3	5.4	7.2	9.0	10.8	12.6	14.4

TABLE 6.9, FUEL CELL HARDWARE VOLUME

The volume of the cryogenic storage tanks chargeable to the fuel cell is

$$V_t = 8.80 + 3.75X10^{-2} P \text{ cubic feet} \qquad (6\text{-}46)$$

where **P** is given by equation (6-42).

6.11 Fuel Cell System for a 60 Day Mission

Neither of the candidate fuel cell systems can be considered as having adequate lives to survive a 60 day mission. As a result the basic hardware weights will have to be more than doubled if the required reliabilities are to be achieved. Further, the cryogenic storage system used in the 30 day mission will require very substantial amounts of venting in order to deliver the required quantities of fluid for 60 days. Hence, the weight of fluids and storage may nearly triple over the value achieved for the 30 day mission. Finally, there will be no increase in the credits for the fuel cell water as neither the radiator nor the water recovery system will require significant weight increases.

Referring to Table 6.7, it was found that the Gemini type fuel cell system weighs on the order of 2000 to 3000 pounds for the 30 day mission. This range would probably increase to the 6000 to 8000 pound range for a 60 day mission as a result of the above cited reasons. These weights are about 30 to 40% of the entire spacecraft weight and are considered totally unacceptable. Indeed, it is unlikely that there would be room or weight for experiments. It may be concluded that the fuel cell system is impractical for a 60 day mission.

7. INTEGRATED FUEL CELL/SOLAR CELL SYSTEM

In part 5 of this study an integrated battery/solar cell power system was analyzed. This system is rather conventional and there is a large backlog of experience associated with it. Another possible integrated power system can be formed by combining the fuel cell with the solar array. Regenerative systems of this type which use the power of the solar array to reverse the fuel cell and generate hydrogen and oxygen have been studied. However, none of the regenerative fuel cells presently in development are expected to be ready for flight test for some years.[79] An alternative approach to such an integrated system is to combine the primary Gemini-type fuel cell with an array and allow the two power sources to share the daylight loads and use the fuel cell alone for the shadow loads.

Only the Gemini system will be considered as it has already been shown to be of lower weight than the Apollo system. Also, only a 30 day mission will be analyzed at the cryogenic storage system is inadequate for a 60 day mission.

7.1 Division of Loads at the Peak Power Level

By adding a solar array to the fuel cell system, the weights of part of the radiator, part of the fuel cell hardware, and part of the reactants and cryogenic storage are traded for the weight of the solar array. The fuel cell must still be adequate to deliver P_s watts (the minimum continuous load varying from 1045 to 2545 watts) during the shadow time. Referring to Table 6.3, two fuel cell system configurations are of interest. These are a two module system with a peak capacity of 1500 watts (at a 99.5% probability of mission success) weighing 136 pounds and a three module system with a capacity of 2625 watts weighing 204 pounds. Since capacity is added in increments of 1125 watts, an excess capacity is likely to be available and it is useful to determine whether or not it should be used in daylight.

Referring to equation (6-41), a one watt increase in a continuous load requires a 0.860 pound increase in the weight of reactants and tankage. Or put in a slightly more useful way, if a load occurs for t hours in a 24 hour day, a 0.0358t pound increase in the weight of reactants and storage is required. Using equation (6-6), if the power supplied by the fuel cell during daylight exceeds P_s, but not 1500 or 2625 watts as appropriate, additional radiator capacity must be added at the rate of 0.04 pounds per watt in excess of P_s. From equation (3-28), the cost of adding solar array is 0.0981 pounds per watt. Equating the weight increases in the fuel cell and solar cell system for the case of the fuel cell delivering less than P_s watts in daylight, it is more economical to add solar array if the load duration exceeds 2.74 hours per day ($t = 0.981/0.0358$). If the load exceeds P_s, it is more economical to add solar array if the load duration exceeds 1.62 hours ($t = 0.0581/0.0358$).

Using these rules we can examine the worst case. The peak load occurs when P_{ehp} (the peak experimental load) and P_s are coincident. Referring to Table 1.2, $P_s + \frac{1}{2} P_{eh}$ of this load occurs for 2.5 hours per day, $\frac{1}{2} P_{eh}$ occurs for 1.5 hours per day, and $P_{ehp} - P_{eh}$ is a transient load. The maximum value of $P_{ehp} - P_{eh}$ is 1000 watts and so is always less than P_s. The fuel cell should supply this load. The load $\frac{1}{2} P_{eh}$ occurs for less than 1.65 hours per day and should be supplied to the limit of the fuel cell capacity even if extra radiator is required. The other $\frac{1}{2} P_{eh}$ of the experimental load occurs only 2.5 hours per day so that if the load $(P_{ehp} - P_{eh}) + \frac{1}{2} P_{eh}$ is less than P_s, the full value of P_s should be supplied by the fuel cell. If the fuel cell can supply all the experimental load without additions to the radiator, it should do so. The fuel cell should never supply more than P_{ehp} because the rest of the load is continuous. The solar array is sized to satisfy $P_s + P_{ehp}$ minus the load satisfied by the fuel cell.

Using these rules for load division, the sizing of the system is simply defined by considering two cases and several subcases.

1. If $P_s \leq 1500$ watts, the two module system is used. In this case $P_s \leq P_{ehp}$ so that the capacity of the system is less than or equal to the experimental load. The subcases are:

   a. If $P_s \geq P_{ehp} - \frac{1}{2} P_{eh}$, the fuel cell should deliver only P_s watts at the peak. The array is then sized to deliver P_{ehp} watts.

   b. If $P_s \leq P_{ehp} - \frac{1}{2} P_{eh} < 1500$, additional radiator should be added so that the fuel cell can deliver $P_{ehp} - \frac{1}{2} P_{eh}$ watts at the peak. The array is sized to deliver $P_s + \frac{1}{2} P_{eh}$ watts.

   c. If $P_{ehp} - \frac{1}{2} P_{eh} \geq 1500$, the fuel cell should deliver the full 1500 watts at the peak. The array is sized to deliver $P_s + P_{ehp} - 1500$ watts.

2. If $1500 \leq P_s \leq 2545$ watts, the three module system is used. In this case P_s may exceed P_{ehp}. The subcases are:

   a. If $P_s \geq P_{ehp}$, the fuel cell has the capacity to supply the full experimental load and should then deliver P_{ehp} watts at the peak condition. The solar array is sized to deliver P_s watts.

   b. If $P_s \geq P_{ehp} - \frac{1}{2} P_{eh}$, the fuel cell should deliver P_s watts at the peak condition. The array is then sized to deliver P_{ehp} watts.

   c. If $P_s \leq P_{ehp} - \frac{1}{2} P_{eh}$, the fuel cell should deliver $P_{ehp} - \frac{1}{2} P_{eh}$ watts, at the peak condition. The array is then sized to deliver $P_s + \frac{1}{2} P_{eh}$ watts.

The size of the array is defined by these peak conditions which last only a few seconds per orbit. When the load is off peak, the array should still be used at full capacity so that the smallest quantities of reactants are consumed. The magnitude of the daylight loads in excess of P_s and their durations are

LOAD	DURATION
P_{eh}	90 min/day
$\frac{1}{2} P_{eh}$	60 min/day
500	1.28 min/day
100	10 min/day
20	120 min/day

TABLE 7.1, SCHEDULE OF LOAD LEVELS AND DURATIONS

In all cases considered above, the solar array has at least the capacity to deliver P_s so that only those sunlight loads in excess of P_s can possibly be satisfied by the fuel cell if the solar array is used to full capacity. Assuming that the transients due to the experiment loads consume insignificant quantities of power,* the loads satisfied by the fuel cells and their sunlight durations are given in the following listing. The cases and subcases are numbered as before.

1. $P_s \leq 1500$ watts
   a. $P_{eh} + P_s - P_{ehp}$ 90 min/day
      $\frac{1}{2} P_{eh} + P_s - P_{ehp}$ 60 min/day
      $500 + P_s - P_{ehp}$ 1.28 min/day
      $100 + P_s - P_{ehp}$ 10 min/day
      $20 + P_s - P_{ehp}$ 120 min/day
   b. $\frac{1}{2} P_{eh}$
      The array can handle all other loads.
   c. The array can handle all daylight loads.
2. $1500 \leq P_s \leq 2545$ watts
   a. P_{eh} 90 min/day
      $\frac{1}{2} P_{eh}$ 60 min/day
      500 1.28 min/day
      100 10 min/day
      20 120 min/day
   b. Same schedule as for 1a above.
   c. Same schedule as for 1b above.

In addition to these daylight loads, the fuel cell supplies P_s watts for 39 minutes of each orbit as does the battery.

7.2 Cryogenic Storage

The preceding results indicate that most of the reactant and storage requirements for the mission will be a result of the shadow time load. This

*If transient loads with a magnitude of 1000 watts are sustained for 6 seconds per day, the total energy which they consume in the mission amounts to only five watt hours.

conclusion is illusory however. Even though the fuel cell will not be consuming reactants for much of the mission, fluid must be drawn from the tanks at a rate at least equal to the minimum steady flow rate due to heat leak. Hence, venting is required.

The cryogenic storage system used with the integrated fuel cell/ solar cell system is the same as that discussed in section 6.7. It consists of two hydrogen tanks and two oxygen tanks. Oxygen storage for the environmental control system is combined with oxygen storage for the fuel cells so that the minimum steady flow rate for oxygen is five pounds per day. This combination will result in significantly lower venting than if the ECS oxygen system were separate.

Expressions (6-14) and (6-15) were given as inequality tests of whether the cryogenic storage system could go through the mission without venting. These same expressions may be used as equations in which case they directly relate the quantity of fluid required to the minimum steady flow rate. In order to give a conservative bias, the constant terms in the expressions are slightly reduced to give the following equations.

$$\frac{W_H}{\dot{w}_{H_{min}}} = 30 + 0.104W_H \qquad (7\text{-}1)$$

$$\frac{W_O}{\dot{w}_{O_{min}}} = 35 + 0.0182W_O \qquad (7\text{-}2)$$

The minimum flow rate for hydrogen is simply the vent rate in pounds per day. The minimum flow rate for oxygen is the sum of the vent rate and the flow rate for life support (five pounds per day). The weight of hydrogen, W_H, is the sum of the weight required for the fuel cells (including a contingency supply) and the weight of fluid vented. The weight of oxygen, W_O, is the sum of the weight required for the fuel cells, the weight of vented fluid and 150 pounds of oxygen for life support. The weight of vented fluid

in either case is the product of the vent rate and the vent time. The vent time can be found by considering the schedule of demands on the fuel cells. Venting will generally be required if the fuel cell is not supplying at least $\frac{1}{2} P_{eh}$ watts.

The sum of the weight of hydrogen and oxygen used by the fuel cell is

$$W_{O+H}^{fc} = \frac{30 \Sigma P_i t_i}{2000 \eta} \text{ pounds} \tag{7-3}$$

where

P_i = the i^{th} load, watts

t_i = the duration of the i^{th} load, hours/day

η = the efficiency of the fuel cell.

The values of P_i and t_i are given for all the various cases in section 7.1. The efficiency will vary only slightly as most of the fuel cell energy is delivered at the P_s load level. Using equation (6-8) and the Gemini efficiency function of Table 6.1 the efficiency is found to vary little from 60%. Using this efficiency and adding an 11% contingency allowance as was done in section 6.6, the total weight of fluids provided for use by the fuel cell is

$$W_{O+H}^{fc} = 0.0278 \Sigma P_i t_i . \tag{7-4}$$

Since hydrogen and oxygen are used in a stoichiometric ratio, the weights W_H^{fc} and W_O^{fc} may be easily determined. Then the venting rates are

$$\dot{w}_{HV} = \frac{W_H - 0.111 W_{O+H}^{fc}}{t_V} \tag{7-5}$$

and

$$\dot{w}_{OV} = \frac{W_O - 150 - 0.889 W_{C+H}^{fc}}{t_V} \tag{7-6}$$

where t_V is the venting time in days. Hence, by using equations (7-1), (7-2), and (7-4) through (7-6) the total weight of each reactant is determined.

By modifying equations (6-16) and (6-18) to include the weight of fluid and subtracting the weight of a separate oxygen system for life support, the total weight of fluids and storage chargeable to the fuel cell part of the system is

$$W_{F+S}^{fc} = -84.0 + 1.1614W_O + 2.25W_H \qquad (7\text{-}7)$$

7.3 Credits

It was found in section 6.9.1 that at least 440 pounds of water must be available if the system is to be credited for a 185 pound saving in the weight of a water recovery system. The water generated is equal to 90% of W_{O+H}^{fc} given in equation (7-4). Hence, if

$$\Sigma P_i t_i \geq 17,600 \qquad (7\text{-}8)$$

the credit for drinking water may be used. The values of $\Sigma P_i t_i$ for the various cases are:

$$1a.\quad 14.7P_s - 3.85P_{eh} - 886 \qquad (7\text{-}9a)$$

$$1b.\quad 10P_s + 0.75\,P_{eh} \qquad (7\text{-}9b)$$

$$1c.\quad 10P_s \qquad (7\text{-}9c)$$

$$2a.\quad 10P_s + 2P_{eh} + 57.6 \qquad (7\text{-}9d)$$

$$2b.\quad 14.7P_s - 3.85P_{eh} - 886 \qquad (7\text{-}9e)$$

$$2c.\quad 10P_s + 0.75P_{eh}\,. \qquad (7\text{-}9f)$$

Using these values, the water credit cannot be applied to cases 1a through 1c. The conditions under which the water credit may be applied to the other cases are:

$$2a.\quad P_s + 0.200P_{eh} \geq 1755 \qquad (7\text{-}10a)$$

$$2b.\quad P_s - 0.262P_{eh} \geq 1260 \qquad (7\text{-}10b)$$

$$2c.\quad P_s + 0.075P_{eh} \geq 1760\,. \qquad (7\text{-}10c)$$

The fuel cells generate very little water as is seen from the preceding discussion of credits for drinking water. However, even with this small amount of water, the additional radiator added to the system for the short duration peak loads can be eliminated by simply using the stored water as a heat sink. These loads are so short that probably no water will be vaporized but only a small temperature rise will result. The remainder of the heat load from the fuel cell is semi-continuous and should be handled by the radiator. Hence, the radiator weight chargeable to the fuel cell is only

$$W_r^{fc} = 0.04 P_s \tag{7-11}$$

in all cases.

As for the heat load of the life support system, the credit due to using a water boiler is found by taking P_{eh} equal to zero in equation (6-39). The credit is then

$$W_{cr} = 6.45 X 10^{-2} W_{wa} \tag{7-12}$$

where

$$W_{wa} = .90 W_{O+H}^{fc} = 0.0250 \Sigma P_i t_i \tag{7-13}$$

If credit is given for elimination of the water recovery system, W_{wa} should be reduced by 440 pounds.

In Appendix B it was shown that water is unsuitable as a propellant for attitude control. The possible attitude control systems are the magnetic torquer and the nitrogen gas mass expulsion system. The magnetic torquer system unfortunately requires significant quantities of power. In order to be competitive with the mass expulsion system, a current of at least 41.3 amperes should be used. To supply a demand of this magnitude, an increase of 108 pounds in the weight of the array or 110 pounds in the weight of the fuel cell hardware and radiator would be required. This addition to the power system weight totally negates any advantage gained

in the attitude control system. Hence, the nitrogen gas mass expulsion system with a weight of 230 pounds should be used with the integrated fuel cell/ solar cell system.

7.4 System Weight Summary

The weight of all components of the power system have been determined above in either numerical or equation form. These weights are now summarized in a convenient listing along with the volume of the system according to the various cases and sub cases defined in section 7.1.

A few comments apply to all cases. First, the radiator weight is

$$W_r = 0.04P_s \tag{7-11}$$

Second the weight of the attitude control system is 230 pounds. Third, the weight and volume of the cryogenic storage system and reactants chargeable to the fuel cell is found by a single procedure with a single set of equations for all cases. The total weight of hydrogen is found by simultaneous solution of equations (7-1) and (7-5). The total weight of oxygen is similarly found from equations (7-2) and (7-6). The weight chargeable to the power system is then given by equation (7-7). The volume of tankage chargeable to the power system is found from equations (6-17) and (6-19) as

$$V_t^{fc} = 1.1 + 0.0193W_O + 0.354W_H \text{ ft}^3 \tag{7-14}$$

The special characteristics of the various cases are now listed.

Case 1. $P_s \geq 1500$ watts

In all three subcases the fuel cell hardware weigh 136 pounds and has a volume of 3.6 cubic feet. There is no credit for drinking water.

a. $P_s \geq P_{ehp} - \frac{1}{2} P_{eh}$ watts

The solar array weight is

$$W_{sa} = 64.6 + 0.0981\ P_{ehp} \tag{7-15}$$

The weight of reactants stored for use in the fuel cell is

$$W^{fc}_{H+O} = 0.409P_s - 0.104P_{eh} - 24.6 \tag{7-16}$$

The total venting time is

$$t_V = 11.5 \text{ hr/day} = 14.4 \text{ days/30 days} \tag{7-17}$$

b. $P_s \leq P_{ehp} - \frac{1}{2} P_{ehp}$ watts 1500

$$W_{sa} = 64.6 + 0.0981\ (P_s + \tfrac{1}{2} P_{eh}) \tag{7-18}$$

$$W^{fc}_{H+O} = 0.278P_s + 0.0208P_{eh} \tag{7-19}$$

$$t_V = 12.5 \text{ hr/day} = 15.6 \text{ days/30 days} \tag{7-20}$$

c. $P_{ehp} - \frac{1}{2} P_{eh} \geq 1500$

$$W_{sa} = -82.5 + 0.0981\ (P_s + P_{ehp}) \tag{7-21}$$

$$W^{fc}_{H+O} = 0.278P_s \tag{7-22}$$

$$t_V = 1\ \text{hr/day} = 17.5 \text{ days/30 days} \tag{7-23}$$

Case 2. $1500 \leq P_s \leq 2545$

In all these subcases, the fuel cell hardware has a weight of 204 pounds and a volume of 5.4 cubic feet.

a. $P_s \geq P_{ehp}$

$$W_{sa} = 64.6 + 0.0981P_s \tag{7-24}$$

$$W^{fc}_{H+O} = 0.278P_s + 0.0556P_{eh} + 1.60 \tag{7-25}$$

$$t_V = 11.5 \text{ hr/day} = 14.4 \text{ days/30 days} \tag{7-26}$$

$$\text{If } P_s + 0.2P_{eh} \geq 1755 \tag{7-27}$$

a 185 pound credit is given for drinking water.

b. $P_s \geq P_{ehp} - \frac{1}{2} P_{eh}$

$$W_{sa} = 64.6 + 0.0981 P_{ehp} \tag{7-28}$$

$$W_{H+O}^{fc} = 0.409 P_s - 0.104 P_{eh} - 24.6 \tag{7-29}$$

$$t_V = 11.5 \text{ hr/day} = 14.4 \text{ days/30 days} \tag{7-30}$$

$$\text{If } P_s - 0.262 P_{eh} \geq 1260 \tag{7-31}$$

a 185 pound credit is given for drinking water.

c. $P_s \leq P_{ehp} - \frac{1}{2} P_{eh}$

$$W_{sa} = 64.6 + 0.0981 (P_s + \tfrac{1}{2} P_{eh}) \tag{7-32}$$

$$W_{H+O}^{fc} = 0.278 P_s + 0.0208 P_{eh} \tag{7-33}$$

$$t_V = 12.5 \text{ hr/day} = 15.6 \text{ days/30 days} \tag{7-34}$$

$$\text{If } P_s + 0.075 P_{eh} \geq 1760 \tag{7-35}$$

a 185 pound credit is given for drinking water.

8. SYS TEM COMPARISONS

8.1 Weight and Volume for a 30 Day Mission

The weight and volume characteristics of the integrated battery/ solar cell system for the fuel cell system and the integrated fuel cell/ solar cell system are summarized in sections 5.3, 6.10, and 7.4 respectively. In Figure 8.1 the weights of the three systems, including all credits and the attitude control system, are compared as functions of the minimum continuous load, P_s. A range of weights is shown for each system; the lower boundary corresponds to the minimum value of the experiment load, P_{eh}; and the upper boundary is for the maximum experiment load. Figure 8.2 is a similar comparison of the volumes of the various systems. From these two figures it is apparent that the battery/ solar cell system is superior to both alternatives in terms of weight and is also the lowest in volume for the most part.

An explanation about the various discontinuities in Figures 8.1 and 8.2 is in order. In the case of the fuel cells, all sudden increases in weight and volume are associated with the addition of another module to the system. In contrast, weight is added on a continuous basis to the battery/ solar cell system; the slight break in the curves for this system at 1800 watts is attributable to the increased weight of the battery charger as the rating exceeds 900 watts (see section 4.8.2). The behavior of the fuel cell/ solar cell system involves a few more considerations. First, at a P_s of 1500 watts another fuel cell module is added to the system and this increased capacity results in a reduction of the solar array area. At low peak loads the net effect is a weight and volume increase while with high peak loads there is a net decrease in weight and volume. Second, depending on P_{eh}, somewhere between values of 1535 watts and 1555 watts for P_s, the system generates enough water to be credited with a 185 pound saving in the weight of a water recovery system. Hence, the system weight is suddenly reduced

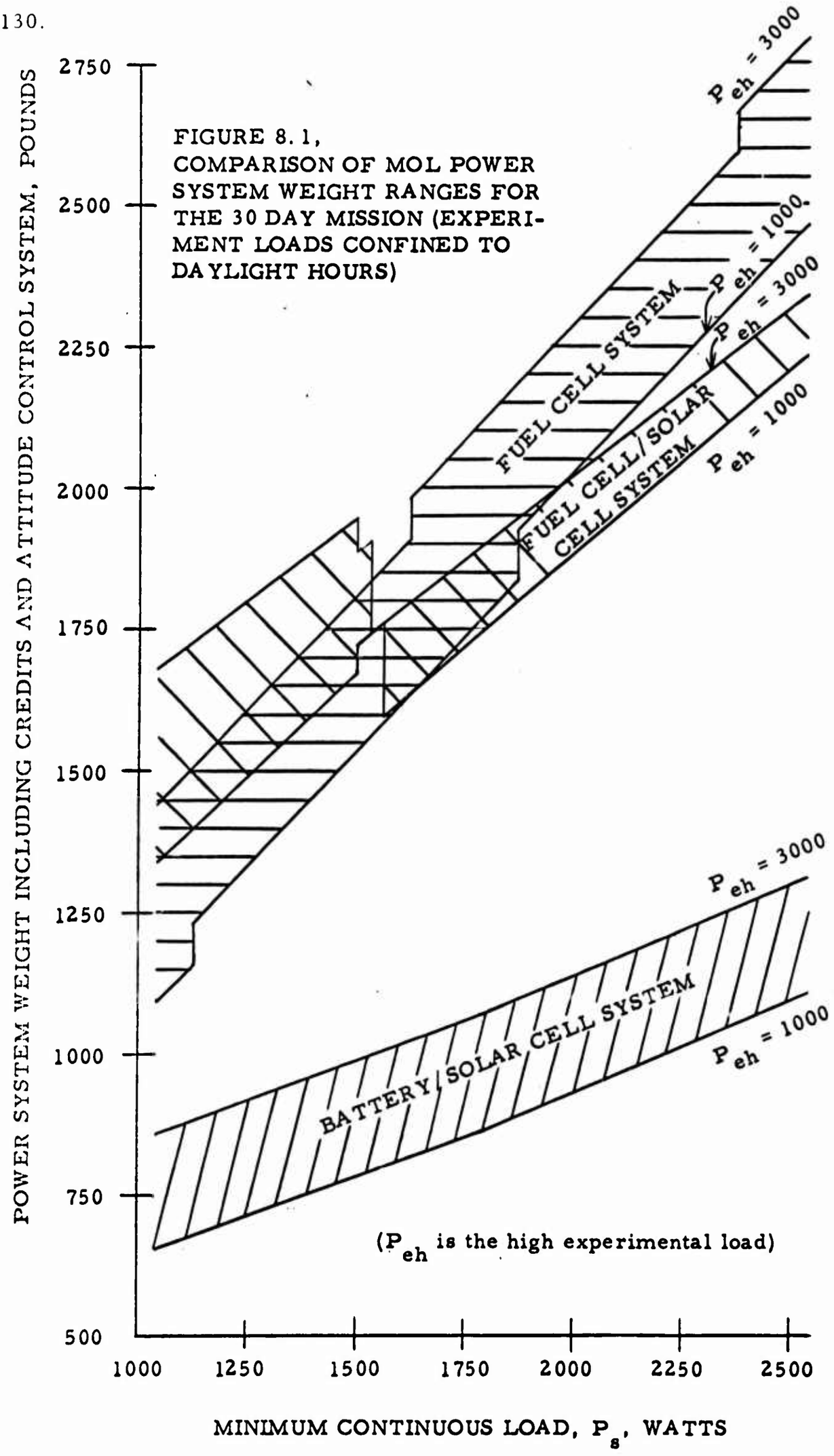

FIGURE 8.1,
COMPARISON OF MOL POWER SYSTEM WEIGHT RANGES FOR THE 30 DAY MISSION (EXPERIMENT LOADS CONFINED TO DAYLIGHT HOURS)

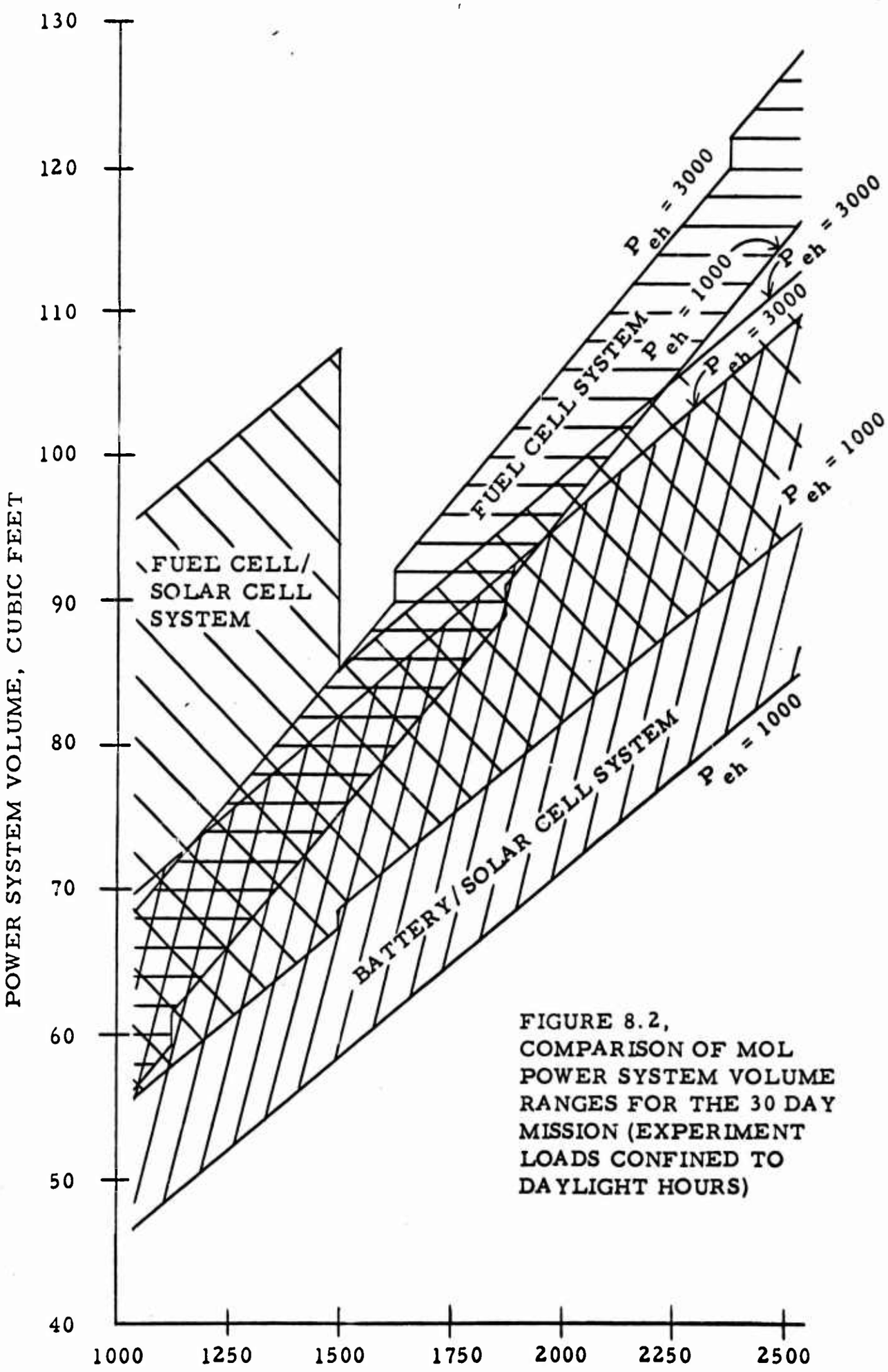

FIGURE 8.2,
COMPARISON OF MOL
POWER SYSTEM VOLUME
RANGES FOR THE 30 DAY
MISSION (EXPERIMENT
LOADS CONFINED TO
DAYLIGHT HOURS)

when sufficient water is available. The very tiny weight penalty incurred by increasing P_{eh} in this range is somewhat artificial since in a real mission a small quantity of stored water could be used to make up the difference between the needs of the crew and the production of the fuel cell. The size of the credit would be reduced of course but a lower overall system weight will result by carrying the supplemental water.

8.2 Analysis of the Weight Differences for a 30 Day Mission

The weight disparity between the battery/ solar cell system and the two alternatives warrants some discussion. The fuel cell system is examined first. Combining equations (6-41) and (6-42), the weight of fluids and storage for the fuel cell system is

$$W_{F+S}^{fc} = -57.4 + 0.860P_s + 0.0717P_{eh} . \qquad (8\text{-}1)$$

The weight of the entire battery/ solar array system (not including attitude control) is given by equations (5-2a) and (5-2b) as

$$W_{B/SC} = 78.6 + 0.352P_s + 0.0981P_{eh}, \quad P_s \leq 1800 \qquad (8\text{-}2)$$

$$W_{B/SC} = 70.6 + 0.356P_s + 0.0981P_{eh}, \quad P_s \geq 1800 \qquad (8\text{-}3)$$

Comparing the equations for the two systems, it is easily seen that the value of W_{F+S}^{fc} is minimized with respect to $W_{B/SC}$ when P_s is minimum (1045 watts) and P_{eh} is a maximum (3000 watts). At these conditions the value of W_{F+S}^{fc} is 317 pounds more than that of $W_{B/SC}$ without including a credit for water. Clearly, the path to reductions in the fuel cell system weight is through increasing the efficiency of the energy conversion process.

The maximum theoretical efficiency of a fuel cell may be expressed as the ratio of the free energy change (ΔF) to the change in heat content (ΔH). The maximum theoretical efficiency is then 83.0%. Using equations (6-9), (6-10), and (6-21), the weight of fluids and storage for an 83% efficient fuel cell used in this mission is

$$W_{F+S}^{fc} = -58.0 + 0.618P_s + 0.0515P_{eh} . \qquad (8-4)$$

Comparing the fuel cell once again to the battery/ solar cell system at the conditions most advantageous to the former, the value of W_{F+S}^{fc} just equals the value of $W_{B/SC}$. Hence, even if the fuel cell hardware could be developed to deliver the theoretical maximum efficiency, the system could be only marginally superior to the battery/ solar cell system as most of the credit for water would be absorbed by the weight of the fuel cell hardware and radiator. It may be concluded then, that even advanced fuel cells are unlikely to displace current state of the art battery/ solar cell systems for this mission.

The weight disparity for the integrated fuel cell/ solar cell system is in part due to the weight of reactants used by fuel cells as discussed above. However, another factor which is of importance is the requirement for venting fluid when the fuel cell is not in use. This fluid is totally wasted and could not result in a reduction in system weight, even if used, as the fuel cell hardware and solar array are sized to the peak power requirement and not an energy requirement. But even the elimination of venting would not make the fuel cell/ solar cell system competitive with the battery/ solar cell system. This fact is best illustrated by an example. Let the value of P_s be 2545 watts (the maximum) and the value of P_{eh} be 1000 watts (the minimum). From equations (7-4) and (7-9d) the weight of hydrogen and oxygen required by the fuel cell is then 764 pounds. Using this value and equation (7-7), the total weight of fluid and storage chargeable to the fuel cell for an unvented system is 893 pounds. Then using equations (7-1), (7-2), and (7-5) through (7-7) the total weight of fluid and storage chargeable to the fuel cell for vented systems is 1525 pounds so that 632 pounds could be saved in the system weight if it is not necessary to vent fluid. However, Figure 8.1 shows that the weight difference between the systems at the specified conditions is over 1000 pounds. Thus the fuel cell/ solar cell system cannot match the battery/ solar cell system in weight.

The power conditions used for this example were chosen to give the fuel cell/ solar cell system the greatest advantage as less fluid will be vented at other power levels while the weight disparity is at least as great. It may be concluded then that neither of the alternatives presented in this study appears to have the potential to displace the battery/ solar cell system for this mission.

8.3 Effect of Requiring Experiments in Shadow on the 30 Day Mission

At the beginning of this study it was specified that all experiments requiring electrical power be performed in daylight. However, this requirement may be an unreasonable restriction in light of the military potential of this program. Hence, the effect of requiring experiments in the earth's shadow should also be considered.

The fuel cell system is unaffected by conditions of shadow or illumination, and hence is not changed by addition of this requirement. The integrated fuel cell/ solar cell system degenerates to the simple fuel cell system as the fuel cell capacity must be adequate to supply the peak load. The solar array will then represent only excess capacity which is never needed and so is redundant. The battery/ solar cell system requires an increase in the size of the battery adequate to satisfy the demand of the high load experiments, P_{eh}. The additional battery capacity need not be sized to the additional peak load, P_{ehp}, as batteries have an excellent ability to handle short duration overloads.

Then weight of the solar cell/ battery system required for this new condition may be found from equation (8-3) by replacing the power level P_s by the sum of P_s and P_{eh}. The weight of the system is then

$$W_{B/SC} = 70.6 + 0.356P_s + 0.454P_{eh} . \qquad (8\text{-}5)$$

A further weight increase suffered by the battery/ solar cell system is in the attitude control system. Since the battery must supply all power during shadow there is no excess available for a magnetic torquer system. Either

extra battery and array capacity could be added to supply the needed power or a 230 pound nitrogen gas mass expulsion system, analyzed in Appendix B, could be used. Referring to section 4.13, 6.46 pounds of battery and array are necessary to provide an extra ampere of current during the shadow time. If the magnetic torquer is to weigh less than the mass expulsion system, at least 41.3 amperes must be used. The weight added to the power system would then be at least 268 pounds or more than the weight of the mass expulsion system. Hence, the 230 pound nitrogen gas attitude control system should be used.

The weight of the battery/ solar cell system required to satisfy the demands of full load experiments in both light and shadow is compared to the fuel cell system weight in Figure 8.3. These weights include the attitude control system and all credits. From Figure 8 3 it is apparent that the fuel cell system has the lowest weight for some of the possible conditions. The combinations of loads which result in equal weights are shown in Figure 8.4. To the right side of the line of equal weight the battery solar cell system has the lowest weight while the fuel cell has the lowest weight to the left of the line.

This example serves to illustrate that power levels and mission durations are not the only determinants of the optimum power system. If shadow time experiments are not required, the fuel cell is 450 to 1500 pounds heavier than the battery/ solar cell system. However, the addition of shadow time experiments not only makes the fuel cell competitive, but also makes it up to 550 pounds lighter than the alternative.

8.4 The 60 Day Mission

Only the battery/ solar cell system was analyzed for the conditions of a 60 day mission as the fuel cell system becomes prohibitively heavy for this long duration. The basic fuel cell hardware does not have sufficient life to be used for 60 days of continuous operation so that this part of the system would probably require complete redundancy to meet reliability

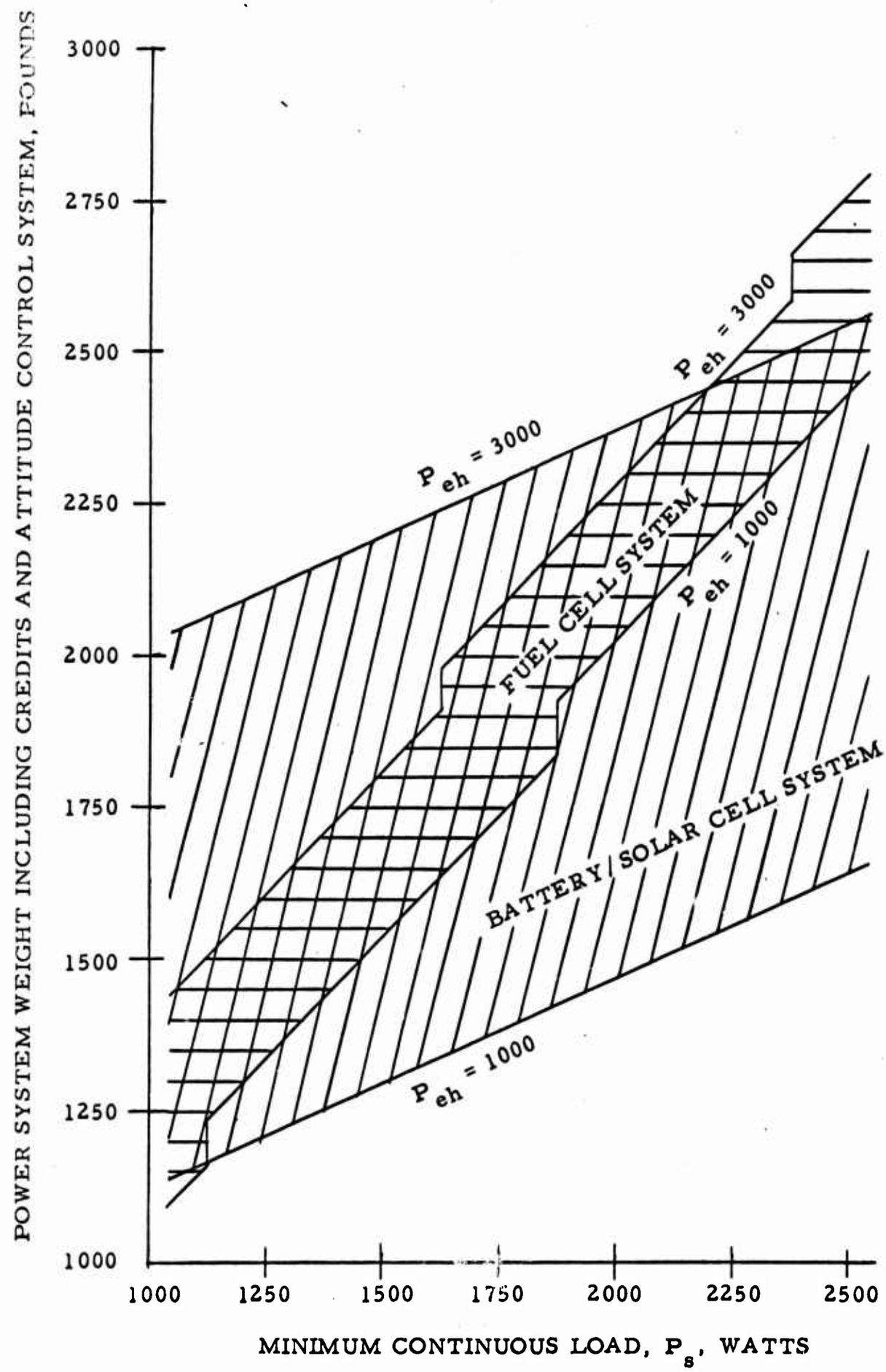

FIGURE 8.3, COMPARISON OF MOL POWER SYSTEM WEIGHT RANGES FOR THE 30 DAY MISSION (EXPERIMENTS REQUIRED DURING SHADOW)

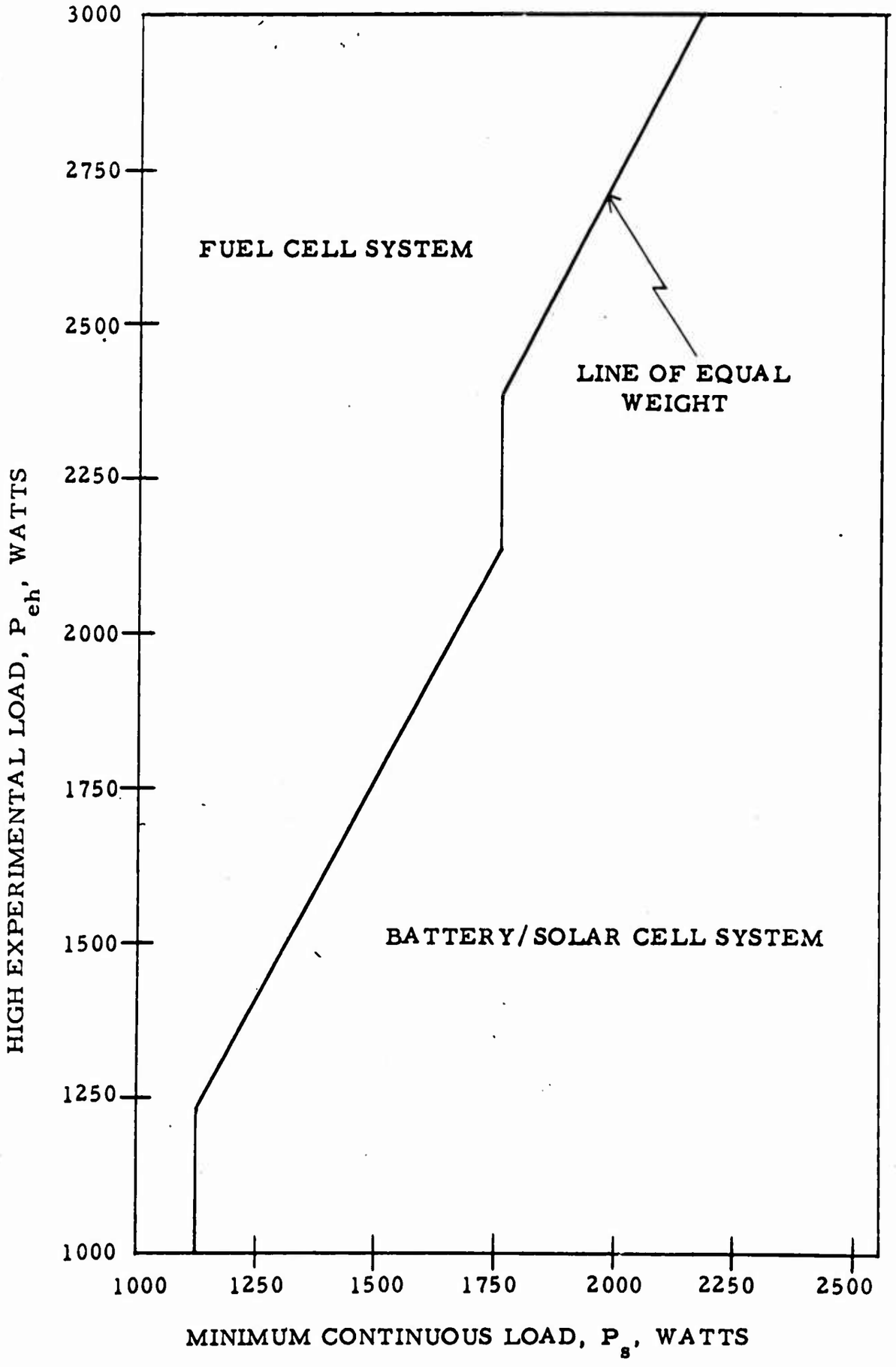

FIGURE 8.4, ZONES OF LOWEST WEIGHT AS FUNCTIONS OF THE ELECTRICAL LOADS FOR THE 30 DAY MOL MISSION (EXPERIMENTS REQUIRED IN SHADOW)

goals. The weight of reactants will be at least doubled if only because the mission length is doubled. Further, the cryogenic storage system does not have the ability to store fluids for 60 days without venting. From these considerations the fuel cell system will more than double in weight when the mission length is doubled.

On the other hand, the battery/solar cell system is essentially unchanged by doubling the mission length. The same battery configuration and weight are adequate for both mission lengths. The only weight increase in this system is a slight addition to the solar array to compensate for increased radiation degradation. Using expressions (5-3a) and (5-3b) the weight increase is a maximum of 15.3 pounds and may be as little as 4.9 pounds if no experiments are required during the shadow time. If experiments are required in shadow, the weight penalty for doubling the mission length ranges from 10.5 to 27.3 pounds depending on the values of P_s and P_{eh}.

If the mission length is to be eventually expanded to 60 days, the battery/solar cell system is the only choice for power. This system has the further advantage of requiring nearly insignificant increases in weight for a doubling of mission length.

CONCLUSION

The characteristics of fuel cell, solar cell, and battery power systems and possible combinations of these systems have been analyzed in detail for the requirements of the Manned Orbiting Laboratory mission. For a mission of 30 days the battery/ solar cell system has the lowest weight of the alternatives by a very wide margin if power for experiments is not required during the shadow time. If such loads are required during the shadow time, either the battery/ solar cell system or the fuel cell system may be the lowest in weight depending on the type and magnitude of the loads. For a 60 day mission only the battery/ solar cell system can be seriously considered for virtually any set of requirements.

APPENDIX A

BATTERY TEMPERATURE ANALYSIS

A.1 Procedure and Derivations

For the analysis of part 4 of this study to be valid, it is necessary to insure that the battery temperature remains at 25 ± 10°C as the battery performance parameters are very much temperature dependent. This appendix describes and analyzes a static heat rejection scheme in which the battery is mounted directly on a cold plate that radiates to space and so maintains this temperature range.

The battery is installed in the equipment and experimental apparatus section of the spacecraft. The ambient temperature in this section is assumed to vary between 0°C and 60°C depending on the heat generation rate of equipment in the spacecraft, whether the spacecraft is in sunlight, and its orientation to sun. In Figure A-1 there is a schematic of the battery package and cold plate showing the heat flows.

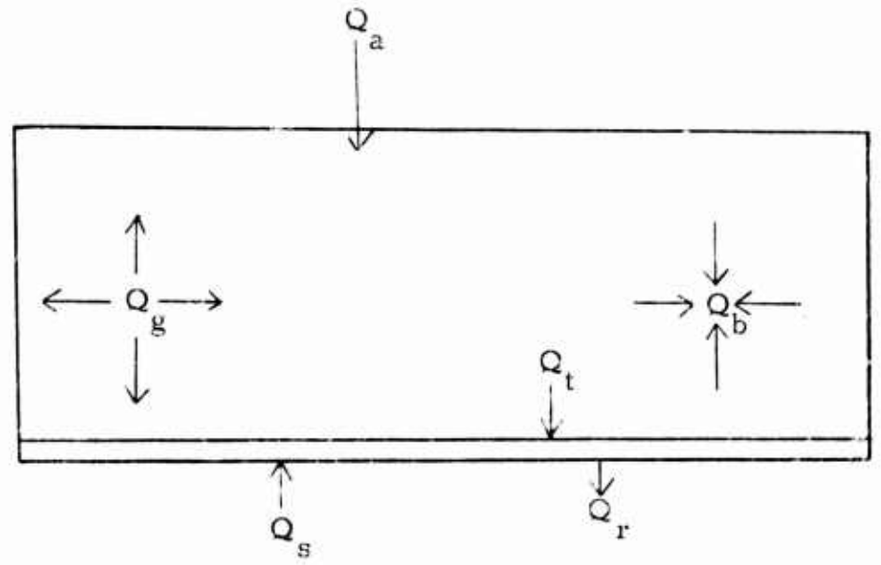

FIGURE A-1, BATTERY SCHEMATIC

The rate qualities shown in the figure are defined as:

Q_a = rate of heat input from surroundings

Q_g = rate of internal heat generation in the battery

Q_s = rate of solar heat input

Q_t = rate of heat transfer from the battery to the cold plate

Q_r = rate of heat radiation from the cold plate

Q_b = rate of heat storage by the battery

It is convenient to sum all the variable heat sources(Q_a, Q_g, and Q_s) as a single variable heat input, Q_i. From conservation of energy considerations:

$$Q_r = Q_t \tag{A-1}$$

$$\text{and} \quad Q_i = Q_b + Q_t . \tag{A-2}$$

The expressions for Q_b, Q_t, and Q_r are

$$Q_b = W_b c \frac{dT}{d\theta} , \tag{A-3}$$

$$Q_t = UA_p(T_b - T_p) , \tag{A-4}$$

$$Q_r = \sigma \epsilon_p A_p T_p^4 . \tag{A-5}$$

where

W_b = battery weight = $3.08 I_s$

c = specific heat = 0.360 BTU/LB - ^oK[64]

U = overall heat transfer coefficient

σ = Stepthan Boltzmann constant = 1.27×10^{-10} BTU/hr/in^2/$^oK^4$

θ = time

ϵ_p = effective emissivity of the plate

A_p = area of the plate

T_p = plate temperature.

The density of a silver-cadmium battery is 0.10 lbs/in^3. Hence,

$$V_b = 10W_b = 30.8I_s \text{ in}^3 . \tag{A-6}$$

The battery dimension perpendicular to the plate is assumed to be 10 inches regardless of battery size so that

$$A_p = W_b = 3.08I_s \text{ in}^2 . \tag{A-7}$$

By substituting equations (A-3) and (A-4) into equations (A-2) and integrating we obtain

$$W_b c\, T_b + UA_p (T_b - T_p)\, \theta = Q_i \theta + E \tag{A-8}$$

where E is the integration constant. When T_b is a minimum, all the generated heat should be radiated to space. Thus,

$$UA_p (T_{bL} - T_{pL}) = Q_{iL} \tag{A-9}$$

and

$$E = W_b c T_{bL} \tag{A-10}$$

where the subscript "L" is for "lowest."

When Q_i is maximum,

$$W_b c(T_{bm} - T_{bL}) + UA(T_{bm} - T_{pm})\, \theta_m = Q_{im} \theta_m \tag{A-11}$$

By combining equations (A-1), (A-5), (A-8), (A-10), and (A-11), the general relationship among all the variables is found as

$$U(T_b - T_p) = \sigma \epsilon_p T_p^4 = \frac{Q_i}{A_p} - \frac{W_b c T_b - E}{A_p \theta_m} \tag{A-12}$$

All quantities but T_b, T_p, ϵ_p, U, and Q_i are known. The quantity Q_i is determined independently of this equation as shown below and will have maximum and minimum values. By assuming a value of I_s (ranges from 41.8 to 101.8)

and setting up equation (A-12) for both the maximum and minimum conditions of Q_i, four independent equations are generated. The four unknowns are T_{pL}, T_{pm}, U, and ϵ_p. The values of T_{bL} and T_{bm} are not really unknown because they are bounded by the range 15 to 35°C. Additionally, the various equal terms of equation (A-14) must have greater values for the highest temperature condition than for the lowest. This fact is easily seen by combining equations (A-4) and (A-5) which gives

$$T_b = \frac{\sigma \epsilon_p}{U} T_p^4 + T_p \qquad (A-13)$$

Equation (A-13) shows that as T_b increases so must $(T_b - T_p)$. Hence, the inequality

$$\frac{Q_{im}}{A_p} > \frac{W_b c (T_{bm} - T_{bL})}{A_p \theta_m} \frac{Q_{iL}}{A_p} \qquad (A-14)$$

may be used to determine the maximum range of T_b. Once a range of interest is selected, values for T_{bm} and T_{bL} may be selected and the four equations generated from equation (A-12) may be solved simultaneously.

A.2 Determination of Q_i

Because the orbit is a polar one, the sun may lie anywhere between 0° and 90° out of the orbit plane. The first case maximizes the shadow time and the second case puts the spacecraft in continuous sunlight. Because of this variation in sun declination, thermal conditions will vary over a wide range. However, only the extremes are of interest here.

From the definition of Q_i,

$$Q_i = Q_s + Q_g + Q_a \, . \qquad (A-15)$$

The solar constant is a 130 watts/ft^2 or 3.00 BTU/hr/in^2 so that the rate of solar heat input is

$$Q_s = 3.00A_p \sin\varphi = 9.24I_s \sin\varphi \qquad (A-16)$$

where φ is the angle between the sun's rays and the radiating plate.

The rate of internal heat generation in the battery is Q_g and it is time variable depending on whether the battery is on charge, overcharge, or discharge. On charge the cell reaction is endothermic and just about balances the I^2R losses. On discharge, the reaction is exothermic and adds to the I^2R losses. On overcharge almost all the charging energy goes into heat.[55,64] The discharge I-V characteristic of a 22 cell silver cadmium battery at 25°C is

$$V_d = 30.6 - \frac{0.198}{C} I_d \qquad (A-17)$$

where I_d is expressed as a function of C.[69] Thus the resistance of the battery is known and the various heat generation rates can be determined from the currents found in section 4.10.2 as

$$Q_d = I_d^2R + I_{ch}^2R = 0.104C \text{ watts}$$

$$Q_{ch} = 0$$

$$Q_{oh} = V_{och}I_{och} = 3.34C \text{ watts.}$$

The capacity of each string, $C/(q-r)$, was found as $0.754I_s$. At any given time three strings are in use so the value of C is $2.26I_s$. Substituting this value and using the conversion factor

$$1 \text{ watt} = 3.42 \text{ BTU/hr},$$

the heat generation rates are

$$Q_d = 0.804I_s \text{ BTU/hr} \qquad (A-18a)$$

$$Q_{ch} = 0 \qquad (A-18b)$$

$$Q_{och} = 26.4I_s \text{ BTU/hr.} \qquad (A-18c)$$

The duration of each of these conditions are:

$$T_d = 39.0 \text{ minutes} = 0.65 \text{ hour}$$

$$T_{ch} = 44.75 \text{ minutes} = 0.745 \text{ hour}$$

$$T_{och} = 9.75 \text{ minutes} = 0.1625 \text{ hours.}$$

These values are for when the sun lies in the orbit plane.

Finally, Q_a is the rate of heat input from the ambient surroundings. If the battery is not insulated, the net rate of heat transfer is

$$Q_a = \sigma \epsilon_b A_b (T_a^4 - T_b^4)$$

where

ϵ_b = battery emissivity

A_b = battery area.

To determine A_b, it will be assumed that the dimension of the cold plate perpendicular to the spacecraft longitudinal axis is 18 inches as shown in Figure A.2.

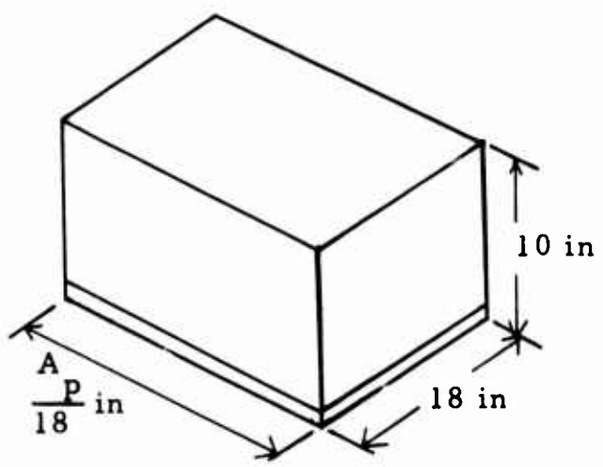

FIGURE A-2, BATTERY PACKAGE DIMENSIONS

Thus,

$$A_b = 360 + 2.11A_p \text{ in}^2,$$

and

$$Q = \sigma \epsilon_b (360 + 6.5I_s)(T_a^4 - T_b^4) \qquad (A-19)$$

The maximum value of Q_i will occur when the sun lies in the orbit plane. At this condition, Q_{och} is a maximum because T_{och} is minimum and so I_{och} is maximum. Also, the battery is overcharged during the last ten minutes of sunlight during which time the spacecraft is broadside to the sun's rays which results in a maximum value of T_a. The contribution of Q_s at this condition can be kept at zero by properly locating the battery package in the spacecraft.

The minimum heat input rate will also occur when the sun lies in the orbit plane because the shadow time is a maximum which results in a minimum value of T_a. At this condition, the battery is generating very little heat but is radiating to the spacecraft interior and transferring heat to the radiating plate. The expressions for Q_{im} and Q_{iL} are then

$$Q_{iL} = Q_d + Q_a$$

$$Q_{iL} = 0.804I_s + \sigma \epsilon_b (360 + 6.5I_s)(T_{aL}^4 - T_{bL}^4) \qquad (A-20)$$

and

$$Q_{im} = Q_{och} + Q_a$$

$$Q_{im} = 26.4I_s + \sigma \epsilon_b (360 + 6.5I_s)(T_{am}^4 - T_{bm}^4) \qquad (A-21)$$

The cell cases are made of stainless steel and are not insulated. The emissivity of unoxidized steel is about 0.10. The values of T_{am} and T_{aL} are 273°K and 333°K respectively.

A.3 Results

When $I_s = 41.8$, the following set of equations is generated.

$$U(T_{bL}-T_{pL}) = 1.27X10^{-10}\epsilon_p T_{pL}^4 = 0.261 + 6.24X10^{-11}[(273)^4-(T_bL)^4]$$

$$U(T_{bm}-T_{pm}) = 1.27X10^{-10}\epsilon_p T_{pm}^4 = 8.25 + 6.24X10^{-11}[(333)^4-T_{bm}^4] - 2.22(T_{bm}-T_{bL})$$

This set of equations has an infinite number of solutions. One such solution is

$$T_{bL} = 297^oK, \quad T_{bm} = 300.8^oK$$

$$T_{pL} = 296^oK, \quad T_{pm} = 299.7^oK$$

$$\epsilon_p = 0.125, \quad U = 0.122.$$

The same is true of the case when $I_s = 101.8$. A solution for this value of I_s is

$$T_{bL} = 297^oK, \quad T_{bm} = 300.8^oK$$

$$T_{pL} = 295.6^oK, \quad T_{pm} = 299.3^oK$$

$$\epsilon_p = 0.175, \quad U = 0.122.$$

The very narrow temperature range is a result of the high heat capacity of the battery. It may be concluded that the simple radiating cold plate is adequate to maintain the battery temperature in the specified limits.

A.4 Weight of Cold Plate

In both cases, the value of U is taken as 0.122. The definition of U is

$$U = \frac{k}{t} \qquad (A-22)$$

where

k = thermal conductivity, BTU/hr/in^2/in/^oC

t = plate thickness, inches.

In order to minimize plate weight, a material with a low conductivity is required so that t may be small. Metals are obviously of little interest as a plate would have to be several inches thick for U to be sufficiently low.

Teflon has been selected as the material for the plate because of its stability in space conditions and low thermal conductivity about 0.021. The emissivity requirements can be met through the use of coatings or with additives in the plate material itself. A sheet 0.172 inches thick with an area equal to A_p will be required. The density of this material is 0.077 lbs/in^3. The added weight due to the radiating plate is then

$$W_p = 0.0408 I_s \qquad (A-23)$$

The volume of the cold plate is $0.53 I_s$ cubic inches. Combining this figure with equation (A-6), the total volume of battery and cold plate is $31.3 I_s$.

APPENDIX B

ATTITUDE CONTROL SYSTEM

The Manned Orbiting Laboratory will probably be oriented in an earth pointing attitude as discussed in section 1.3. In this attitude the gravity gradient torque will aid the control system in balancing disturbance torques due to solar radiation pressure, aerodynamic pressure, crew movements, and magnetic torques generated by electrical loops in the spacecraft. In this appendix, first order estimates of the characteristics of inertia wheel, magnetic torquer, and mass expulsion systems are found in order to provide a basis for evaluating attitude control systems used with the power systems discussed in the text.

B.1 Vehicle Characteristics

For purposes of analysis, the MOL cylinder is assumed to be a solid of uniform density 41 feet long and 10 feet in diameter with a weight of 19,000 pounds. The Gemini capsule is assumed as a solid cone of uniform density 13 feet high and 10 feet in diameter at the base with a weight of 6,000 pounds. Using these assumptions, the vehicle center of mass is 5.7 feet from the cylinder center of mass. The geometric center is displaced 2.45 feet from the center of mass as shown in Figure B-1.

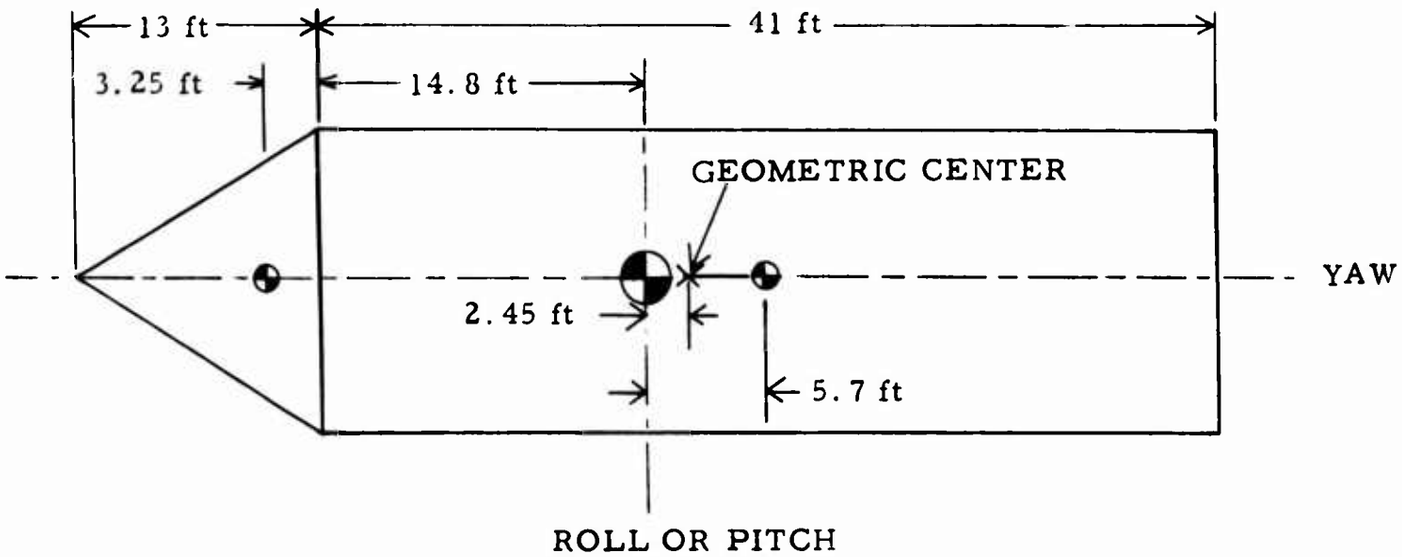

FIGURE B.1, VEHICLE WITHOUT SOLAR ARRAYS

The moment of inertia about the yaw axis (or longitudinal axis) which is aligned with the local vertical is

$$I_y = 8,760 \text{ ft-lb-sec}^2 . \tag{B-1}$$

The moments of inertia about the other two axes (roll and pitch) are

$$I_r = I_p = 93,600 \text{ ft-lb-sec}^2 . \tag{B-2}$$

These moments of inertia are for the spacecraft without arrays.

The other extreme is when the spacecraft has arrays totalling 1250 ft^2 and weighing 1000 pounds. Such large arrays are not required for even the maximum possible peak power but are used only to demonstrate how little an effect the arrays have. Because the arrays weigh 1000 pounds, the cylinder weight is reduced to 18,000 pounds. The vehicle center of mass is then 5.3 feet from the cylinder center mass and the geometric center is displaced 11.5 feet from the center of mass as shown schematically in Figure B.2.

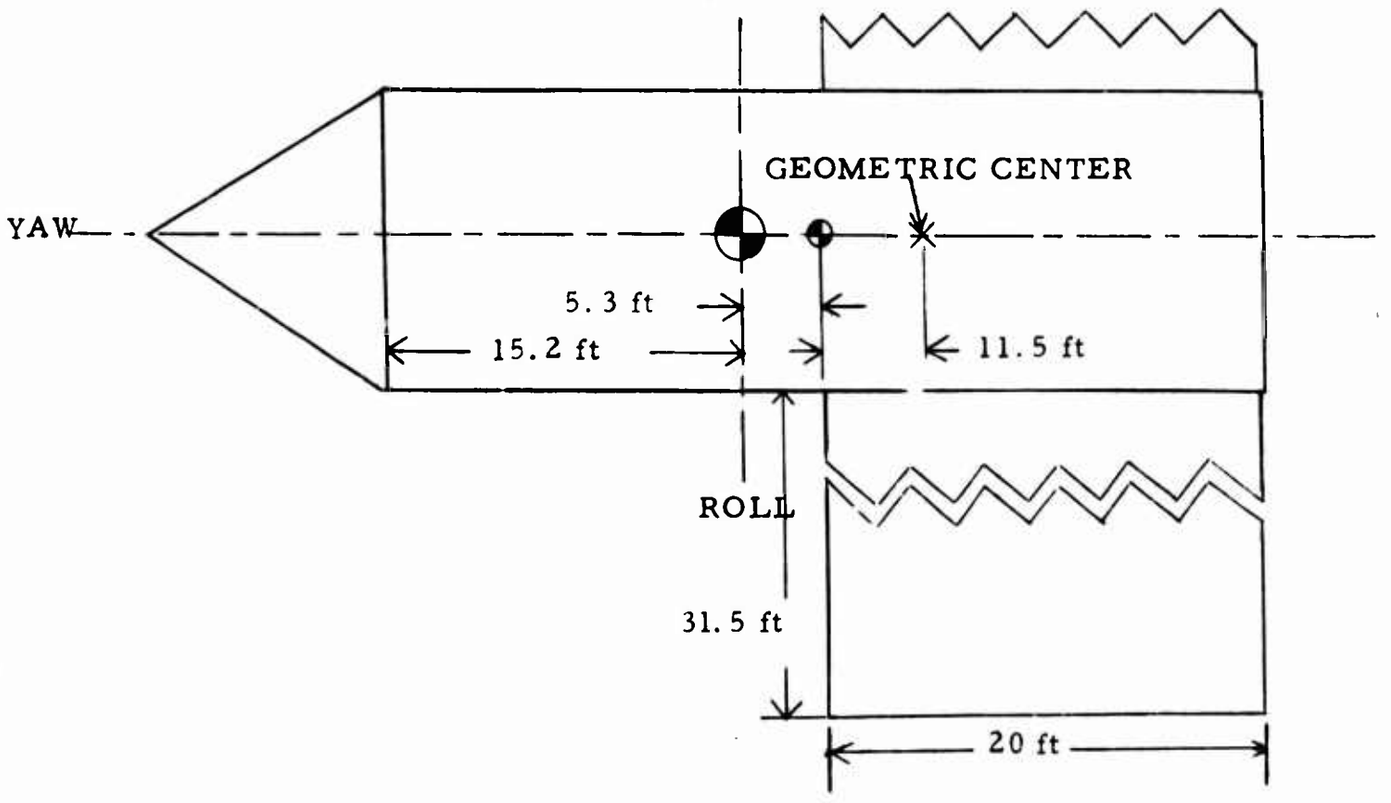

FIGURE B.2, VEHICLE WITH SOLAR ARRAYS

The moments of inertia of a vehicle with these large arrays are

$$I_y^a = 24,400 \text{ ft-lb-sec}^2 \tag{B-3}$$

$$I_r^a = 98,200 \text{ ft-lb-sec}^2 \tag{B-4}$$

$$I_p^a = 111,500 \text{ ft-lb-sec}^2. \tag{B-5}$$

The yaw axis moment of inertia has tripled, but this fact will be of little consequence as seen below.

B.2 Gravitational Torques

The gravitational torque may be expressed as[51]

$$T_g = \frac{3K}{2r^3} \Delta I \sin 2\theta \text{ ft-lbs} \tag{B-6}$$

where

K = gravitational constant = 1.408×10^{16} ft^3/ sec^2

r = orbit radius = 2.25×10^7 feet

ΔI = difference between longitudinal and the transverse moment of inertia

θ = angle of inclination between the longitudinal axis and orbit plane.

The pointing accuracy required for reconnaissance experiments is assumed to be ± 0.001 radian. At the maximum permissible misorientation, the gravity gradient torque for a vehicle without solar arrays is

$$T_g = 7.06 \times 10^3 \text{ ft-lbs} \tag{B-7}$$

about the roll and pitch axes. For a vehicle with solar arrays, the restoring torque about the pitch axis is

$$T_{gp}^a = 6.15 \times 10^3 \text{ ft-lbs.} \tag{B-8}$$

Similarily about the roll axis,

$$T_{gr}^a = 7.26 \times 10^3 \text{ ft-lbs.} \tag{B-9}$$

These torques tend to restore the vehicle orientation to the null point.

B.3 Solar Radiation Pressure Torque

The solar radiation pressure torque for a reflecting body* is[51]

$$T_s = 2P_s r_s A_s \cos^2\varphi \tag{B-10}$$

where

P_s = radiation pressure = $9.25X10^{-8}$ lb/ft^2

r = distance between center of mass and center of radiation pressure

A_s = surface area projected to the sun

φ = angle of incidence.

The maximum torque comes when φ is zero. This torque for a vehicle without solar arrays is

$$T_s = 2.16X10^{-4} \text{ ft-lb.} \tag{B-11}$$

For a vehicle with solar arrays, the torque is generated about the roll axis and is maximum of

$$T_s^a = 3.77X10^{-3} \text{ ft-lb.} \tag{B-12}$$

Comparing with equation (B-7) and (B-9) these torques are insignificant.

B.4 Aerodynamic Torques

The aerodynamic torque is[51]

$$T_a = P_a r_a A_a \sin\alpha \tag{B-13}$$

where

P_a = aerodynamic pressure = $8X10^{-6}$ lbs/ft^2 at 250 nm

r_a = distance between center of mass and center of pressure

A_a = surface area exposed to airstream

α = angle of attack.

When $\alpha = 90^\circ$, the torque on the spacecraft without solar arrays is

$$T_a = 9.3X10^{-3} \text{ ft-lb.} \tag{B-14}$$

---

*A reflecting body generates the highest torques.

For the vehicle with solar arrays, the torque is generated about the roll axis and has a magnitude of

$$T_a^a = 1.63X10^{-1} \text{ ft-lb.} \qquad \text{(B-15)}$$

As in the case of radiation torques, the aerodynamic disturbance torques are negligible compared to the gravitational restoring torques. Torques due to crew motions and currents in electrical loops are of no greater magnitude than the solar radiation or aerodynamic torques.[51] Hence, it may be concluded that the gravity gradient torque is adequate to maintain the vehicle orientation to well within ± 0.001 radian even in the presence of these disturbances.

B.5 Maneuvering

Since the mission principally concerns reconnaissance experiments, the crew will command short duration reorientations in order to gain fixes on ground targets. In one source where attitude control systems for manned military reconnaissance satellites are considered, it was estimated that the crew would require an average of 10 maneuvers per orbit. Since experiments are nominally conducted in only four orbits per day (see section 1.2), 40 maneuvers will be required per day. The torque and momentum requirements of each maneuver are estimated to be

$$T = 2X10^{-4}I \qquad \text{(B-16)}$$

$$H = 5X10^{-4}I \qquad \text{(B-17)}$$

where I is the moment of inertia about the axis of rotation.[51] The maneuvers only involve the pitch and roll axes. In the case of the spacecraft with solar arrays, command rotations about the yaw axis are prohibited as yaw axis rotation is controlled by the array pointing requirement (see section 3.13).

For the vehicle without solar arrays, the torque and momentum requirements for each maneuver about the roll or pitch axis are

$$T = 18.7 \text{ ft-lb} \tag{B-18}$$

$$H = 46.8 \text{ ft-lb-sec.} \tag{B-19}$$

For the vehicle with solar arrays, it is assumed that half the maneuvers are about the roll axis and half about the pitch axis. The torque and momentum requirements for each maneuver about the respective axes are

$$T_r^a = 19.6 \text{ ft-lb} \tag{B-20}$$

$$H_r^a = 49.05 \text{ ft-lb-sec} \tag{B-21}$$

$$T_p^a = 22.3 \text{ ft-lb} \tag{B-22}$$

$$H_p^a = 55.8 \text{ ft-lb-sec.} \tag{B-23}$$

There will be some requirements for control about the yaw axis in either type of vehicle. If no solar arrays are included, yaw rates must be limited. If solar arrays are included, yaw rates must be limited and controlled to specified values. For the vehicle without solar arrays the torque and momentum requirements are assumed to be

$$T_y = 1 \text{ ft-lb} \tag{B-24}$$

$$H_y = 2.5 \text{ ft-lb-sec.} \tag{B-25}$$

For the vehicle with solar arrays

$$T_y^a = 3 \text{ ft-lb} \tag{B-26}$$

$$H_y^a = 7.5 \text{ ft-lb-sec.} \tag{B-27}$$

It is assumed that there will be about 5 corrections in the yaw rate per orbit or about 80 per day.

B.6 Inertia Wheels

Inertia wheels are spinning bodies which can store or release momentum by simply being accelerated or decelerated. These devices are particularly useful when periodic torques must be generated or compensated. The

torques for maneuvering are of this type as the vehicle should be returned to the stable orientation after being disturbed.

In reference 51 (pages 29 and 30) the power requirements and weight of a single axis inertia wheel system are graphically presented as functions of the torque and momentum requirements for three representative maximum wheel speeds. Using the data presented therein, the characteristics of an inertia wheel system are summarized in Tables B-1 and B-2 below

MAXIMUM WHEEL SPEED, RPM	500	2000	6000
PEAK POWER, WATTS	650	2000	5000
WEIGHT, LBS	170	100	75

A. WHEELS CONTROLLING ROLL AND PITCH

MAXIMUM WHEEL SPEED, RPM	500	2000	6000
PEAK POWER WATTS	50	110	230
WEIGHT, LBS	30	19	18

B. WHEEL CONTROLLING YAW

TABLE B.1, INERTIA WHEEL CHARACTERISTICS OF VEHICLE WITHOUT SOLAR ARRAYS

MAXIMUM WHEEL SPEED, RPM	500	2000	6000
PEAK POWER, WATTS	680	2050	5300
WEIGHT, LBS	170	100	75

A. WHEEL CONTROLLING ROLL

MAXIMUM WHEEL SPEED, RPM	500	2000	6000
PEAK POWER, WATTS	800	2400	6500
WEIGHT, LBS	200	110	80

B. WHEEL CONTROLLING PITCH

MAXIMUM WHEEL SPEED, RPM	500	2000	6000
PEAK POWER, WATTS	130	340	750
WEIGHT, LBS	50	30	23

C. WHEEL CONTROLLING YAW

TABLE B.2, INERTIA WHEEL CHARACTERISTICS OF VEHICLE WITH SOLAR ARRAYS

It is immediately seen from Tables B. 1 and B.2 that addition of solar arrays has only a small effect on the weight of an inertia wheel system. For a three wheel system, solar arrays add 50 pounds (13.5%) at 500 RPM, 21 pounds (9.6%) at 2000 RPM and 10 pounds (5.9%) at 6000 RPM. If there is excess power available with the solar array system, these weight increases can be offset by slightly increasing the wheel speed. The peak power requirements may be considered as transients since momentum is merely the product of torque and time. Referring to equations (B-16) and (B-17), the time associated with each maneuver is approximately 2.5 seconds. The weights given in the above two tables include wheels, motors, and control circuits.

B.7 Magnetic Torquers

A single axis magnetic torquer consists of a coil of wire (hundreds of turns) and a control circuit. By passing current through the coil a magnetic dipole moment is generated and exerts a torque which tends to align the dipole in the direction of the earth's local magnetic field in the manner of a simple compass.[29] The moment generated is simply

$$\bar{M} = NI\bar{A}_L = \text{ampere-turn-ft}^2 \qquad \text{(B-28)}$$

where

N = the number of loops

I = the current, amperes

$\bar{A}_L$ = area enclosed by the loop, ft^2.

The torque generated is[51]

$$T_m = 6.86X10^{-6}\bar{M}X\bar{B} \text{ ft-lb} \qquad \text{(B-29)}$$

where $\bar{B}$ is the flux density of the geomagnetic field in gauss. The magnetic dipole of the earth is actually canted 11.4^o from the polar axis.[30a] However, if this angle of cant is neglected, the resulting error has only second order effects.[30b] An approximate expression for B is then[51]

$$B = \frac{1.43X10^{10}}{r^3} (\sin^2\psi + 4\cos^2\psi)^{\frac{1}{2}} \text{ gauss} \qquad (B-30)$$

where

r = the orbit radius, nautical miles

ψ = the angle between r and earth's axis.

Since the orbit is polar, the magnitude of B varies with location in the orbit but the variance is the same for all orbits in the mission. If the inclination is less than 90°, the dipole effectively processes at the earth rotation rate and so has different strengths for each orbit.

The quantity $(\sin^2\psi + 4\cos^2\psi)^{\frac{1}{2}}$ is henceforth defined as the quantity G. The value of G is a maximum of 2.0 when $\psi = 0^{\circ}$ which corresponds to the location over either of the poles. At the equator, $\psi = 90^{\circ}$ and G has the minimum value of 1.0.

By combining equations (B-28), (B-29), and (B-30), the magnetic torque generated about a given axis is

$$T_m = 1.88X10^{-6} NIA_L G \sin\gamma \qquad (B-31)$$

where γ is the angle between the loop dipole and the earth's axis. If loops are located in each of the planes determined by the roll, yaw, and pitch axes, each axis will lie in two of these planes and torques can be generated about each axis by use of two loops. If the loop areas are the maximum size permitted by the dimensions of the cylinder, the following torques may be generated:

$$T_m^{\,y} = 1.475X10^{-4} N_y I_y G \sin\gamma_y \text{ ft-lb} \qquad (B-32)$$

$$T_m^{\,r} = 7.70X10^{-4} N_r I_r G \sin\gamma_r \text{ ft-lb} \qquad (B-33)$$

$$T_m^{\,p} = 7.70X10^{-4} N_p I_p G \sin\gamma_p \text{ ft-lb.} \qquad (B-34)$$

The superscripts y, r, and p indicate that the loop plane is perpendicular to the yaw, roll, or pitch axis. The two torques generated by coils in the planes containing the axis of interest may be used. For instance, if it is desired to generate a torque about the roll axis, both $T_m^{\,y}$ and $T_m^{\,p}$ may be used.

Since torques must be available at any time during sunlight, the system should be sized to the worst case which occurs when the spacecraft is above the equator (G = 1.0). At this location, $\gamma_y = 90^o$ because of the earth-pointing orientation. The values of γ_r and γ_p may be selected at will by proper placement of the coils in the spacecraft. The angles γ_r and γ_p are selected as 45^o at G = 1 as no other combination will give a larger sum of T_m^r and T_m^p at G = 1.0. With these specifications, a unique set of values of NI for the three axes could be determined from the torque requirements of section B.4 and equations (B-32) through (B-34). However, such a solution results in immense values of $N_y I_y$ relative to the other values of NI because T_m^r and T_m^p together provide the yaw axis torque which is very small. Further, T_m^y is least efficient of the three torques in terms of the weight and power required as shown below.

The product of coil weight and current for a circular coil is[30c]

$$WI = \frac{16d\,\rho\,M^2}{VD^2} \qquad \text{(B-35)}$$

where

d = wire density, lbs/ft^3

ρ = resisitivity, ohm-ft

M = dipole moment, ampere turn-ft^2

V = power supply voltage = 25 volts

D = coil diameter, feet

Equation (B-35) may also be used with rectangular coils (as with T_m^r and T_m^p) by using for D the diameter of a circle of equivalent area. The diameter associated with T_m^y is the vehicle diameter or 10 feet. The diameter associated with the other two torques is the diameter of a circle with an area of 410 ft^2, 22.9 feet. If aluminum wire is used,

$$d = 168.5 \text{ lbs/ft}^3$$

$$\rho = 9.30 \times 10^{-8} \text{ ohm-ft.}$$

The values of WI are then

$$(WI)_y = 1.00X10^{-10} M^2 \text{ lb-amp} \tag{B-36}$$

$$(WI)_{p,r} = 1.90X10^{-11} M^2 \text{ lb-amp.} \tag{B-37}$$

From these equations, one sees that there is no point in including a coil to generate $T_m{}^y$ as the other two coils are much more efficient and together can generate torques about all three axes. Hence, the problem is reduced to supplying a coil for $T_m{}^r$ large enough to satisfy pitch maneuver and a coil for $T_m{}^p$ large enough to satisfy roll maneuvers. Using equations (B-33) and (B-34) and the torque requirements of section B.4, at G = 1, $\gamma_p = \gamma_r = 45^o$ the following values of NI are determined. For a vehicle without solar arrays:

$$(NI)_{p,r} = 35000 \text{ amp-turn.} \tag{B-38}$$

For a vehicle with solar arrays:

$$N_r{}^a I_r{}^a = 40,900 \text{ amp-turn} \tag{B-39}$$

$$N_p{}^a I_p{}^a = 36,000 \text{ amp-turn.} \tag{B-40}$$

Using these values and the areas of the loops, the values of M are found from equations (B-28) and can be substituted into equations (B-37) to find these weight-current products:

$$(WI)_{p,r} = 3920 \text{ amp-lbs} \tag{B-41}$$

for the vehicle without solar arrays and

$$(WI)_r{}^a = 5350 \text{ amp-lbs} \tag{B-42}$$

$$(WI)_p{}^a = 4150 \text{ amp-lbs} \tag{B-43}$$

for the vehicle with solar arrays. From these equations, it is immediately apparent that the solar cell system need not suffer a weight increase in the attitude control system, relative to the vehicle without solar arrays, if the current is increased by only 13.7%. Either spacecraft would require two

coils and both coils would be operated together only when making yaw axis corrections, and then only at very low currents. The currents may be considered as transients of 2.5 seconds duration.

For comparison, the product of weight and current* for the inertia wheel systems assuming operation of only one wheel at a time are given in Figure B.5 below.

MAXIMUM WHEEL SPEED RPM	500	2,000	6,000
WI	9,630	17,500	33,600

A. VEHICLE WITHOUT SOLAR ARRAYS

MAXIMUM WHEEL SPEED, RPM	500	2,000	6,000
WI	13,450	24,000	46,300

B. VEHICLE WITH SOLAR ARRAYS

TABLE B.3, WEIGHT-CURRENT PRODUCT FOR INERTIA WHEEL SYSTEMS

Comparing Table B.3 with equations (B-41) through (B-43) and taking into account two coils in each system, the magnetic torquer requires much less weight and power than the inertial wheel system while being much more flexible in trading one for the other. The magnetic torquer system is much superior to the inertia wheel system for this mission.

B.8 Mass Expulsion Systems

Mass expulsion attitude control systems generally use cold gases as propellants because of the requirement for thousands of starts and thrusting times of only a few seconds. The most common gas used in such systems is nitrogen although water will also be considered as it is the product of the fuel cell reaction.

B.8.1 System Requirements

The system will require one set of four symmetrically located thrusters for the roll axis and one such set for the pitch axis. A set of

*Total weight times peak current of largest wheel.

eight symetrically located thrusters are required for the yaw axis. The roll and pitch thrusters fire in pairs while two pairs of yaw thrusters are fired at once. This arrangement results in only rotational forces.

The vehicle without solar arrays has the following torque and thrusting time requirements:

$$T_r = T_p = 18.7 \text{ ft-lb}, \quad t_p = t_r = 50 \text{ sec/day}$$

$$T_y = 1.0 \text{ ft-lb}, \quad T_y - 200 \text{ sec/day}$$

The vehicle center of mass is displaced 14.8 feet from the nearest end of the cylinder and the cylinder radius is 5 feet (see Figure B.1). Using these dimensions as the available moment arms, the thrust requirements of each thruster are

$$F_r = F_p = \frac{18.7}{2(14.8)} = 0.63 \text{ pounds}$$

$$F_y = \frac{1.0}{4(5)} = 0.05 \text{ pounds.}$$

The sum of the thrust-time products for the entire mission is 4980 lb-sec.

The vehicle with solar arrays has the following torque and thrusting time requirements.

$$T_r^a = 19.6 \text{ ft-lb}, \quad t_r = 50 \text{ sec/day}$$

$$T_p^a = 22.3 \text{ ft-lb}, \quad t_p = 50 \text{ sec/day}$$

$$T_y^a = 3 \text{ ft-lb}, \quad t_y = 200 \text{ sec/day.}$$

The vehicle center of mass is displaced 15.2 feet from the nearest end of the cylinder (see Figure 3.2). The thrust requirements of each thruster are then

$$F_r^a = 0.64 \text{ pounds}$$

$$F_p^a = 0.74 \text{ pounds}$$

$$F_y^a = 0.15 \text{ pounds.}$$

The sum of the thrust-time products for the entire mission is 7730 lb-sec.

B.8.2 Nitrogen as a Propellant

Nitrogen used for attitude control is cryogenically stored and vaporized by expansion. Assuming the gas is warmed to -60°F before delivery and is expanded through a 5:1 nozzle, the specific impulse is about 80 seconds. Since the thrusting periods are very short, significant amounts of propellant will be spent in thrust buildup and tailoff because of the finite valve opening and closing times. An effective value of specific impulse is then assumed to be 70 seconds.

Using the simple relationship

$$W_{prop} = \frac{Ft}{I_{sp}} \qquad \text{(B-44)}$$

the propellant weight requirement for the vehicle without solar arrays is 71.0 pounds. For the vehicle with solar arrays the requirement is 110.3 pounds. These values are raised to 80 pounds and 125 pounds respectively to provide some reserve for contingencies. The same Beech analysis used in section 6.7 also includes analysis of nitrogen storage. Using that study, the dry storage system weights for one tank nitrogen storage are approximately 57.5 and 65 pounds respectively for 900 psi storage pressure.

The thrusters may be clustered on the spacecraft so that only one feed line is needed to satisfy each cluster. There will be eight feed lines, each nominally about 22 feet long. Assuming a delivery pressure of 100 psia, aluminum feed lines with an outside diameter of 0.40 inch and an inside diameter of 0.30 inch should be adequate. The weight of feed lines for either system is then 9.5 pounds.

With a chamber pressure of 100 psia, the nozzles are very small and differ little between the systems. The weight of nozzles and valves is estimated to be one pound per thruster or 16 pounds per system. The weight of control circuitry and wiring should add another 10 pounds. The weight of the mass expulsion system for the vehicle without solar arrays is then about 175 pounds while the vehicle with solar arrays requires about 230 pounds for the attitude control system.

Comparing these weights with equations (B-41) through (B-43), the magnetic torquer system for the spacecraft without solar arrays must use at least 44.6 amperes to be lighter than the mass expulsion system. The current for the vehicle with solar arrays is 41.3 amperes. These results apply for a 30 day mission.

For the 60 day mission, the weight of propellant is doubled. The tankage weights increase to 72.5 pounds and 87.5 pounds respectively. All other hardware should remain the same. The system weights are then about 268 and 372 pounds respectively. Comparing once again with the magnetic torquer system, the magnetic torquer system requires at least 29.2 amperes to weigh less than the nitrogen gas system in the case of the vehicle without solar arrays. The corresponding current for the vehicle with solar arrays is 25.5 amperes

B.8.3 Water as a Propellant

Water is generated by the fuel cells and may be put to use as a propellant in which case a credit can be applied to the fuel cell system for the weight saved (if any). Assuming the water is at 70°F, the specific impulse achieved by expansion through a 5:1 nozzle is about 80 seconds or the same as nitrogen. Hence, the same weight of water will be required as nitrogen gas in the previous section. Since only three or four pounds of water are used per day the water temperature can easily be maintained by including the storage tank in the environmental control system coolant loop.

At 70°F, the water must be at a pressure of 0.36 psia or less to form steam. However, at this extremely low pressure, the nozzles would have to be quite large to achieve the required thrusts. To obtain pressures of interest (about 20 psia) the temperature must be raised to about 230°F. With a Gemini fuel cell system, there should be no heat source in the spacecraft with a temperature of over 110°F. Hence, the water would have to be electrically heated and maintained at 230°F in insulated tanks. About 2300 watt hours per pound would be required to heat and vaporize

the water. Assuming a fuel cell efficiency of about 60%, two pounds of reactants would be required to generate enough energy to heat and vaporize one pound of water. Using such a scheme, an additional 160 pound of reactants would be required not to mention the weight of thrusters, lines, and storage for the water and fuel cell reactants. It may be concluded that an attitude control system using water as a propellant is unattractive, compared to the alternatives, if the only heat source is electrical.

BIBLIOGRAPHY

1. Anderson, G. M., "Nuclear Reactor Systems," Astronautics and Aerospace Engineering, May 1963, pp. 27-36.

2. Alibrando, A. P., "Apollo Fuel Cell Progress Termed 'Sound'," Aviation Week and Space Technology, January 20, 1964, pp. 32-33.

3. Amsterdam, M. F. et al, Research on Improved Solar Generator, September, 1962, ASD-TDR-62-245, AD 289, 691.

4. "Batteries May Replace LEM Fuel Cell," Aviation Week and Space Technology, March 8, 1965, p. 17.

5. Blatz, W. J. et al, "Gemini Design Features," Astronautics and Aeronautics, November, 1964, pp. 30-40.

6. Bleymaier, Brigadier General J. S., "Mapping Out the MOL," Air Force and Space Digest, June, 1964, pp. 43-46.

7. Bonnett, E. W. and Englar, K. G., "An Early Capability Medium Space Station," AIAA Paper No. 64-339.

8. Briggs, R. W. et al, "4 KW Solar Photovoltaic Power System Design Study," ASD-TDR-62-158, March 1962, pp.: a. 67-74, b. 159, c. 186, d. 215, e. 265, f. 274.

9. Carpenter, Captain R. T., "Space Isotopic Power Systems," Astronautics and Aerospace Engineering, May 1963, pp. 68-72.

10. Carson, W. N. Jr., "Auxiliary Electrode for Charge Control," Proceedings, 18th Annual Power Sources Conference, 1964, pp. 59-61.

11. Carson, W. N. Jr. and Hadley, R. L., "Auxiliary Electrode Space Cells," AIAA paper No. 64-752.

12. Chandler, William A., "Cryogenic Storage for Space Electrical Power," Astronautics and Aeronautics, May 1963, pp. 97-101.

13. Cheney, E. O. et al, "Open Cycle Fuel Cell System for Space Applications," ASME paper No. 64-WA/AV-15.

14. Cherry, W. R., "Solar Cells and the Applications Engineer," Astronautics and Aerospace Engineering, May 1963, pp. 54-57.

15. Cherry, W. R., "Solar Energy Systems for Space Application," Proceedings, 17th Annual Power Sources Conference, 1963, pp. 12-14.

16. Cherry, W. R. and Zoutendyk, J. A., "The State of the Art in Solar Cell Arrays for Space Electrical Power," AIAA paper No. 64-738.

17. Clark, W. W. et al, "Alkaline Battery Evaluation," June 1964, APL-TDR 64-76, AD 602 676, pp. 209.

18. Coffman, S. W. et al, "Advanced Fuel Cell Applications for Space Missions," AIAA paper No. 64-723.

19. "A Conceptual Design for a Multi-Kilowatt Power Level Photovoltaic Power System," Aerospace Electrical Division, Westinghouse Electric Corporation, Lima, Ohio, 1965.

20. Conners, John W., "Systems Engineering of Fuel Cell Powerplants," AIAA paper No. 64-748.

21. Cooley, W. C., "Solar Direct-Conversion Power Systems," IRE Transactions on Military Electronics, Vol. MIL 6, No. 1, January 1962, pp. 91-98.

22. "Cryogenic Storage System for the Manned Orbiting Laboratory," Beech Aircraft Corp., DD14297, October 6, 1964.

23. Du Pont, P. S. "Syncom 2 Electrical Power System," AIAA paper No. 64-456.

24. "Electrical Power Generation Systems for Space Applications," NASA SP-79.

25. Evans, G. E., "Reliability Engineering of Fuel Cells for Space Power," AIAA paper No. 64-746.

26. Evans, W. and Menetrey, W. R., "Direct Solar Conversion," Volume V of Energy Conversion Systems Reference Handbook, September 1960, WADD-TR-60-699. AD257, 788, pp.: a. V-A-120-123, b. V-A-84.

27. Evans, W. et al, "Solar Panel Design Considerations," Space Power Systems, ed. by N. W. Snyder, Academic Press, New York, 1961, pp. 79-109.

28. Fink, D. E. "Air Force Moves Quickly to Exploit MOL," Aviation Week, September 6, 1965, pp. 22-23.

29. Fischell, R. E., "Passive Magnetic Attitude Control for Earth Satellites," Advances in the Astronautical Sciences, Volume II, ed. by Horace Jacobs, Western Periodicals Inc., North Hollywood, California, 1963, p. 155.

30. "Flywheel Stabilized, Magnetically Torqued Attitude Control System for Meteorological Satellites," May 1965, NASA CR-232, pp.: a. 2.2-1, b. 3.2-9, c. 3.2-25.

31. Frink, A. M., Jr., "Sealed Cadmium-Silver Oxide Batteries," Proceedings, 17th Annual Power Sources Conference, 1963, pp. 114-116.

32. "General Electric Fuel Cell," Interavia, no. 8, 1965, pp. 1297-1299.

33. Gould, C. L., "Solar Cell Power Systems for Space Stations," IEEE Transactions on Aerospace, Vol. AS-2, No. 2, April 1964, p. 760.

34. Greenstein, J. L. and Hunter, J. R., "A Preliminary Design of an Early Manned Space Station," AIAA Paper No. 64-335.

35. Gregory, Dr. Derek P., "Hydrogen-Oxygen Cells of the Bacon Type," A Lecture to the UCLA Course on Electrichemical Energy Conversion, August 6, 1963.

36. de Haas, E. and Winkler, S. H., "Electrical Power System for Lunar Excursion Module," Radio Corporation of America, Astro-Electronics Division, Princeton, N.J., October 1962, AED Report No. C-2033.

37. Hamilton, R. C., "Ranger Spacecraft Power System," Space Power Systems, ed. by N. W. Snyder, Academic Press, New York, 1961, pp. 19-27.

38. Hendel, F. J., "Recovery of Water During Space Missions," ARS Journal, December 1962, pp. 1847-1859.

39. Hendel, F. J., "Water Sources During Manned Space Missions," Proceedings of the Fifth International Symposium on Space Technology and Science, Tokyo, 1963, pp. 1101-1106.

40. Hinton, J. F. and Hagen, R. W., "A Vehicle Integrated Power System for a Manned Orbiting Space Vehicle," SAE paper 921D, October 1964.

41. Iles, P. A., "Present Status of Silicon Solar Cells," IRE Transactions on Military Electronics, Vol. MIL 6, No. 1, January 1962, pp. 5-13.

42. Ingling, W. G. and Clark, W. W., "Evaluation of Secondary Batteries," Proceedings, 17th Annual Power Sources Conference, 1963, pp. 122-124.

43. Kovacik, V. P., "Dynamic Energy Conversion," Astronautics and Aerospace Engineering, May 1963, pp. 84-88.

44. Ladner, J. E. and Ragsdale, G. C., "Earth Orbital Lifetime," January 1964, NASA TN D-1955.

45. Luft, W., "Effects of Electron Irradiation on N on P Silicon Solar Cells," IEEE Transactions on Aerospace, April 1964, pp. 747-758.

46. "Manned Environmental System Assessment," NASA CR-134, pp. 74-77.

47. Mathews, C. W., "The Gemini Program," Astronautics and Aeronautics, November 1964, pp. 22-29.

48. Menetry, W. R., "Solar System Design," Volume IX of Energy Conversion Systems Reference Handbook, September 1960, WADD TR 60-699, AD 256, 748.

49. Miluschewa, S., RCA Internal Data on Earth Radiation Belts, January 29, 1964 and May 26, 1964.

50. "MOL and Beyond," Space/Aeronautics, June 1964, pp. 52-75.

51. Nichol, K. C. et al, "Research and Investigation on Satellite Attitude Control," March 1965, AFFDL-TR-64-168, part I, pp. 24-60.

52. Normyle, W. J., "Air Force Given Manned Space Role," Aviation Week, August 30, 1965, p. 23.

53. "Optics, Batteries Considered for LEM," Aviation Week and Space Technology, April 12, 1965, p. 30.

54. Rappaport, P. J. and Frink, A. M., Jr., "Sealed Nickel-Cadmium and Silver-Zinc Batteries," Power Systems for Spaceflight, ed. by M. A. Zipkin and R. N Edwards, Academic Press, New York, 1963, pp. 211-219.

55. Preusse, K. E. and Shair, R. C., "Thermal Analysis of Hermetically Sealed Nickel-Cadmium Cells for Space Applications," AIAA Paper No. 64-751.

56. Private Communication from K. R. Hahn of Pratt and Whitney, East Hartford, Connecticut, July 1965.

57. Private Communication with W. R. Hangen, Manager of Solar Cell Marketing, RCA, Mountain Top, Pennsylvania, September 1964.

58. Private Communication with L. Muhlfelder, RCA Astro-Electronics Division, Heightstown, N. J., August 1965.

59. Private Communication with Bernard Randall of Pratt and Whitney, East Hartford, Connecticut, April 1965.

60. Private Communication from J. H. Rodgers, Beech Aircraft Corporation, Boulder, Colorado, October 1964.

61. Private Communication with members of the Power Systems Group RCA Astro-Electronics Division, Heightstown, N. J., October 1964.

62. Ray, K. A. and Winicur, D. H., "A Large Area Solar Cell Array," AIAA Paper No. 64-525.

63. "Research Study on the Use of Auxiliary Electrodes in Sealed Silver-Cadmium Cells," Prepared by General Electric Co. for Goddard Space Flight Center, June 1963, NASA, CR-55014.

64. Schulman, I. M., "Secondary Batteries for Energy Storage in Space," Energy Conversion for Space Power, ed. by Nathan W. Snyder, Academic Press, New York, 1961, pp. 479-496.

65. Scott, W. C., "Development of the Power Supply for the Transit Satellite," Space Power Systems, ed. by N. W. Snyder, Academic Press, New York, 1961, pp. 49-79.

66. Shair, R. C., "Sealed Secondary Cells for Space Power Systems," AIAA Paper No. 64-455.

67. Shair, R. C. and Gray, W., "Hermetically Sealed Nickel-Cadmium Batteries for the Orbiting Astronomical Observatory Satellite," Power Systems for Space Flight, ed. by M. A. Zipkin and R. N. Edwards, Academic Press, New York, 1963, pp. 221-239.

68. Shair, R. C. et al, "Design Development and Manufacture of Storage Batteries for Future Satellites," Prepared by Golton Industries for Goddard Space Flight Center, July 1963, NASA CR 60819.

69. Shair, R. C., et al, "Silver-Cadmium Batteries," Proceedings, 18th Annual Power Sources Conference, 1964, pp. 50-54.

70. Shaw, R. H. and Thompson, R. A., "Hydrogen-Oxygen Fuel System for Space Vehicles," ARS Paper No. 2560-62.

71. Smylie, R. E. and Reumont, M. R., "Life Support Systems," Manned Spacecraft: Engineering Design and Operation, ed. by P. E. Purser et al, Fairchild Publications, 1964, pp. 137-159.

72. Snyder, N. W. and Karcher, R. W., "Solar Cell Systems for Space Vehicles," Space Power Systems, edited by N. W. Snyder, Academic Press, New York, 1961, pp. 3-17.

73. Southman, D. L., "Power Systems Comparisons for Manned Space Station Applications," AIAA Paper No. 64-721.

74. Space Data, TRW Space Technology Laboratories, Redondo Beach, California, 1965, pp.: a. 24-26, b. 64-66.

75. Stafford, G. B., "Space Power Subsystem Capabilities," AIAA Paper No. 65-468.

76. Stoup, E. R., "The Battery for the International Ionosphere Satellite Ariel I," Power Systems for Space Flight, ed. by M. A. Zipkin and R. N. Edwards, Academic Press, New York, 1963, pp. 249-260.

77. Stump, F. C. et al, "Study Progress Report: Manned Orbital Space Station: Power Conversion and Control," Aerospace Electrical Division, Westinghouse Electric Corporation, Lima, Ohio, February 1963, Report No. SID-63-36-6, pp.: a. 18-19, b. A-122-123.

78. Szego, George, "Space Power Systems State of the Art," AIAA Paper No. 64-525.

79. Szego, G. C. and Cohn, E. M., "Fuel Cells for Aerospace Application," Astronautics and Aerospace Engineering, May 1963, pp. 107-111.

80. Tarneja, K. S. and Rossi, V. A., "Second Quarterly Progress Report - Dendritic Silicon Solar Cell Panel," February 1963, AD 401-794.

81. Thelen, Alfred, "The Use of Vacuum Deposited Coatings to Improve the Conversion Efficiency of Solar Cells in Space," Energy Conversion for Space Power, ed. by N. W. Snyder, Academic Press, New York, 1961, pp. 29-47.

82. Thomas, U. B., "Battery Considerations for a Communications Satellite," Energy Conversion for Space Power, ed. by N. W. Snyder, Academic Press, New York, 1961, pp. 497-514.

83. "Titan Rockets for Civil and Military Spacecraft," Interavia, May 1965, pp. 686-689.

84. Tonelli, D. A. and Regnier, E. P., "Radioisotope Power Generating System for a Manned Space Laboratory," ASME Paper No. 65-AV-18.

85. "Transcript of the Conference on Secondary Space Batteries," Vol. II, NASA and Interagency Advanced Power Group, June 1963, pp. A-27-28.

86. "USAF Continues MOL Definition Effort," Aviation Week, March 15, 1965, pp. 85-93.

87. Wallman, H. and Barnett, S. M., "Evaluation of Water Recovery Systems for Space Vehicles," Medical and Biological Problems of Space Flight, ed. by G. H. Bourne, Academic Press, New York, 1963, pp. 225-235.

88. Wolverton, R. W. et al, Flight Performance Handbook for Orbital Operations, John Wiley and Sons, Inc., New York, 1963, pp. 6-16 to 6-19.

89. "World Missile and Space Encyclopedia," Missiles and Rockets, May 11, 1964, p. 45.

90. Zylstra, D. L., "DOD Approves Pre-MOL Flights," Missiles and Rockets, April 19, 1965, pp. 12-13.

91. Zylstra, D. L., "Douglas Wins Epochal MOL Contract," Missiles and Rockets, August 30, 1965, pp. 14-15.